

Publication No.
FHWA-
HIF-20-004
December 2019

Post-Hazard Engineering Assessment of Highway Structures using Remote Sensing Technologies



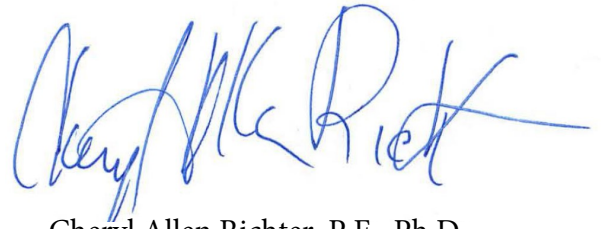
U.S. Department
of Transportation

**Federal Highway
Administration**

Research, Development, and Technology
Turner-Fairbank Highway Research Center
6300 Georgetown Pike
McLean, VA 22101-2296

FOREWORD

This report describes applications of remote sensing technologies for post-hazard damage inspection of highway structures. A literature review is presented of various remote sensing platforms used in post-hazard bridge applications including space-borne, airborne, ground-based and water-based systems. On real world applications, the report presents demonstration of unmanned aerial systems (UAS) and unmanned water systems (UWS) at two bridge sites in Maryland and a mock-up laboratory study of bridge movement using photogrammetry technique.



Cheryl Allen Richter, P.E., Ph.D.
Director, Office of Infrastructure
Research and Development

Cover image sources, from top, left to right: Silent Falcon, FHWA; FHWA; Seafloor Systems; CEE HydroSystems.

The FHWA is the source for all images not otherwise credited in this document.

Notice

This document is disseminated under the sponsorship of the U.S. Department of Transportation in the interest of information exchange. The U.S. Government assumes no liability for the use of the information contained in this document.

The U.S. Government does not endorse products or manufacturers. Trademarks or manufacturers' names appear in this report only because they are considered essential to the objective of the document. They are included for informational purposes only and are not intended to reflect a preference, approval, or endorsement of any one product or entity.

Quality Assurance Statement

The Federal Highway Administration (FHWA) provides high-quality information to serve Government, industry, and the public in a manner that promotes public understanding. Standards and policies are used to ensure and maximize the quality, objectivity, utility, and integrity of its information. FHWA periodically reviews quality issues and adjusts its programs and processes to ensure continuous quality improvement.

TECHNICAL REPORT DOCUMENTATION PAGE

1. Report No. FHWA-HIF-20-004	2. Government Accession No.:	3. Recipient's Catalog No.	
4. Title and Subtitle: Post-Hazard Engineering Assessment of Highway Structures using Remote Sensing Technologies		5. Report Date: December 2019	
		6. Performing Organization Code:	
7. Authors: Jalinoos, F., Agrawal, A.K., Brooks C., Amjadian, M., Banach, D., Boren, E.J., Dobson, R., and Ahlborn, T.		8. Performing Organization Report No.:	
9. Performing Organization Name and Address: The City College of New York 160 Convent Ave, New York, NY 10031		10. Work Unit No. (TRAIS):	
		11. Contract or Grant No.: DTFH61-14-D-00010 0209	
12. Sponsoring Agency Name and Address: Office of Research, Development, and Technology Federal Highway Administration 6300 Georgetown Pike McLean, VA 22101-2296		13. Type of Report and Period Covered: Final Report	
		14. Sponsoring Agency Code:	
15. Supplementary Notes: Frank Jalinoos was the Contracting Officer's Representative (COR).			
16. Abstract: There are approximately 615,000 bridges in the United States. Many of these bridges serve as critical parts of the transportation network locally, regionally and nationwide, and are essential for transportation of goods and people before, during and after extreme natural hazards. This report presents a detailed study on engineering post-hazard assessment of bridges with focus on geo- and hydraulic hazards. The objective of post-hazard assessment is to collect engineering data related to the behavior and damage to bridges. The report presents a detailed investigation on post-hazard engineering assessment through: (i) literature review of the current state of the art on post-hazard assessment for geo- and hydraulic hazards including data needs and gaps; (ii) field evaluation using unmanned aerial systems (UAS) for 3D photogrammetry of two bridge structures in Maryland as well as field evaluation using unmanned water systems (UWS) for developing bathymetric profiles; and, (iii) investigation on resolution of bridge movement detection using UAS through testing of a scaled bridge model. It has been demonstrated that UAS and UWS are invaluable and powerful technology for collecting engineering data after an extreme natural hazard event. However, numerous knowledge gaps exist in full implementation of an engineering data collection program.			
17. Key Words: Bridge damage assessment, geo- and hydraulic hazard, remote sensing technology, unmanned aerial system (UAS), unmanned water system (UWS).		18. Distribution Statement: No restrictions. This document is available to the public.	
19. Security Classification (of this report): Unclassified	20. Security Classification (of this page): Unclassified	21. No of Pages: 88	22. Price:

SI* (MODERN METRIC) CONVERSION FACTORS

APPROXIMATE CONVERSIONS TO SI UNITS

Symbol	When You Know	Multiply By	To Find	Symbol
LENGTH				
in	inches	25.4	millimeters	mm
ft	feet	0.305	meters	m
yd	yards	0.914	meters	m
mi	miles	1.61	kilometers	km
AREA				
in ²	square inches	645.2	square millimeters	mm ²
ft ²	square feet	0.093	square meters	m ²
yd ²	square yard	0.836	square meters	m ²
ac	acres	0.405	hectares	ha
mi ²	square miles	2.59	square kilometers	km ²
VOLUME				
fl oz	fluid ounces	29.57	milliliters	mL
gal	gallons	3.785	liters	L
ft ³	cubic feet	0.028	cubic meters	m ³
yd ³	cubic yards	0.765	cubic meters	m ³
NOTE: volumes greater than 1000 L shall be shown in m ³				
MASS				
oz	ounces	28.35	grams	g
lb	pounds	0.454	kilograms	kg
T	short tons (2000 lb)	0.907	megagrams (or "metric ton")	Mg (or "T")
TEMPERATURE (exact degrees)				
°F	Fahrenheit	$5(F-32)/9$ or $(F-32)/1.8$	Celsius	°C
ILLUMINATION				
fc	foot-candles	10.76	lux	lx
f	foot-Lamberts	3.426	candela/m ²	cd/m ²
FORCE and PRESSURE or STRESS				
lbf	poundforce	4.45	newtons	N
lbf/in ²	poundforce per square inch	6.89	kilopascals	kPa

APPROXIMATE CONVERSIONS FROM SI UNITS

Symbol	When You Know	Multiply By	To Find	Symbol
LENGTH				
mm	millimeters	0.039	inches	in
m	meters	3.28	feet	ft
m	meters	1.09	yards	yd
km	kilometers	0.621	miles	mi
AREA				
mm ²	square millimeters	0.0016	square inches	in ²
m ²	square meters	10.764	square feet	ft ²
m ²	square meters	1.195	square yards	yd ²
ha	hectares	2.47	acres	ac
km ²	square kilometers	0.386	square miles	mi ²
VOLUME				
mL	milliliters	0.034	fluid ounces	fl oz
L	liters	0.264	gallons	gal
m ³	cubic meters	35.314	cubic feet	ft ³
m ³	cubic meters	1.307	cubic yards	yd ³
MASS				
g	grams	0.035	ounces	oz
kg	kilograms	2.202	pounds	lb
Mg (or "T")	megagrams (or "metric ton")	1.103	short tons (2000 lb)	T
TEMPERATURE (exact degrees)				
°C	Celsius	$1.8C+32$	Fahrenheit	°F
ILLUMINATION				
lx	lux	0.0929	foot-candles	fc
cd/m ²	candela/m ²	0.2919	foot-Lamberts	f
FORCE and PRESSURE or STRESS				
N	newtons	0.225	poundforce	lbf
kPa	kilopascals	0.145	poundforce per square inch	lbf/in ²

TABLE OF CONTENTS

CHAPTER 1. THE STATE OF THE ART OF REMOTE SENSING TECHNOLOGIES AND ANALYSIS OF NEEDS AND GAPS	1
INTRODUCTION.....	1
STATE OF THE ART OF REMOTE SENSING TECHNOLOGIES.....	3
Space-borne Technologies.....	4
Airborne-Based Technologies	6
Ground-Based Technologies	7
Water-Based Technologies.....	18
Monitoring-Based Nondestructive Evaluation Technologies	21
Social Media-Based Technologies	23
ANALYSIS OF NEEDS AND GAPS	24
Data Needs in Post-Hazard Damage Assessment	24
Gaps in Post-Hazard Damage Assessment.....	28
CHAPTER 2. FIELD DEMONSTRATION OF SELECTED REMOTE SENSING TECHNOLOGIES.....	35
INTRODUCTION.....	35
ASSESSMENT OF TUCKAHOE CREEK BRIDGE	38
CONCLUDING REMARKS.....	48
CHAPTER 3. LABORATORY EVALUATION OF SELECTED REMOTE SENSING TECHNOLOGIES OF A MOCK BRIDGE FOR MOVEMENT DETECTION.....	49
INTRODUCTION.....	49
MODEL BRIDGE AND EQUIPMENT.....	51
Model Bridge.....	51
Camera System.....	51
Unmanned Aircraft System (UAS)	51
TRANSLATION MOVEMENT EXPERIMENT.....	52
ROTATION MOVEMENT EXPERIMENT	54
SETTLEMENT MOVEMENT EXPERIMENT.....	56
POST-PROCESSING OF DATA	59
RESULTS AND DISCUSSION	59
Translation.....	59
Rotation	60
Settlement.....	61
Results Summary.....	61
CONCLUDING REMARKS.....	62
CHAPTER 4. CONCLUSIONS AND RECOMMENDATIONS FOR FUTURE STUDY..	64
CONCLUSIONS	64
RECOMMENDATIONS FOR FUTURE STUDY	65
Field Evaluation of the Technology	65
Evaluation of Bridge Movements.....	65
ACKNOWLEDGMENTS	67
REFERENCES.....	68

LIST OF FIGURES

Figure 1. Illustration. Potential remote sensing technologies for post-hazard damage assessment of highway structures.	3
Figure 2. Illustration. InSAR results obtained from a simple span bridge showing progressive settlement over the considered period.....	5
Figure 3. Photo. A rotary-wing unmanned aerial vehicle (UAV) over Disaster City, Texas.	8
Figure 4. Photo. Examples of UAV with different capabilities useful for post-hazard damage assessment of structures.	9
Figure 5. Photo. A fixed wing UAV used to collect CRS data.....	11
Figure 6. Photo. Examples of UAS helicopter models.	13
Figure 7. Photo. A quadcopter UAS used for inspection of a steel bridge.	13
Figure 8. Illustration. Detection of defective area of a girder using a ground-based LiDAR sensor.	16
Figure 9. Illustration. Mobile LiDAR used for scanning the Mackinac Bridge and toll plaza.....	17
Figure 10. Photo. An Unmanned Water System in operation.....	19
Figure 11. Photo. Examples of Unmanned Water System.....	19
Figure 12. Illustration. Bridge pier scanning using a commercial fish finder sonar app, where the footing of a bridge pier can be seen as indicated by arrow.....	21
Figure 13. Photo. Field implementation of sensors on the bridge in Rome, New York.....	22
Figure 14. Illustration. Carbon Scanner tested by searching “#winterstorm” over New York City on March 19, 2013.	24
Figure 15. Photo. Water mark collected in the aftermath of Hurricane Sandy in the New York City area.....	25
Figure 16. Graph. Computer water surface elevation of Hurricane Sandy in the New York City area.....	26
Figure 17. Illustration. Digitally filtered and migrated 300 MHz GPR data.	26
Figure 18. Illustration. Spatial availability of coastal elevation data.....	32
Figure 19. Illustration. LiDAR data availability for Maryland.....	33
Figure 20. Photo. UWS platform collecting data at the Tuckahoe Creek bridge site. (UWS is highlighted in the grey circle).	36
Figure 21. Photo. UWS platform collecting data at the Bacon Ridge Branch site (UWS is highlighted in the grey circle).	36
Figure 22. Photo. The hexacopter platform collecting bridge image data at the Tuckahoe Creek site.	37
Figure 23. Photo. UWS (highlighted by grey circle) can be seen returning to Tuckahoe Landing in a UAS-collected image after obtaining sonar data near the bridge.	37
Figure 24. Illustration. Data collection paths (shown in red) of the UWS at Tuckahoe Creek. ...	39
Figure 25. Illustration. Contour bathymetry measurements at Tuckahoe Creek reached 30 ft (9.1m) near bridge piers 8 and 9 (white arrow).	39
Figure 26. Illustration. A combination of collected bathymetry data (black outline), NOAA bathymetry data (white outline), and LiDAR elevation data (outside white outline) that can be used as an input for hydraulic modeling (Tuckahoe Creek).	40
Figure 27. Illustration. Wider scale of watershed data in Tuckahoe Creek.	41

Figure 28. Illustration. DJI Phantom 3A aerial imagery (outlined in black) reconstructed into an orthophoto image with 3D elevation data shown on top of an GIS Basemap displaying WorldView satellite imagery (Tuckahoe Creek).	42
Figure 29. Photo. Photo of the Tuckahoe Creek bridge site taken with the Phantom 3A UAS. ..	42
Figure 30. Photo. Close-up photo of the Tuckahoe Creek Bridge taken with the Phantom 3A UAS.	43
Figure 31. Photo. DJI Mavic imagery of a pier cap and the side of the bridge.	43
Figure 32. Illustration. Model of bridge cap-beam (Tuckahoe Creek Bridge) with its measured height.	44
Figure 33. Illustration. (A) Model of a bridge pier (Tuckahoe Creek Bridge) and (B) its measured length compared to that shown in (C) its drawing details.	44
Figure 34. Photo. The Bacon Ridge Branch site as collected from the DJI Phantom 3A UAS. ..	45
Figure 35. Illustration. Data collection paths of UWS with depths at Bacon Ridge Branch (Note: Red color indicates deeper values).	46
Figure 36. Illustration. Comparison of bathymetric sonar data from Bacon Ridge Branch collected using UWS in 2013, 2014, and 2017.	46
Figure 37. Photo. High-resolution UAS-collected imagery of riprap at Bacon Ridge Bridge.	47
Figure 38. Photo. Data collection by UWS at Bacon Ridge Branch (1 ft = 0.3048 m).	47
Figure 39. Photo. Mounting LiDAR sensor on a UAS.	50
Figure 40. Photo. Photo of the scaled model bridge. The bridge dimensions are 3 ft High × 6 ft Wide × 2.7 ft Deep (91 cm H / 183 cm W / 83 cm D).	50
Figure 41. Illustration. Data collection set-up. Red lines indicate position of transects which were used to create distance from target and path for camera system positions. The figure also illustrates the height of the camera system.	52
Figure 42. Illustration. Picture of model bridge with position of markers 1 to 7.	53
Figure 43. Illustration. Picture of model bridge with position of markers 1 to 8.	54
Figure 44. Illustration. Picture of model bridge with position of markers 1 to 4.	55
Figure 45. Photo. Amount of rotation in the model bridge element was verified with ground measurements.	55
Figure 46. Equation. Estimated angle of rotation.	56
Figure 47. Illustration. Picture of model bridge with position of coordinate markers 1-6. Additional markers 7 and 8 used for reporting Z-axis position.	56
Figure 48. Photo. The model bridge with a raised section used to represent bridge settlement for the UAS data collection.	57
Figure 49. Photo. Certified remote pilot collecting imagery from the UAS of the model bridge in the settlement scenario.	58
Figure 50. Photo. The model bridge with settlement in place as collected from the UAS with 36 megapixel camera at 50 ft (15m) height.	58
Figure 51. Graph. Scatter plots comparing the measured differences of markers 1 and 6 against estimated differences for each position.	60

LIST OF TABLES

Table 1. Sample county LiDAR dataset metadata information.	32
Table 2. Coordinates of markers for the translation experiment (Unit: cm).....	53
Table 3. Coordinates of markers for the roattaion experiment (Unit: cm)	55
Table 4. Coordinates of markers for the settlement experiment (Unit: cm).....	57
Table 5. Measured vs. estimated distance between markers 1 and 6 for the translation design 1 movement experiment (Unit: cm).....	59
Table 6. Measured vs. estimated distance between markers 1 and 8 for the translation design 2 movement experiment (Unit: cm).....	60
Table 7. Measured vs. estimated degrees and distance between marker 2 at postion 0 and reported row postion (Unit: cm).....	61
Table 8. Measured vs. estimated distance between bridge surfces at markers 7 and 8 (Unit: cm)	61
Table 9. Accuracy of the UAS in measuring three different movements of the model bridge. ...	62

LIST OF ABBREVIATIONS

2D	Two Dimensional
3D	Three Dimensional
ASV	Autonomous Surface Vehicle
Caltrans	California Department of Transportation
CRS	Commercial Remote Sensing
DEM	Digital Elevation Map
DIC	Digital Image Correlation
FAA	Federal Aviation Administration
FHWA	Federal Highway Administration
FPV	First Person Viewer
GIS	Geographic Information System
GNSS	Global Navigation Satellite System
GPR	Ground Penetrating Radar
GPS	Global Positioning System
IBIS-FS	Image by Interferometric Survey for Structures
IMU	Inertial Measurement Unit
InSAR	Interferometric Synthetic Aperture Radar
IRSV	Integrated Remote Sensing and Visualization
LDV	Laser Doppler Vibrometer
LiDAR	Light Detection and Ranging
NBI	National Bridge Inventory
NDT	Nondestructive Testing
NIST	National Institute of Standards and Technology
NOAA	National Oceanic and Atmospheric Administration
NSF	National Science Foundation
NSMP	National Strong-Motion Project
ROV	Remotely Operated Vehicle
SAR	Synthetic Aperture Radar
SHM	Structural Health Monitoring
UAS	Unmanned Aerial System
UAV	Unmanned Aerial Vehicle
UMV	Unmanned Marine Vehicle
USDOT	U.S. Department of Transportation
USGS	U.S. Geological Survey
USV	Unmanned Surface Vehicle
UWS	Unmanned Water System

This page is intentionally left blank.

CHAPTER 1. THE STATE OF THE ART OF REMOTE SENSING TECHNOLOGIES AND ANALYSIS OF NEEDS AND GAPS

INTRODUCTION

As per current National Bridge Inventory (NBI) (FHWA 2018), there are approximately 615,000 bridges in the United States. These bridges serve as critical parts of the transportation network locally, regionally and nationwide, and are essential for transportation of goods, services and people. The vulnerability of highway bridges to extreme natural hazards is becoming more significant as the average age of bridges in the United States is reaching 50 years (against a design life between 60-70 years) and about 9 percent of bridges are in poor condition (FHWA 2018; Adkins 2016). Post extreme event damage to bridges is well noted in the literature including earthquakes (Watanabe et al. 1998; Basoʒ et al. 1999; Pamuk et al. 2005; Wang and Lee 2009; Duwadi 2010; Yen 2010), scour (Melville, 1992; Richardson et al. 1993; Kerenyi and Guo 2010), tsunami after an earthquake (Kosa 2011; Akiyama et al. 2013), hurricanes, storm surge and flooding (*PCI Journal* 2005; Robertson et al. 2007; Padgett et al. 2008; Lee et al. 2012; Stearns and Padgett 2012), geo-hazards such as mudslides, slope stability, rock fall and underground void (Liao et al. 2010; Mansour et al. 2011), and tornado and high-wind events (Burgess et al. 2014; Graettinger et al. 2014). A special editorial report published in *PCI Journal* in 2005 has discussed the damage sustained by precast/pre-stressed concrete bridges and other structures in the path of the Hurricane Katrina in the Gulf Coast region (*PCI Journal* 2005). These structures, in particular the 5.4 miles (8.7 km) twin I-10 Bridge, suffered severe damage from flooding and extremely high speed winds.

The economic impact of damage to bridges during future extreme natural hazards can be mitigated by addressing observed vulnerabilities during the past natural events. In order to do this, it is important to develop an engineering assessment plan during and after extreme hazard events so that important perishable data (i.e., data that cannot be replicated once the event has subsided) could be collected and lessons learned could be implemented in the current and future bridge design and maintenance practices. The extent of damage to bridge infrastructures during extreme natural hazards, such as scour, earthquakes, mud slides, tsunamis, hurricanes, etc., is likely to be widespread. In such situations, current NBI “damage” inspection and evaluation technologies, which mostly rely on visual and nondestructive inspection by direct access to the damaged structure, may not be efficient for collecting important data on impacts of these hazards on bridges.

Remote sensing, in general terms, is the practice of collecting and measuring spatial information about an object, region, or a natural event, such as earthquake, hurricane, wildfire, etc. using images acquired at a distance from the data source (Campbell and Wynne 2011; Falkner 1995; Aronoff 2005). However, from a damage assessment perspective, remote sensing may be regarded as a form of nondestructive testing (NDT) or structural health monitoring (SHM) method, where the sensors are not in physical contact with the structure and the use of remote sensors eliminates the need for direct access to bridges for post-hazard assessment. Hence, remote sensing technologies—consisting of non-contact sensing tools such as optical/radar satellites and aerial (fixed wing aircraft) imageries, vision-based sensors (thermal and high-resolution cameras) and unmanned aerial systems (UAS)—have tremendous capabilities and

potential for assessing large number of bridges rapidly after an extreme event without interfering with rescue and emergency response operations. Engineering assessments by these technologies could also aid in the emergency response and management. For example, remote sensing through satellites and aerial imagery after an earthquake has become an invaluable tool for disaster response and damage assessment (Tralli et al. 2005; Stramondo et al. 2006; Pittore and Wieland 2013; Liu et al. 2018). Use of UAS during recent hurricanes has demonstrated their significance in post-disaster response and assessment of structures (Steimle et al. 2009; Stow et al. 2018; Jordan et al. 2018). As such, these remote sensing technologies are becoming complementary to local and regional airborne methods, and to traditional in situ field measurements and ground-based sensor networks (Tralli et al. 2005).

The use of remote sensing technologies for post-hazard damage assessment of highway structures has been a subject of great attention in the United States over the past decade. In a recent work, Alipour (2016) carried out a study on review of technologies that transportation agencies employ nationwide to assess damage to bridges in the aftermath of extreme events and the procedures that they use to undertake emergency response activities. The author carried out a nationwide survey to identify the types of hazards, the type of damage detection for post-hazard damage assessment of bridges, and the readiness of State transportation agencies with emergency response plans. It was concluded that hydraulic hazards such as scour, flood and debris flows are common causes of bridge failures across the nation. The survey also revealed that visual inspection (either cursory or hands-on) and NDT techniques are the most frequently used methods for assessing damage to bridges. Both these inspections methods require direct access to the bridge. It has also been reported that sonar survey is one of the most commonly used inspection methods by hydraulic engineers in many States. This study also shows that 86 percent of the States have an emergency response plan for extreme events, although not all of the plans are specifically focused on assessment of bridge damage. The survey also noted that most States do not take advantage of emerging technologies such as Light Detection and Ranging (LiDAR), Interferometric Synthetic-Aperture Radar (InSAR), and aerial imagery using UAS for post-hazard damage assessment of bridges. However, these technologies can be efficiently utilized for collecting data from damaged infrastructures in a wide area immediately after the occurrence of an extreme hazard when time is crucial and direct access to the affected area can be dangerous and may not be possible.

Remote sensing technologies can play a key role in assessment of the integrity of highway structures after an extreme hazard and can also be an important component of an emergency response plan. Olson et al. (2016a, 2016b, and 2016c) have developed a uniform methodology for rapidly assessing, coding, and marking highway structures in the aftermath of an extreme natural hazard. This work provides a general guidance on structural assessment of different types of highway structures, including bridges, tunnels, culverts, walls, and overhead signs impacted by natural hazards, such as earthquake, tornado, hurricane, scour, and fire. This assessment process consists of four stages: Fast Reconnaissance, Preliminary Damage Assessment, Detailed Damage Assessment, and Extended Investigation. The authors proposed a coding and marking procedure to physically and digitally mark an affected structure to facilitate communication between responders from different agencies. The digital coding and marking can be carried out by an app designed for smart devices such as smartphones and tablets. These marks and associated information help the responders know whether the structure has been inspected and is safe. Although the guidelines have been proposed for damage assessment of a highway structure

using traditional inspection practices, they can also be effectively used for remote sensing inspection using unmanned aerial and water vehicles.

STATE OF THE ART OF REMOTE SENSING TECHNOLOGIES

This section presents a detailed review of state of the art of different types of remote sensing platforms and sensors that can be used for post-hazard engineering assessment of bridges. Depending on the level of their operations with respect to the location of the structure of interest on the Earth, these remote sensing technologies can be categorized into four different groups:

1. **Space-borne (10-1000 km (60-620 mi)):** Satellite-based technologies.
2. **Airborne (0-10 km (0 -6 mi)):** Manned or unmanned aircrafts-based technologies.
 - **High altitude systems: Manned aircrafts and large UAS**
 - **Low altitude systems: Small UAS (max 120 m)**
3. **Ground-based:** Vehicle-based, stand-off, and monitoring technologies.
4. **Water-based:** Unmanned water system (UWS).

Figure 1 illustrates the schematic view of these technologies and their operation levels with respect to the structure of interest on the earth. It should be noted that the maximum allowable altitude for a UAS is 400 ft (120 m) above ground level (AGL) (FAA 2016).

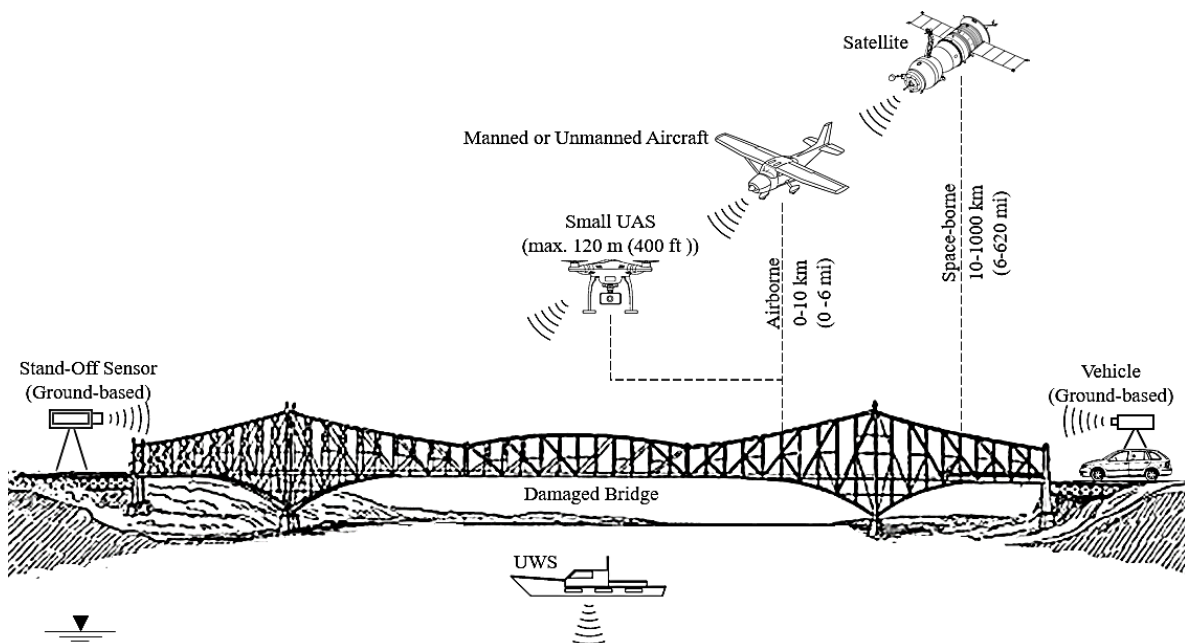


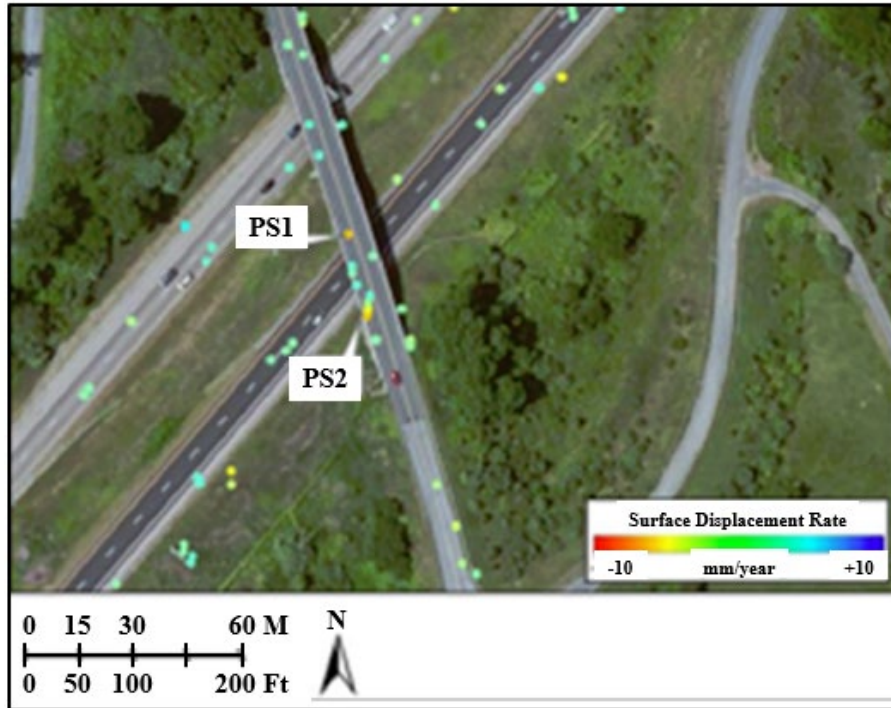
Figure 1. Illustration. Potential remote sensing technologies for post-hazard damage assessment of highway structures.

Space-borne Technologies

Satellite-based technologies represent one of key examples of space-borne technologies for remote sensing of bridges and other highway structures. Earth observation satellites are useful remote sensing technologies for rapidly acquiring information from regions impacted by natural hazards (Ostir et al. 2003; Niu et al. 2018). Because of rapid developments in this technology and its impacts on all human activities, online tools such as Earthnow (<https://earthnow.usgs.gov/observer/> & <https://earthnow.com/>) provide real-time video observations of the Earth. These tools can be used to assess broad-area damage in a particular region from high resolution images and videos immediately after an event.

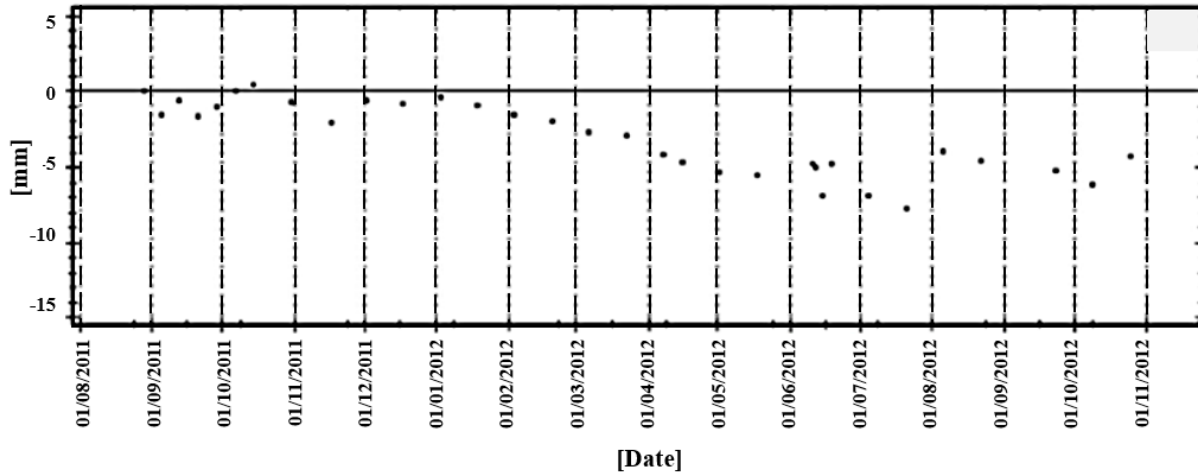
Satellites used for damage assessment are usually equipped with InSAR technology (Sousa et al. 2014). InSAR can collect data from an object on the ground, based on the acquisition of two Synthetic Aperture Radar (SAR) images taken from two points that are different both in time and space. Differences between the phases and amplitudes of these images are the key to the extraction of useful data from the images. The SAR sensor is often installed on space-borne (satellite) or airborne platforms positioned at high stand-off distances with respect to the bridge so that the data can be collected without any interference to the traffic. InSAR is very effective in the evaluation of global metrics of bridges, such as bridge settlement or bridge movement in its own plane (Acton 2013; Milillo et al. 2018). InSAR can monitor multiple bridges within a single radar image, detect and quantify vertical movement in millimeters, evaluate deck deflation and settlement of bridge supports. This sensor can effectively monitor the displacement of bridges at regular intervals while minimizing traffic disruption (Cusson et al. 2012; Sousa et al. 2014). However, at least 20 radar scenes are required and accuracy depends on the number of scenes and orientation of the structure (Sousa et al. 2014). InSAR has also been used to detect sink holes, unstable slopes, and to conduct infrastructure assessments (Hoppe et al. 2016).

Satellite imagery is also useful for modeling changing bridge characteristics. The same techniques of photogrammetry can be used to create elevation models of the bridge and surrounding areas. One drawback of the satellite imagery is the decreased resolution compared to both manned and unmanned aerial collection methods. However, one of the most significant benefits is that the satellite imagery does not require mobilization to travel to the impacted site. This also means that there is a possibility of data being collected while the extreme hazard is occurring, even if the region is inaccessible. Wolf et al. (2016) have used satellite remote sensing technology to monitor the surface displacement of geotechnical assets such as retaining walls, unstable slopes, rock-fall sites, cut slopes, embankments, and tunnels. They have proposed to use satellite InSAR technology to assess these geotechnical asset conditions and monitor their long-term performance. This technique has been found to be much more cost-effective and efficient than current geotechnical asset management procedures requiring frequent site visits (Bouali et al. 2016; Wolf et al. 2016). Three common remote sensing techniques, including optical imagery acquired via satellite, unmanned aerial system, and LiDAR data acquired from a stationary sensor, have been used by Bouali et al. (2016) to evaluate 14 slopes within a 24-km railroad corridor in southeastern Nevada for rock-fall hazard. This work found that the terrestrial LiDAR is preferable among the three technologies for monitoring slow slope deformation (accuracy=0.8 in/yr) and for identifying the areas of rapid deformation.



Source: USDOT

A. The simple span bridge located at Route 635 over Interstate 81.



Source: USDOT

B. Time history of the settlement at point PS1 (see figure 2-A for location of point PS1).

Figure 2. Illustration. InSAR results obtained from a simple span bridge showing progressive settlement over the considered period.

Acton (2013) led a research project on the application of remote sensing technologies for transportation infrastructures with focus on the detection of sinkhole and the monitoring of landslides around highway infrastructure. The research used InSAR on spaceborne satellite platforms, and LiDAR and photogrammetry using ground-based platforms to investigate geo-hazards such as sinkhole, landslide, rockslides and bridge settlements. The main objective of the work was to demonstrate the capability of InSAR data to detect and monitor geo-hazards and

movement of highway infrastructures. The other objective of the project was to develop image analysis algorithms to identify geo-hazards relevant to transportation infrastructures and validation of these algorithms using InSAR data as input to detect locations of geo-hazards. The geo-hazards considered in this study included subsidence due to sinkhole formation, movements due to landslides and rockslides, and bridge settlements. The area of interest (AOI) for the investigation consisted of a 40 km by 40 km region near Middlebrook, Virginia. Furthermore, in order to validate the image analysis algorithms, additional data collected from Vancouver, Canada and Wink, Texas were also used. The InSAR data collected by Acton (2013) included 32 images acquired between 29th August 2011 and 25th October 2012, representing 14 months of monitoring over the area of interest shown in figure 2. The resolution of the displacement data was estimated to be less than 0.4 in (1 cm).

Acton (2013) analyzed image data using graph-theoretic and parametric approaches. In the graph-theoretic approach, an optimization process is conducted to identify regions of subsidence. However, a major limitation of this approach is the lack of capability to exploit the evolution of features (such as settlement) over time, which is the main advantage of InSAR data acquisition. The parametric approach, which utilizes both spatial data and temporal dimension, can discover trends in space and time that are consistent with certain geophysical or structural phenomena. A field validation study was conducted to confirm the InSAR-driven results using ground-based remote sensing technologies, including LiDAR, digital photogrammetry and traditional surveying methods. The study showed that the analysis of InSAR using image analysis algorithms had strong field evidence of subsidence in 78 percent of the cases.

Zebker et al. (2017) developed a prototype comprehensive space-borne InSAR displacement monitoring system to measure mm-level surface displacement in transportation infrastructures. As an example, they used the monitoring system to analyze possibility of subsidence in rural roads in the Bushkill Creek and Lewiston Narrows in Pennsylvania.

Airborne-Based Technologies

Light general aviation manned aircrafts are the most common types of airborne platforms used for aerial survey and damage inspection of highway structures. It is relatively easy to maintain sensors installed on such platforms compared to space-borne platforms. However, their swaths are smaller and they need more time to cover a large area. These aircrafts are usually equipped with optical LiDAR sensors also (Toth and Jozkow 2016). LiDAR is an efficient remote sensing technique to measure displacements of objects (e.g., lateral displacement of the deck in a highway bridge after an extreme natural hazard) on the Earth by identifying the travel time and speed of the laser pulse between the sensor and the object.

One benefit of manned aircraft is the ability to survey several study sites in a relatively short duration of time. The higher altitude of this collection method means that it is possible to increase the size of the study site to cover a larger area. In addition, this collection method is particularly useful when the collection site is difficult to access or is at a significant distance. Imagery taken through the use of manned aircraft can be used to create 3D models of the bridge using photogrammetry. An ideal sensor for this collection method would be a photogrammetry-focused camera. Such a camera provides high resolution imagery and geotags each photo to aid in 3D reconstruction. It is also possible to collect other types of imagery such as thermal data.

Once collected, the imagery can be converted into geo-referenced ortho-mosaics and digital elevation models. Bian et al. (2011) have used terrestrial LiDAR and aerial photography (commercial DSLR camera at the altitude 1000 ft (305 m)) for the evaluation of deck joints in bridges. Chen et al. (2011) have used aerial photography to inspect bridges. The authors set up a high-resolution camera on a Cessna C210L plane flying at 1000 ft (305 m) to take pictures of large cracks and joint opening on bridge decks and highway pavements. It was found that this technique is capable of detecting large defects on bridge decks, which can help in identifying the movement patterns of the bridge after an extreme natural hazard. Hauser and Chen (2009) also used high-resolution (sub-inch) aerial photography and automated imaging to map the wear surface conditions. They have shown that this technique is capable of detecting the cracks on a bridge surface from aerial photos. They found that the method is useful in monitoring movements of a bridge at the expansion joint.

Ground-Based Technologies

Unmanned Aerial-Based Technologies

UAS operators in both the public and private sectors must adhere to statutory and regulatory requirements. Public aircraft operations (including UAS operations) are governed under the statutory requirements for public aircraft established in 49 USC § 40102 and § 40125. Additionally, both public and civil UAS operators may operate under the regulations promulgated by the Federal Aviation Administration. The provisions of 14 CFR part 107 apply to most operations of UAS weighing less than 55 lbs. Operators of UAS weighing greater than 55 lbs may request exemptions to the airworthiness requirements of 14 CFR part 91 pursuant to 49 USC §44807. UAS operators should also be aware of the requirements of the airspace in which they wish to fly. The FAA provides extensive resources and information to help guide UAS operators in determining which laws, rules, and regulations apply to a particular UAS operation. For more information, please see <https://www.faa.gov/uas/>.

The term UAV refers to the aircraft itself; UAS refers to the UAV and all the equipment used to control the aircraft, such as ground-based controllers and communication systems.

UAS have played a significant role in hurricane relief efforts in the aftermath of recent Hurricanes Harvey, Irma, and Maria in the fall of 2017. To expedite the recovery process in the wake of these strong tropical storms, the Federal Aviation Administration (FAA) allowed commercial UAS operators to carry out preliminary damage assessment of private and public properties for insurance companies through special waivers under Part 107 (Rockwell 2017; Craft 2017). Several telecom companies also effectively used UAS to inspect damage to cell towers in the affected areas (Sydell 2017). However, there was very limited use of UAS in assessing damage to bridges.

However, UAVs are drones flying in the air only. Research on the use of UAS following a natural disaster was carried out by American Red Cross following the 2010 Haiti earthquake for collecting data from the damaged area (American Red Cross 2015). The American Red Cross team also conducted structural assessment flights at the Disaster City at the Texas A&M University in coordination with the Center for Robot-Assisted Search and Rescue (CRASAR), as shown in figure 3. Disaster City is a 52-acre training facility administered by the Texas A&M

Engineering Extension Service that is used to simulate different types of disaster scenarios with varying degrees of destruction (American Red Cross 2015).



© 2018 Measure UAS, Inc.

Figure 3. Photo. A rotary-wing unmanned aerial vehicle (UAV) over Disaster City, Texas.

The American Red Cross team identified three groups of UAS with the capabilities that are applicable for structural integrity assessment (see figure 4):

- **Group 1:** Hand-launched, lightweight, low payload UAVs (see figure 4-A) that are useful for local and interior airborne surveillance/monitoring of damage. The UAVs in this group weigh under 21 lbs and can operate at attitudes under 1,000 ft (305 m). They are often powered by batteries.
- **Group 2:** Long endurance reconnaissance and surveillance UAVs (see figure 4-B) that are useful for wide-area airborne surveillance/monitoring of damage. The UAS in this group weigh between 21 and 50 lbs (9.5 and 22.6 kg) and operate at attitudes up to 3,500 ft (1,067 m). Their payload capacity are limited, but they can still carry electro-optic camera and communication systems.
- **Group 3:** Long endurance, large payload UAVs (see figure 4-C) that are useful for wide-area airborne surveillance/monitoring of damage. These UAS have large engines and can carry significantly more payload than those in Group 2. They weigh up to 1,320 lbs (600 kg) and have operational attitudes up to 18,000 ft (5,486 m) mean sea level.

For applications to bridge scour monitoring, UAS can be used to collect aerial imagery of the bridge and the river bank. While the imagery collected is typically limited to above water features, high-resolution imagery collected can be used to create 3D reconstruction of a bridge and its surroundings by using appropriate onboard sensor. If scour is impacting the bridge to

cause any kind of movement, UAS can be used to measure these movements for use in analytical models to determine safety and vulnerability of the bridge (see Chapter 3).



© 2018 Lockheed Martin
A. Example of Group 1



© 2018 Silent Falcon
B. Example of Group 2



© 2018 Textron Systems
C. Example of Group 3

Figure 4. Photo. Examples of UAV with different capabilities useful for post-hazard damage assessment of structures.

There are a number of UAS platforms that can be used for the post-hazard assessment of bridges, including bridge scour monitoring. Depending on the payload and battery capacity, flight time could last between 20-30 minutes, including the time for launching and landing operations. The UAVs can carry payloads in the range of 3.5 lb (1.6 kg) to 22 lb (10 kg), and can fly up to 3.1 mil (5 km) from the base (FAA, 2016). These platforms can be equipped with high-resolution cameras to collect high-resolution optical imagery for 3D model, including ortho-photos and base map creation, infrared camera to collect thermal infrared imagery and near-infrared LiDAR for creating 3D models of roadways and bridges. Resolution of 3D model using UAS could be better than 0.5 in (1.3 cm), depending on the resolution of the camera. An on-board Global

Positioning System (GPS) with Inertial Measurement Unit (IMU) allows for flying programmed way points assigned through Ground Station software using a Google Earth interface. A stabilized gimbal can keep the camera pointed downward. A First Person Viewer (FPV) feature of these platforms allows the pilot to see the field of view of the camera and provides a readout of the altitude, speed and battery voltage. Some UAS platforms have built-in collision avoidance to avoid any forward movements toward the obstacle.

Various studies have incorporated LiDAR to construct the river bathymetry above the normal water surface for use in conjunction with sonar data (Sotiropoulos and Khosronejad 2016) as well as to map the bathymetry (at 0.5 in resolution) in semi-transparent water (Irish et al. 2016). The Scanning Hydrographic Operational Airborne LiDAR System (SHOALS) uses airborne LiDAR to take bathymetry measurements of up to 131 ft (40 m) along a coastal environment with a vertical accuracy of +/- 0.50 ft (0.15 m) (Irish et al. 2016). Data collected by the system was used to assess the underwater performance of sand being used as beach fills as well to assess damage due to storms or ship groundings. Repeated measurement along an inlet provided information required to develop a sediment budget. Bathymetric LiDAR technology has recently advanced to the stage where it can be deployed on small hexacopter and octocopter UAS systems with at least 11 lb (5 kg) lift capability. This increases the possibility of deploying bathymetric LiDAR instead of manned aircraft used currently. Where water conditions allow for light penetration (i.e, relatively clear waters), bathymetric LiDAR can be a useful solution for creating bathymetric data needed for hydraulic modeling.

Otero et al. (2016) have investigated the applicability of optical and LiDAR sensors to detect cracks in concrete and to measure displacement of bridge components. These sensors can also be used for the post-hazard damage assessment of bridges. Objectives of their research were (i) developing and evaluating prototype image processing algorithms for concrete crack detection and classification, (ii) developing and evaluating three-dimensional (3D) models based on LiDAR data to identify signs of displacements of bridge components, and (iii) evaluating the effectiveness of the image processing algorithms and 3D models with data collected using an UAS. They developed image processing algorithms for post-hazard detection and classification of large cracks in reinforced concrete (RC) members of bridges. To detect such cracks, Otero et al. (2016) have developed a five-step algorithm based on an unsupervised learning approach in MATLAB to extract pixels that belong to concrete cracks from images. To classify the cracks, the resulting binary images from the detection algorithm were processed to identify cracks as transversal, longitudinal, block, or alligator. They also verified the accuracy of these algorithms using images collected by UAS.

In 2006, the U.S. Department of Transportation (USDOT) initiated a research program to conduct an extensive research on Commercial Remote Sensing & Spatial Information (CRS&SI) technologies for developing smarter and more efficient methods, processes and services for transportation infrastructure development, construction and condition assessment. The main focus of this multi-phase program was on the application of Commercial Remote Sensing (CRS) products, including remote sensing technologies and data from non-contact and above-ground platforms, such as satellites, manned aircrafts and UAS. Outcomes of a few studies through this program are discussed in the following for post-hazard assessment of bridges.

O’Neil-Dunne (2015) conducted research on using commercial remotely sensed imagery by a UAS for disaster response and recovery during geo- and hydro-hazards, such as landslide and flooding. This research focused on making an automated approach to damage assessment of transportation infrastructure by identifying or characterizing damage from high-resolution aerial imagery acquired by modern CRS technologies in the aftermath of devastating natural hazards, such as Hurricane Irene in 2011. Objectives of this research were (i) to develop, calibrate and implement a decision support system for identifying road and bridge damage from high resolution commercial aerial images and (ii) to estimate the amount and type of fill material required for repairs using digital surface models derived from lightweight UAS programmed to fly over the impacted area. A rule-based expert system was also developed using the eCognition software platform to automate the detection of damage to roads because of flooding and debris. The system was tested and validated across numerous satellite images for three areas affected by natural disasters in Vermont, Colorado, and New York. Two applications were considered for this validation: (i) river and stream flooding such as flooding events in Vermont during August 2011 and in Colorado during September 2013 that washed out or covered roads, disrupting partially or fully a transportation network, and (ii) coastal flooding that deposited sand and other debris on roads, but then receded as observed during Hurricane Sandy in New York City in October 2012.



Source: USDOT

Figure 5. Photo. A fixed wing UAV used to collect CRS data.

UAS were used by O’Neil-Dunne (2015) to gather CRS imagery because of their highly rapid and accurate actions, and low cost flights compared to traditional satellite and aerial systems, which are either cost prohibitive, ineffective, or unresponsive during a crisis, particularly when weather and atmospheric conditions are unfavorable. As shown in figure 5, O’Neil-Dunne (2015) selected the fixed wing UAS because of its simplicity, safety features, and robust flight management and planning software. The UAS was equipped with a 16 megapixel camera with a resolutions as fine as 0.8 in/pixel (2 cm/pixel) to acquire images from a stockpile considered as a fill caused by a geo-hazard. The data collected was processed to estimate the volume of the fill. The accuracy of this estimation was checked by comparing with data from a ground-based LiDAR technology.

Brooks et al. (2015) have evaluated the effectiveness of data collected by UAS for bridge damage inspection and road/traffic monitoring. They used several UAS of different sizes (i.e.,

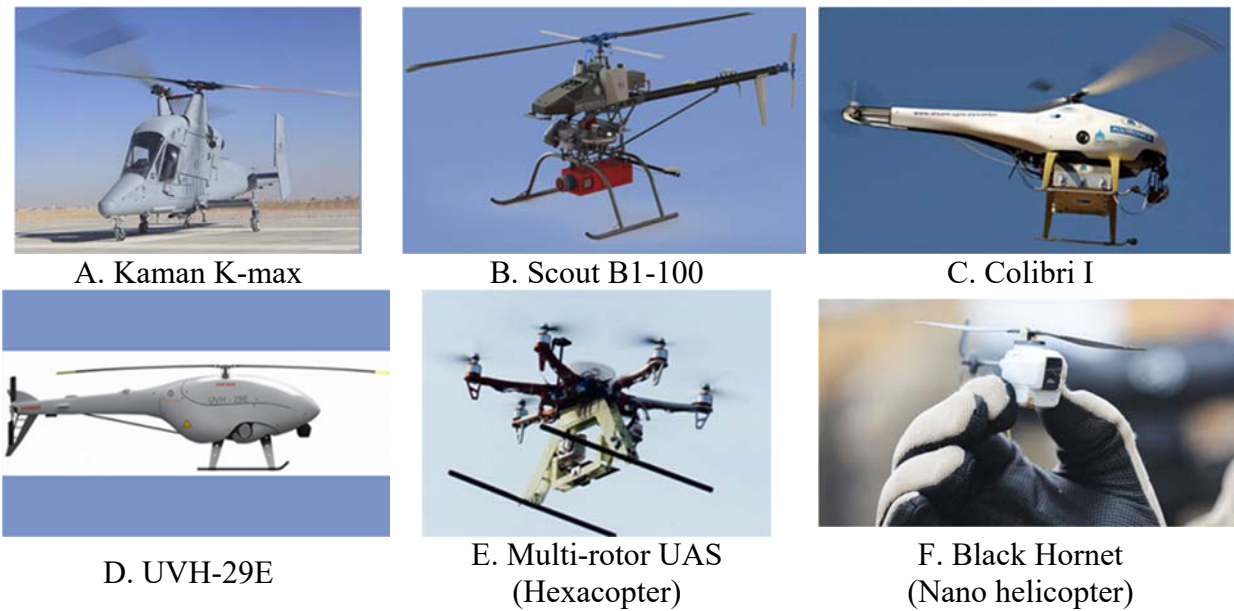
micro-UAS to mid-sized ones), type (i.e., quadcopter, hexa-copter, and aerostat/blimp), and flight times in this study. The results showed that the UAS technology is significantly capable of improving the assessment of bridge health, confined space conditions, roadway asset types, and monitoring of traffic.

Stow et al. (2015) have provided a detailed approach on end-to-end design of time-sensitive remote sensing systems (TSRSS) that can be used to collect timely information on magnitude and extent of damage in the aftermath of natural hazards to support emergency management decision-making. The study focused exclusively on airborne platforms such as UAS due to their greater flexibility and lower altitude of operation. They have discussed the process and the steps of data collection from airborne remote sensing technologies from image analysis to implementation, and have noted that the main limitations to the implementation of remote sensing technologies into practice are institutional in nature (e.g., funding, technology coordination and acceptance, and government regulations).

Baiocchi et al. (2013) have studied the application of UAS for post-earthquake damage assessment of buildings. This study is also of significance for assessment of bridge components such as piers (columns), girders and decks, which are also key components of buildings damaged during earthquakes. Their work shows that micro UAS can easily meet the need for the survey of both the roofs and the facades of tall buildings or dangerous places (one such application could be a collapsed bridge site) where the conventional surveying techniques using high precision total stations, Global Navigation Satellite System (GNSS) receivers and laser scanners alone may not be effective. They developed a flight planning software to optimize the data collection from damaged buildings using commercial multi-rotor micro UAS. In another paper, Baiocchi et al. (2014) have presented a more comprehensive study on their developed software and its application in data acquisitions using UAS.

Ruggles et al. (2016) have conducted a study on the evaluation of the resolution and accuracy of images acquired by small UAS platform and camera configurations to establish 3D point cloud models of a large landslide that occurred in 2013 near Page, Arizona. It was found that multi-rotor UAS were able to improve the resolution by more than 16 percent compared to fixed-wing UAS. However, the accuracy of the points in the point cloud model depends on the selected camera and the image resolution. It is quite independent of the UAS platform. These findings are relevant to bridge applications as 3D point cloud models are required to reconstruct the bridge site.

Nedjati et al. (2016) have proposed a remote sensing system that can be used by earthquake response managers in the early hours following an earthquake in dense urban areas. The system uses recent developments in the area of earthquake detection, data fusion, and medium-scale UAS helicopters. Figure 6 shows several examples of UAS helicopters that may be used for post-hazard response management and damage assessment. A system with abilities similar to that in Nedjati et al. (2016) and data fusion would provide a more accurate overview of a bridge system.



© 2016 *Natural Hazards Journal*

Figure 6. Photo. Examples of UAS helicopter models.



Source: USDOT

Figure 7. Photo. A quadcopter UAS used for inspection of a steel bridge.

Zink and Lovelace (2015) have evaluated the safety and effectiveness of UAS technology for the inspection of bridges owned by the Minnesota Department of Transportation. The authors inspected four different types of bridges using different types of sensors (imaging devices) such as still image, video and infrared cameras installed on a quadcopter UAS. Figure 7 shows this UAS next to a steel bridge. The authors concluded that it is safe to use UAS for bridge inspection because this technology generally has a very low risk for inspection personnel and public. They also concluded that UAS are more effective when they are used for inspecting large-sized bridges. More specifically, they found that UAS are very useful for determining stream or river bank conditions upstream or downstream of a bridge crossing a river as well as for capturing large overall aerial maps of dynamic bank erosion and lateral scour conditions. The authors also found that the UAS that have the ability to direct cameras upward and the ability to fly without a

GPS can be very effective for damage assessment of bridges, particularly after a major extreme natural hazard.

Karpowicz et al. (2014) have conducted a review study on the application of UAS in supporting geotechnical field investigations involving landslides, rock-fall and other steep terrain. The study presented a review on using UAS technologies by DOTs in States such as Arkansas, Georgia, Michigan, North Carolina, Ohio, Utah, Washington, and West Virginia. This study showed that little research has been performed by DOTs on the use of UAS for landslide or other steep terrain investigations.

Darrow et al. (2016) used UAS-acquired photography and other types of remote sensing technologies, including Differential GPS Device, Optical Imagery, LiDAR, and InSAR, to monitor and analyze several frozen debris lobes in Brooks Range of Alaska. Frozen debris lobes are formed on the mountain slopes made up of soil, rocks, trees, and ice in areas with cold weather, such as northern region of Alaska in the United States (Darrow et al. 2016). They are slow moving landslides and are considered as a type of geo-hazard for highway infrastructures in such regions.

Stand-off Remote Sensing Technologies

In stand-off remote sensing, high-precision sensors are installed on a fixed support or a temporary support, such as a tripod, and placed at certain distance from a bridge or other highway structures to acquire data remotely. Examples of stand-off sensors include high-resolution digital cameras (Ja'uregui et al. 2003; Jiang et al. 2008; Ahlborn et al. 2013), laser vibrometers (Mallet et al. 2004; OBrien and Malekjafarian 2016), and IBIS-FS (Image by Interferometric Survey for Structures) interferometric radar system (Sofi et al. 2017). In general, a high accuracy assessment of damage in bridge components, especially in deck and girder surfaces, requires lower stand-off distance of the sensors from the bridge (Vaghefi et al. 2012).

Although the remote sensing technology is primarily based on analysis of image data acquired through satellites or airborne platforms, vibration assessment of bridges during dynamic events can also be carried out remotely using technologies such as GPS (Nakamura 2000; Kaloop and Li 2009). For example, Nakamura (2000) have investigated the application of GPS to measure suspension bridge girder displacements induced by wind forces. An existing suspension bridge was selected to conduct field measurements during the strong wind season. The results obtained from the numerical model and the test model in a wind tunnel agreed well with the semi-static displacements of the girders. It was concluded that GPS method is reliable and useful for measuring the response of long-span bridges during strong winds. Wipf et al. (2011) have also used high-resolution GPS units to determine the best optimization methods to measure movement of a highway bridge and to compare the precision and accuracy of monitoring results. Data was collected once a month for eight months and compared to total station data. Results indicated that the GPS system was more precise than the total station, and that the change in length between abutments was 0.014 in per degree Fahrenheit for the GPS systems and 0.018 in per degree Fahrenheit for the total station

Measurement of dynamic vibration of bridges is of significant importance in identifying current condition of critical bridge members. During an extreme hazard situation, such as hurricane,

dynamic deflection of a bridge can be measured quite accurately by tools such as Laser Doppler Vibrometer (LDV) without directly accessing the bridge element to be monitored (Tabatabai et al. 1998, Nassif et al. 2005). A LDV system is a non-contact portable instrument that measures surface vibration through the principle of interferometry (Doppler Effect) and can provide both velocity and displacement measurement with time (Chen 2018). Nassif et al. (2005) have shown that LDV measurement of deflection in girders of a bridge is comparable to that carried out by contact sensors such as geophone sensor. Helmerich et al. (2012) also used LDV to measure deformation of masonry arch bridges under test loads. The vibrations from points and regions of crucial structural importance to a bridge can be systematically collected remotely by using three types of laser vibrometers: (i) Point LDV (PLDV), (ii) Scanning LDV (SLDV) and (iii) Remote Sensing Vibrometer (RSV). In this set up, PLDV is used to calibrate the SLDV to provide a vibration signature for a spatial region; while RSV is employed to generate the vibration curve for one focal point for a long-time duration. The space and time-evolved vibration map collected using these three laser vibrometers yields a valuable temporal and spectral signature of the structure of a bridge due to the extremely high resolutions in the space and frequency domains. All these high-resolution vibration measurements can be done as automatically programmed from as far as up to 1,000 ft (305 m) using the most advanced models of laser vibrometers. When used during strong winds and hurricanes, space and time-evolved vibration maps of long-span bridges, such as suspension bridges, will serve as extremely valuable datasets (that are not currently available) to verify current design guidelines and potential modes of failure of these bridges.

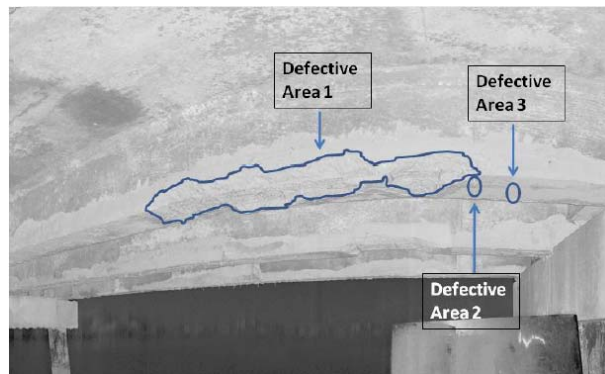
IBIS-FS is a microwave interferometry-based system for monitoring response of bridges or other structures under static and dynamic conditions. This technique is able to remotely measure the response of the bridge in real-time from up to 0.6 mi (1 km) in all weather conditions, while keeping the accuracy in the range of 0.4 mil (0.01 mm) (Xing et al. 2014). Zhnag et al. (2016) used IBIS to monitor dynamic behavior of concrete bridges. In a recent work, Sofi et al. (2017) employed an IBIS-FS sensor to detect changes in the natural frequencies of a pedestrian bridge, considering the change in the stiffness of the bridge because of structural deterioration over a specific time. They compared the fundamental frequency of the bridge obtained by IBIS-FS to that obtained from conventional acceleration measurement technique and concluded that there is a high level of consistency between these two types of measurements.

Images captured by high-resolution stand-off digital cameras can be analyzed by approaches such as 3D Optics to measure depth and height information. Optical interferometry can also be used to detect cracks, spalls, and scaling on the concrete deck from the analysis of digital images (Hatta et al. 2005). In another method, called Spectral Analysis, measurement of spectral reflectance or absorption of light (both visible and IR) from a target surface is carried out by a camera with a range of color bands, termed as multispectral or hyperspectral EO imaging (Vaghefi et al. 2012). The process can be performed with a backpack unit and hand-held spectro-radiometer. However, a vehicle-mounted device is also conceivable (Ahlborn et al. 2010).

Digital Image Correlation (DIC) is used to correlate two electro optical images separated in space or time. This technique is performed by automated computer algorithms, which are able to measure changes between the two images to determine the displacement of features in the image plane (Hutt and Cawley 2008). This method is useful for measuring global metrics of a

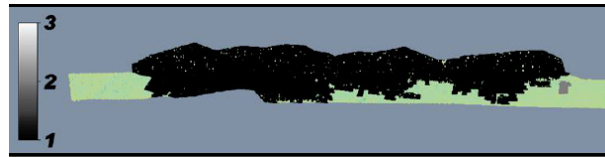
bridge, such as bridge settlement, transverse bridge movement, vibration of the bridge or one of its structural elements, and change in the length of the bridge (Vaghefi et al. 2012).

Hauser and Chen (2009) and Chen et al. (2016) have found the ground-based LiDAR sensor quite useful in the identification of surface damage on bridges components, and load testing of bridges. For example, they have shown that the mass loss due to instability on a bridge pile cap/floor beam can be easily identified by LiDAR scan and a damage detection algorithm. The data acquired by LiDAR sensor can be used to compute the volume and area loss under each girder, as shown in figure 8. As another example, the LiDAR sensor was utilized to monitor the load test of a three-span newly constructed bridge. The static loading was applied by two heavy 50-ton trucks at fixed locations of the bridge. The deflection of the entire span was determined with an accuracy of 3 mm before and during truck loading (Hauser and Chen 2009).



Source: USDOT

A. Defective Areas



Source: USDOT

B. Image Processing Results

Figure 8. Illustration. Detection of defective area of a girder using a ground-based LiDAR sensor.

Hauser and Chen (2009) have developed a remote sensing and visualization system for transportation infrastructure operations and management. They carried out a proof-of-concept study on the applications of remote sensing technologies, such as ground-based LiDAR scan and Small Format Aerial Photography (SFAP), for the inspection of highway bridges and development of an Integrated Remote Sensing and Visualization (IRSV) bridge data diagnostic system. The IRSV system, which is essentially a Bridge Data Management System (BDMS) with a large visualization format, integrates aerial photographic imaging, LiDAR bridge scan and damage evaluation, large data and spatial display system, and an ontology-based knowledge evaluation system. The two remote sensing technologies used are the most viable CRS tools for bridge system management. LiDAR can produce high resolution 3D optical images that are very effective in the evaluation of condition of a bridge, such as large permanent deformations, overload cracking and different kinds of surface erosions.

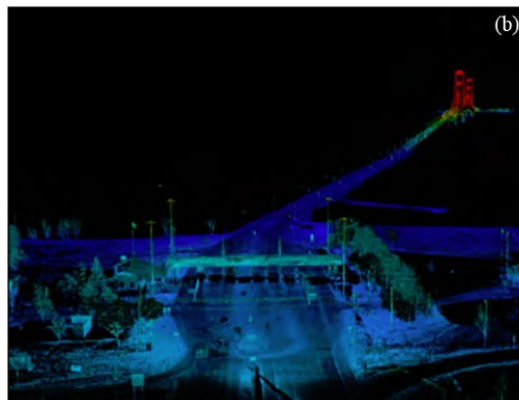
Vehicle-Based Technologies

Some remote sensing sensors, such as LiDAR and LDV, can be mounted on a vehicle-based platform. For example, figure 9-A shows a LiDAR mounted on top of a vehicle. It is observed from figure 9-B that LiDAR technology in combination with high-resolution digital photography in a StreetView-style system can be very effective for reviewing and understanding the condition of a bridge. It also can be helpful in creating 3D models of a bridge and its ambient condition (Chen 2010; Vaghefi et al. 2012; Gong 2016).



Source: USDOT

A. Mobile LiDAR Truck



Source: USDOT

B. LiDAR scan of the Mackinac Bridge

Figure 9. Illustration. Mobile LiDAR used for scanning the Mackinac Bridge and toll plaza.

Radar is another sensor that has the capability to be mounted on a vehicle for bridge damage assessment (Morey 1998). It measures the distance to an object based on transmission of a radio signal to the object and detection of the reflected signal. The distance is calculated by measuring the travel time and the velocity of the wave propagation. The SAR sensor is an example of radar to detect subsurface features of bridges. This sensor can be effectively mounted on a ground-based platform such as a vehicle. The advantage of this technique is its capability to increase cross-range resolution and operating frequency that allows subsurface imaging with higher qualities and finer details (Ahlborn et al. 2013).

Water-Based Technologies

Platform

Unmanned water systems (UWS)—also known as unmanned surface vehicles (USV), unmanned marine vehicles (UMV), and autonomous surface vehicles (ASV)—have been used since 2004 for disaster recovery operations, but in limited applications, in single areas, and in short deployment durations. Murphy et al. (2011a) have used three underwater remotely operated vehicles (ROVs) to inspect critical infrastructure and to assist with victim search and recovery at six sites in the Iwate Prefecture following the Tohoku Earthquake and Tsunami. They customized Advanced Electro-Optical System (AEOS) man-portable unmanned surface vehicle and two commercially available underwater vehicles for inspection of the Rollover Pass bridge in the Bolivar peninsula of Texas in the aftermath of Hurricane Ike. A preliminary domain analysis with the vehicles identified key tasks in subsurface bridge inspection (mapping of the debris field and inspecting the bridge footings for scour), control challenges (navigation under loss of GPS, underwater obstacle avoidance, and stable positioning in high currents without GPS), possible improvements to human-robot interaction (having additional display units so that mission specialists can view and operate on imagery independently of the operator control unit, incorporating 2-way audio to allow operator and field personnel to communicate while launching or recovering the vehicle, and increased state sensing for reliability). They have also discussed the cooperative use of surface, underwater, and aerial vehicles, and achieved seven milestones in the development of a fully functional UMV for bridge inspection: standardized mission payloads, integrated health monitoring, improved teleoperation through better human-robot interaction, 3D obstacle avoidance, improved station-keeping, capability to handle large data sets, and supporting cooperative sensing.

Brown (2009) have described the use of a waterborne robot for conducting bridge inspections in conditions that would be unsafe for human divers. The robot is part of a floating platform and is fitted with acoustic sensors that can capture images above and below the water's surface. It was used to inspect for scour and debris at the Rollover Pass Bridge in Texas, that was damaged in September 2008 during Hurricane Ike. Steimle and Hall (2006) developed a cost effective USV for monitoring and assessment of costal environment and structures. This vehicle can handle a variety of instrumentation with payloads up to 225 lb (102 kg) in up to 3 ft (0.9 m) waters. It can be driven manually by a radio controller.

Brown et al. (2010) have developed a new UWS with onboard embedded controller, GPS, depth sensor, and a digital compass. This UWS was tested at different location across the country including Alaska's North Slope, the harbors of Illinois, and various riverine environments in Michigan. Figure 10 shows this UWS in operation.



Source: FHWA

Figure 10. Photo. An Unmanned Water System in operation.



© 2015 CEE HydroSystems

A. Example of a small bathymetric survey boat



© 2018 Seafloor Systems

B. Example of a small catamaran bathymetric survey boat

Figure 11. Photo. Examples of Unmanned Water System.

Unmanned bathymetric survey boats come in a variety of shapes and sizes, but all collect bathymetric data using a combination of single or multi-beam sonar, GPS positioning, optical imagery / video, and onboard data management systems. These systems prove especially beneficial when conventional bathymetry data collection methods are not practical or safe. Through the use of UWS, data collection can be completed in a short amount of time as

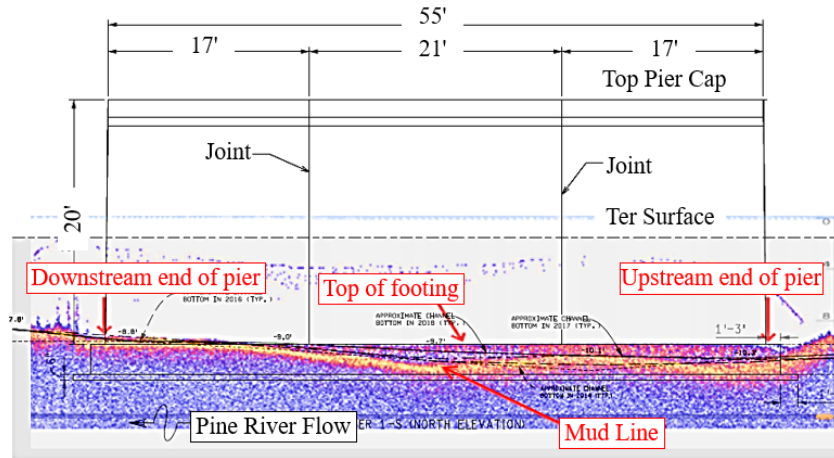
compared to other manual methods. They can also be deployed in unsafe, post-event conditions where rapid data collection is needed. Some systems can now operate in relatively swift waters with control ranges of up to 1.2 miles (2 km). Catamaran style systems can handle debris relatively well. The specifics depend on the platform selected, but the increasing capabilities of UWS merit their consideration for operation in challenging conditions.

Examples of other types of bathymetric survey boats include a mono hull platform (see figure 11-A) and a catamaran platform (see figure 11-B). There are newer bathymetric survey boats such as CEE-USV (Shierenbeck, 2018) with the capability of high maneuverability and an effective range of up to about 3000 ft (76 m) and a maximum speed of 9 knots (4.6 m/s). They are useful for high-speed river cross sections.

Sensor

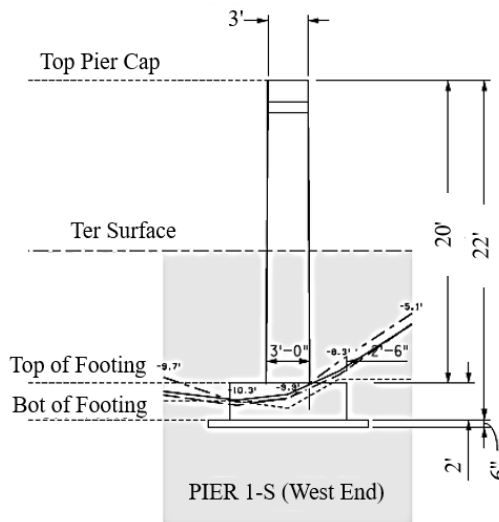
Although many advanced approaches for measuring scour holes are available, a plumb bob is used frequently as a part of the visual inspection program to measure scour depths. For example, Nassif et al. (2002) used a magnetic sliding collar and sonar to measure and map scour at 10 sites and these data were validated by measurements using a plumb bob. However, using this tool to map a large area is not practical. Other cost effective technologies for detecting scour holes could be the ones being used for finding fish, such as commercial fish finders. The sensor, which cost approximately \$250, is castable (meaning that it can be operated from the shore while still taking bathymetry measurements). Additionally, the unit uses integrated GPS and Wifi, which can create and send detailed maps to any smartphone device within 328 ft (100 m). The device can scan depths between 1.6 ft (0.5 m) and 262 ft (80 m). For example, figure 12 shows the scanning of the pier of a bridge using a commercial fish finder.

Single beam sonar (or fathometer) is a widely used method that uses sound waves to measure the depth of a waterway. Measurements of the elapsed time between pulse generation and return is used to determine the depth. Single beam soundings only occur directly underneath the sonar transducer and therefore only provides a single path of data. Typically, single-beam sensors are cheaper, require less processing, and are less complex as compared to multi-beam or side-scan sonar. However, single-beam data collection would take longer to cover a larger, deeper, and more complex region as more passes are required to obtain proper coverage. Multi-beam sonar is a more advanced and expensive technology than single-beam sonar and can provide up to 100 percent coverage of the waterway bottom, since the emitted sound waves are in the shape of a fan. This technology proves especially useful for larger or more complex areas to be scanned. Data collected using this type of sonar tends to be higher in spatial resolution, revealing features that may be missed by a single-beam sonar and requires less time to be collected. Equipment tends to be more complex in nature, requiring advanced data understanding and processing. Side-scan sonar emits pulses from the sides of the platform to form a wider swath of data collection on the waterway bottom. Data collected tends to be high resolution, showing items of interest (such as debris from hazardous conditions). However, since the beams are generated from the sides of the platform, the area directly underneath the sensors is not detected and therefore requires multiple passes in order to achieve 100 percent bottom coverage. Side-scan units tend to be fairly expensive and require advanced data understand and processing.



© 2018 Deeper UAB

A. Profile of the river obtained from the app



© 2018 Deeper UAB

B. Details of one of the piers

Figure 12. Illustration. Bridge pier scanning using a commercial fish finder sonar app, where the footing of a bridge pier can be seen as indicated by arrow.

Interferometric sonar has been investigated for shallow water (around 13.3 ft (4m)) bathymetric mapping since traditional side-scan and multi-beam systems are not as effective in these regions. Gostnell (2005) has carried out a preliminary investigation of this technology and has compared results with those using multi-beam sonar in shallow water. Results indicated that the standard deviations of the interferometric sonar data was about 3–5 times greater than multi-beam sonar data, which was expected due to the higher data density of the interferometric data (Gostnell 2005). Additionally, sand-waves of heights 4 in (10 cm) or greater and boulder and rocks outcrops with diameters of 6 ft (1.8 m) or greater were also detected by the interferometric sonar.

Monitoring-Based Nondestructive Evaluation Technologies

Because of significant progress in SHM technologies in other industries, many bridges have also been instrumented with health monitoring systems with different sensors, such as

accelerometers, tilt meters, etc. During extreme hazards, such as hurricane, response of the bridge can be measured in real-time using these installed sensors. These data can be analyzed after the hazard has ended to find any abnormal behavior or signs of damage to a bridge component. Other sensors, such as inclinometers, can be used to determine the integrity of the bridge after the hazard. For example, Sumitro and Hodge (2006) have developed a smart bridge monitoring system that uses Fiber Optic Displacement Sensor to monitor the long-term degradation in highway bridges through measurement of the global deformational behavior of bridge structural elements, such as, pier tilt, bearing anomalies, deck deflection and rotation due to live loads, environmental loads and long term pre-stress effects. Usefulness of this technology in measuring bridge responses has been determined through experimental and field studies. Swartz et al. (2016) have also proposed an automated remote flow detection arrays based on bio-inspired flow sensors for monitoring scour around bridge piers and abutments. This scour detection system is able to provide remote scour information to bridge owners through a format that is not only easily understandable, but also very helpful in decision making. They have demonstrated the capability of the proposed system to detect and monitor scour by carrying out proof-of-concept experiments in the laboratory and the field. Another example is the work done by Washer (2010). He has developed a bridge monitoring technology based on the application of low-cost sensor arrays, located on the superstructure and bridge pier. The system is used to measure long term settlements, scour and other structural displacements leading to instability or collapse of a bridge. The system was installed on a bridge in Rome, New York, with a history of bearing-related issues that needed to be monitored (see figure 13).



Source: TRB

A. Individual sensor



Source: TRB

B. A three sensor array

Figure 13. Photo. Field implementation of sensors on the bridge in Rome, New York.

Such scour monitoring systems can be very useful for assessing bridge stability after an extreme hydraulic event (Deng and Cai 2009). Radchenko et al. (2013) have proposed a new

methodology for real time scour monitoring of bridges. In this method, sensors called “Smart Rocks” are deployed around the foundation of a bridge as field agents. These sensors use wireless communications to send the change in their positions to a nearby mobile station to be used for scour analysis (Chen et al. 2015). Azhari et al. (2014) have proposed a low-cost and simple scour depth sensor fabricated using piezoelectric poly Vinylidene Fluoride (PVDF) polymer strips. These sensors are deployed at the locations where the potential of scour is high. Scour is detected when the sensor generates a time-varying voltage signal because of being directly exposed to water flow. Recently, an innovative spiral time domain reflectometry (TDR) sensor has also been developed by Gao and Yu (2015) for scour detection. This sensor consists of a copper wire TDR waveguide wrapped spirally around a mounting rod. It has been shown that the spiral TDR sensor is about four times more sensitive in detecting the scour depth than the straight TDR sensor.

Liang (2017) developed a Hydrologic Disaster Forecast and Response (HDFR) system to assess and forecast hydrologic disasters. This system includes a set of integrated software tools that are capable of streamlining hydrologic prediction workflows based on data from multiple reliable sources such as government organizations (meteorological and hydrological observations from ground and space-borne sensors) and weather model forecasts. The main objective of the project was to develop a decision-support tool in operations where extensive areas need to be monitored for extreme weather events and/or where accurate hydrologic predictions are required (Liang, 2017).

Social Media-Based Technologies

Waters and Cervone (2014) have investigated the use of social networks and CRS technologies to assess impacts of natural events such as hurricane and flood (Hydro-hazards) on transportation infrastructures. Key concept of this research is the collection of imagery of transportation infrastructure conditions in the aftermath of natural hazards through social media for post-hazard assessment of structures. In particular, this research investigated on finding hot spots for collecting CRS images after major natural events, such as floods, hurricanes, tornados, and earthquakes, using social media. A scanning software called Carbon Scanner was developed by Waters and Cervone (2014) to access and collect social media data by primarily browsing twitter in real-time and also searching in the other sources such as videos, photos, news reports. The developed software was effectively used to filter tweets by keywords and hashtags, allowing the research team locate road, bridge and natural hazard condition reports, as illustrated in figure 14. The scanned information can be helpful in generating alerts for areas with significant twitter activity, where natural hazards were potentially occurring. This information can give near real-time insight about hot spots for which remote sensing data should be acquired. It was shown that social media during a disaster can provide an immediate assessment of people’s response to a developing hazard. Application of this approach for engineering assessment of transportation infrastructures can be explored by collecting and analyzing photographs of affected bridges through social media platforms. The social media tools, such as twitter, can also be used to instruct people on collecting certain damage data and transmit through twitter. Examples for such data include the water surge levels during hurricanes. Waters and Cervone (2014) also sought to determine the efficacy of the data sources in assessing the damage produced by three major flooding disasters; the flooding and damage to the US eastern seaboard in late October

2012 resulting from Hurricane Sandy, the floods in late June 2013 in the city of Calgary, Alberta, and the catastrophic flooding that occurred in the State of Colorado in mid-September, 2013.



Source: USDOT

Figure 14. Illustration. Carbon Scanner tested by searching “#winterstorm” over New York City on March 19, 2013.

ANALYSIS OF NEEDS AND GAPS

Data Needs in Post-Hazard Damage Assessment

The main objective of post-hazard damage assessment of a bridge using remote sensing technologies is to collect important data related to the behavior of the bridge, observed damage and nature of loading during an extreme hazard so that these data can be used to evaluate current design guidelines and develop strategies aimed at enhancing resiliency of bridges during extreme hazards. Furthermore, immediately after an event, remote sensing technologies can be used to identify bridges that have collapsed or must otherwise be closed in order to identify safe routes for emergency (and other traffic) operations. The data needs are described in the following.

Bridge Movement Data

There are three types of bridge movements that are important to evaluate the impact of hazard scenarios on bridge elements: *translational*, *rotational*, and *settlement movement* (Ettema et al. 2006). Scour, for example, may cause a bridge to sink vertically (settlement), may reduce the longitudinal support of a pier, causing tilting, or may reduce the bridge’s ability to support itself in the stream-wise direction (Guo et al. 2009). Bridge piers are also susceptible to rotational movement due to liquefaction and movement of supporting soils during an earthquake (Palermo et al. 2011; Han et al. 2009). Bridge movement can be measured using methods such as DIC, InSAR, and high-resolution aerial imagery. In addition to these technologies, GPS has also been used to collect bridge movement measurements (Nakamura 2000). Both long-term movement

(e.g., foundation settlement) and short-term motion (e.g., vibration during dynamic events such as earthquakes) can be measured by these tools (Meng et al. 2011).

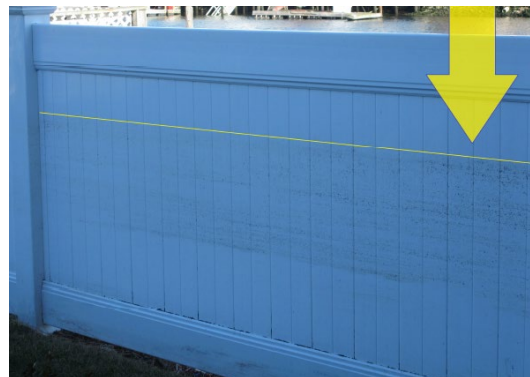
Bathymetry Data

Knowing the locations and dimensions of scour holes near bridge piers can be useful in enhancing the understanding of the development of predictive guidelines and equations for further scour modeling efforts (Huizinga 2017). During an in-depth study of eight bridges along the Missouri and Mississippi Rivers, scour holes were identified at most piers for which bathymetry data could be retrieved, except for piers that were located on river banks, bedrocks outcrops, or had riprap protection. In addition to scour detection at a selected study site, bathymetry data over time can also be very valuable in understanding the development of scour over time.

Hydraulic Data

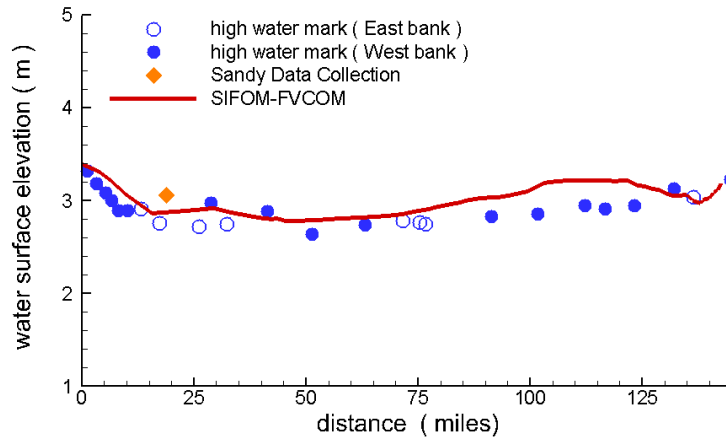
Wave Surge

Water surface elevation during flooding caused by a hurricane in an urban area is a very important perishable data that can be used to calibrate computer modeling of flow during hurricanes. For example, figure 15 shows an example of water mark that was collected in the aftermath of Hurricane Sandy in the New York City Area. Figure 16 shows the plot of computer water surface elevation through computer modeling and its comparison with observed water surface elevations through measured water marks. Water marks data (similar to that in figure 15) on various structures and locations in the New York City region were collected after the Hurricane Sandy in 2012 manually, which is very time-consuming and inefficient. Quality and quantity of these data can be improved substantially by using remote sensing tools such as aerial imagery from an UAS. Resolution of digital cameras in currently available UAS is sufficient to collect this data with much higher level of accuracy in position (location) because of coordinate measurement by a GPS and automated detection of water mark height through digital image processing.



© 2012 Dr. Hansong Tang

Figure 15. Photo. Water mark collected in the aftermath of Hurricane Sandy in the New York City area.

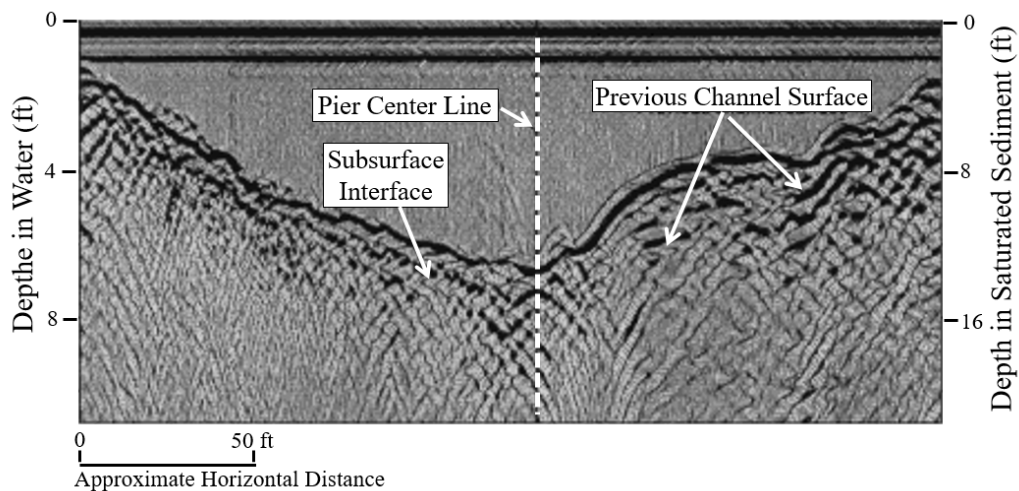


© 2012 Dr. Hansong Tang

Figure 16. Graph. Computer water surface elevation of Hurricane Sandy in the New York City area.

Sub-bottom Profiling (Lower Frequency-10 kHz)

Evidence of previous (paleo) scour holes can be detected through the use of low frequency acoustic and ground penetrating radar (GPR) in shallow waterways as shown in figure 17 (Placzek and Haeni 1995). Advantages of using GPR to detect scour holes include a continuous image of the channel and sub-channel, safe data acquisition during peak flow (remote data collection), rapid data collection across the water’s surface, accurate two- or three-dimensional models of the waterway’s bottom (up to 32.8 ft (10 m) in depth) and sediment (up to a depth of 1 ft (0.3 m)). Anderson et al. (2007) have assessed multiple sites in Missouri for scour using a GPR and have found two instances of paleo-scour holes at approximately the same location, but at different heights. Hence, assessment of sub-bottom of a river near piers and abutments can give important data on formation of scour holes during extreme flooding.



Source: USGS

Figure 17. Illustration. Digitally filtered and migrated 300 MHz GPR data.

3D Data of the Contributing Watershed for Hydraulic Modeling

Satellite image photogrammetry can be used to create digital surface models over large areas of land (Stumpf, 2017). For example, a Chinese satellite sensor, ZiYuan-3 (ZY-3), launched in early 2012, uses three high-resolution panchromatic cameras to collect imagery that can be used for stereographic purposes. The tri-camera system operates at two different resolutions, which allows for three-fold stereo capabilities, and therefore, more stable geometric conditions. The accuracy of the DSM is 8.2 ft (2.5 m) to 9.8 ft (3 m), depending on the type of terrain and ground sampling distance of the orthophoto, which was 8.2 ft (2.5 m) in the study by Kornus et al. (2015).

Aerial LiDAR (collected via aircraft or satellite) can provide elevation data for the surrounding watershed, especially in areas where in-situ data is difficult to collect. Because of NOAA's Digital Coast program, terrestrial LiDAR datasets have been rapidly progressing in the amount of data, resolution, and accuracy. With high-resolution Digital Elevation Map (DEM) data available from LiDAR, hydraulic modeling should incorporate these models as compared to using other readily available lower resolution (32.8 ft (10 m) or 98.4 ft (30 m)) DEM datasets. Furthermore, rapid evolution of UAS is enabling the use of heavier-lift capacity platforms and new onboard sensors including LiDAR. By collecting LiDAR data at a much lower altitude as compared to manned aircraft or satellite-based LiDAR units, the resulting resolution of a LiDAR-based DEM is rapidly increasing.

Aerial photography and photogrammetry can provide users with a broad overview of the area of interest as well as detailed elevation information about the landscape. By collecting high-resolution, overlapping aerial imagery, 3D models of the landscape can be reconstructed using photogrammetric 3D image processing software. By collecting this imagery at lower elevations through the use of UAS, the high-resolution imagery is reconstructed in a high-resolution DEM (sub- cm or mm depending on the input imagery). Detailed measurements can be made from these high-resolution models, which can also serve as elevation inputs into hydraulic modeling. Photogrammetry is the most useful for areas without significant shrub and tree cover, as it uses natural color images that reflect surface conditions and do not penetrate surface canopy (McGlone et al. 1980). Aerial photography can be collected via manned or unmanned aircraft. A relatively affordable UAS is able to create high-resolution elevation data.

To create an input dataset for hydraulic modeling, it can be important to create an integrated above and below water digital elevation model of the landscape and bathymetry. This task was performed in this research (see Chapter 2) for the bridge over Tuckahoe Creek in Easton, Maryland, by combining three different datasets. Field data collected by a UWS in this research produced a 3.75 ft (1.1 m) resolution dataset for an area approximately 195,000 ft² surrounding the bridge. The remainder of bathymetry data was obtained from NOAA's Digital Coast Program and was processed in Geographic Information System (GIS) software to include only negative (bathymetric) values. This provided the bathymetry data for sections of the river for which data could not be collected by the UWS. It is important to note that the Digital Coast data only extended a certain extent upstream of the watershed's outlet. The remainder of the watershed's elevation data was obtained from LiDAR data, which was collected during multiple aerial flights. The three datasets were merged together to cover the entirety of the watershed at a

resolution of 2 ft (0.60 m). This merged dataset can be used for advanced hydraulic and scour modeling using software such as SRH-2D (Lai 2010).

Having access to data and imagery of bridge elements prior and post-hazard can provide vital information on the extent of damage to a bridge (and its elements) during the event. This type of data could be standard pictures (2D) or processed elevation imagery (3D), which can be used to make detailed comparison measurements. Comparison data can be documents such as bridge plans or designs, previous inspection reports, digital images, or processed data. These types of analyses can be qualitative or quantitative in nature, depending on the type of comparison data that is available. Furthermore, this type of data can provide detailed historical information to determine how bridge condition has progressed over time.

Gaps in Post-Hazard Damage Assessment

As part of the research study, gaps in engineering post-hazard assessment of bridges have been identified through consultation with subject matter experts from industry, government and academics. These gaps are discussed separately for geo-hazards (e.g., seismic) and hydraulic hazards. It has been observed from the nationwide survey of transportation agencies by Alipour (2016) that 86 percent of the States have an emergency response plan for extreme events. However, these plans are mostly focused on emergency response and recovery, and do not focus on engineering post-hazard assessment. As noted earlier, major hazards requiring detailed post-hazard assessment are geo-hazards (earthquakes, landslide, etc.) and hydro-hazards (hurricanes, flooding, etc.). Among geo-hazards, seismic hazards pose the risk of causing most-widespread damage to highway infrastructures.

Seismic Hazard

Post-hazard engineering assessment program exists more for seismic hazards than for other hazards because of the risk of massive and widespread damage during earthquakes, but even this is true only for a few high seismic States. Additional reason for focusing on seismic assessment may also be due to extensive research on seismic effects by researchers worldwide. Strong ground motion recording during earthquakes are fundamental to understanding and characterizing the behavior of bridges during seismic events. The U.S. Geological Survey (USGS) National Strong-Motion Project (NSMP) has the primary Federal responsibility for acquiring strong motion records of significant earthquakes in the United States recorded by networks of sensors placed in the ground and in man-made structures¹. These recordings are disseminated by USGS and used by researchers and transportation agencies across the country for research and design of bridges.

A number of State Departments of Transportation (DOTs) have post-earthquake assessment program in place. Most prominent among these programs is the post-earthquake program of California Department of Transportation (Caltrans)². This manual provides detailed guidance on components of a bridge to be investigated in the event of an earthquake. Caltrans used an

¹ <https://earthquake.usgs.gov/monitoring/nsmp/>

² http://www.dot.ca.gov/hq/esc/earthquake_engineering/PEQIT/PEQIT_Manual_2013.pdf

advanced seismic risk analysis software package called REDARS³ (Risks from Earthquake Damage to Roadway Systems) to improve its ability to face a strong earthquake event. This software helps disaster decision makers assess various seismic-risk-reduction scenarios for pre-earthquake planning. Caltrans and USGS also use ShakeCast⁴ (ShakeMap Broadcast) for both pre-earthquake planning and emergency operation. Many other State DOTs also have their own guidelines for post-earthquake inspection/investigation of structures, including bridges, for example “Post-earthquake bridge inspection guidelines” for New York State Department of Transportation (O’Connor 2010), “Handbook for the post-earthquake safety evaluation of bridges and roads” for Indiana Department of Transportation (Ramirez et al. 2000), “Pacific Northwest Seismograph Network (PNSN) ground-motion processing and notification software” for Oregon and Washington State DOTs (Ranf et al. 2007). These guidelines are well detailed and provide detailed recommendations on inspection of bridges after an earthquake to collect important engineering data. USGS has issued a detailed plan to coordinate post-earthquake investigations through coordination between National Institute of Standards and Technology (NIST), National Science Foundation (NSF) and State DOTs (Holzer et al. 2002). Under this plan, various centers and institutes such as Earthquake Engineering Research Institute (EERI), Mid-America Earthquake Center (MAE) at the University of Illinois at Urbana-Champaign, Multidisciplinary Center for Earthquake Engineering Research (MCEER) at the University at Buffalo, New York, and Pacific Earthquake Engineering Research Center (PEER) at the University of California, Berkeley, are supported to carry out detailed investigations after an earthquake. A “Post-Earthquake Investigation Field Guide” by EERI⁵ also provides detailed guidance on post-earthquake inspection of structures, including bridges. USGS uses an application called ShakeCast for automating near-real-time maps of ground motion and shaking intensity to be used by emergency responders and for facilitating notification of ground motion intensity levels at specific facilities.

While the post-earthquake assessment discussed above is largely based on visual aided by nondestructive tools and cameras, there has been significant progress on post-earthquake inspection using remote sensing technologies. A detailed literature review on this has already been provided in the first section of this chapter. It has been noted based on discussions with subject matter experts on the use of remote sensing technologies for post-earthquake assessment that major gaps in this area are institutional in nature and are the same as those for hydraulic hazards. These needs largely relate to the absence of a post-seismic bridge assessment program being in place at State DOTs and will be discussed in detail with hydraulic hazard assessment.

Hydraulic Hazard

It has been noted from discussions with subject matter experts that State DOTs typically monitor the safety of bridges during a flooding event and do not carry out in-depth investigation after a flooding or hurricane event, although some DOTs do carry out underwater inspection using

³ <http://www.dot.ca.gov/newtech/operations/redars/index.htm>

⁴ <https://my.usgs.gov/confluence/display/ShakeCast/Home>

⁵ <https://www.eeri.org/projects/learning-from-earthquakes-lfe/post-earthquake-investigation-field-guide/>

sonars as a part of safety assurance program for bridges. These inspections do lead to useful data in understanding scour and hydraulic effects on bridge foundations.

Gaps in engineering post-hazard assessment of bridges can be categorized as: Institutional and Technological Gaps.

Institutional Gaps

Institutional gaps in post-hazard assessment of bridges occur because of the absence of a well-developed plan for engineering assessment in the event of a hazard. Major reasons for the institutional gaps are (i) financial/budgetary constraint of State DOTs, (ii) lack of technically educated/trained engineers in using remote sensing technologies that include understanding of concepts of image processing, data analysis, photogrammetry and electronics, (iii) lack of adequate training and continued education on the use of remote sensing technologies, (iv) lack of timely access to these technologies by the State DOT engineers for carrying out post-hazard assessment, and (v) lack of availability of sufficient number of trained engineers, in-house or outside, for carrying out post-hazard assessment. However, the biggest gap is related to preparedness of State DOTs in developing and continually updating a post-hazard assessment program with guidelines on data collection and list of identified expertise that can be mobilized rapidly.

With rapid progress in remote sensing technology, a number of States are planning to adopt UAS for regular transportation operations such as bridge inspections by MNDOT (<http://www.dot.state.mn.us/>), MTDOT (<http://www.mdt.mt.gov/>), MDOT (<https://www.michigan.gov/mdot/>), NJDOT (<http://www.state.nj.us/transportation/>) etc. Some DOTs have also identified the use of UAS for emergency response, although it is not focused on engineering data collection. The institutional gap in engineering hazard assessment can be addressed by developing a comprehensive program that can utilize remote sensing technologies, including UAS, after an extreme hazard. Key components of such a program and major challenges and future research directions, as also identified by Otero et al. (2016), to realize the application of LiDAR-UAS system for inspection and post-hazard assessment of bridges, are as follows:

- **Experience of Inspectors and Data Management:** The challenges for effective implementation of remote sensing technologies, particularly UAS equipped with LiDAR, UWS equipped with sonar, include the lack of experience of inspectors with remote sensing techniques, difficulty with data management because of enormous amounts of data, and software limitations.
- **Size of UAS and Technologies:** Small or micro UAS are more favorable for bridge inspection because they meet critical mission requirements such as maneuverability in tight spaces, extended flight durations, water-resistant capabilities, and on-board computer for data storage and/or real-time data transmission. Developments in UAS are needed to (i) operate in GPS denied environment, (ii) perform under-deck inspections and (iii) perform in-contact inspection of selected members. Without these developments, advantages associated with UAS-based inspection, such as accessibility, economy and reliability, will not be realized.

- **Software Resources:** A majority of software using UAS data are based on photogrammetry. There is a need for developing software that can automate the bridge orientation and deviation computations based on the remote sensing data obtained through UAS or other remote sensing technologies. There is also a need for software tool and knowledgebase for translating photogrammetry information into assessment information that can be used by bridge engineers without having expertise in understanding photogrammetry data.
- **Outreach to Stakeholders:** It is recommended to design a plan for State DOTs and other owner agencies in the United States to incorporate UAS as tools for bridge inspections, since the same tool can also be used for post-hazard assessment.
- **UAS Program Coordinator:** Since the use of UAS for bridge assessment is still in exploratory phase, State DOTs need to have a program coordinator familiar with post-hazard assessment data needs for seismic/hydraulic hazards and familiar with key aspects of UAS and sensors that could be used with UAS, including limitations of these sensors. This person could be someone involved with UAS operations for inspections and transportation infrastructure management also.
- **Remote Pilot Database:** A database of licensed remote pilots for UAS with their training and qualification details is needed. Remote pilots could be from the same State or adjoining States, and should have training in flying UAS and interpreting collected data. During and immediately after an extreme hazard, these pilots could be mobilized for rapid assessment of bridges so that the mobility could be improved and important perishable data could be collected.
- **Readiness of Assessment Tools:** State DOTs should have a number of UAS with sensors (high resolution cameras, LiDAR, infrared cameras, etc.) or should have a catalog of consultants owning UAS for rapid mobilization. UAS could be rented for post-hazard assessment if the States don't have their own UAS program.
- **Guideline on Data Collection:** A brief guideline on data to be collected during different hazards needs to be developed so that the assessment can begin during or immediately after the hazard.
- **Budget Allocation:** State DOTs should have planned budget line for post-hazard assessment of bridges so that the program coordinator can recruit qualified remote pilots to collect necessary data useful for improving the understanding of bridges during such hazards. This kind of program may not require substantial costs of maintenance, since UAS are going to be used increasingly in transportation infrastructure management. The sustainability of the program can be improved substantially by incentivizing consultants so that they can train their bridge inspectors with necessary additional training for post-hazard aspects and can maintain UAS that could be used during both regular inspection and post-hazard assessment. A post-hazard inspection certification process can further incentivize consulting engineers participate in this program.

Technological Gaps

Although numerous applications of UAS for post-hazard assessment have been demonstrated during last few years, there are a number of technological gaps in fully realizing the potential of UAS. These gaps are described below.

(i) High Resolution DEMs for Advanced Hydraulic Analysis

Readily available high-resolution bathymetry data exists for some coastal regions of the United States through NOAA’s Office for Coastal Management’s Data Access Viewer (<https://coast.noaa.gov/dataviewer/>) (see figure 18). However, data coverage is not 100 percent along coastal regions. For example, the Atlantic Coast appears to have widespread coverage of LiDAR data that could be used for bathymetric data. The Pacific Coast does not appear to have as widespread coverage, or at least coverage that extends further inland. Likewise, while some of the Great Lakes coastal regions have coverage (southeast Michigan and southern Lake Erie), but other regions such as Lake Superior, Lake Michigan, Lake Huron, and Lake Ontario, have minimal coverage. Depending on the area of interest, acquiring bathymetric data via LiDAR may prove to be difficult or not possible due to lack of coverage.



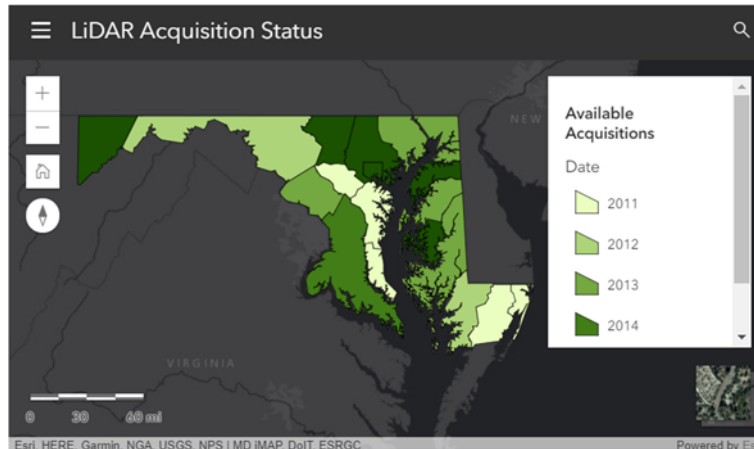
Source: NOAA

Figure 18. Illustration. Spatial availability of coastal elevation data.

Maryland’s Mapping & GIS Data Portal [<http://imap.maryland.gov/Pages/default.aspx>], iMAP, provides access to numerous remote sensing imagery and datasets (see figure 19). The Maryland LiDAR server contains focused areas, pre-defined DEMs, and point cloud data that can be used to retrieve bathymetry information. Reviewing the metadata of these datasets reveals the difference in point spacing, DEM resolution, and vertical accuracy between counties. Retrieving a dataset is quite simple and requires the user to select a region of interest and an email account, with delivery of the dataset typically occurring within 30 minutes. Table 1 provides metadata information for three counties in Maryland and shows the range in point spacing, DEM resolution, and vertical accuracies. Other counties in Maryland have DEM resolutions and vertical accuracies up to 6.6 ft (2 m).

Table 1. Sample county LiDAR dataset metadata information.

County	Date	Point Spacing (m)	DEM Resolution	Vertical Accuracy (RMSE) (cm)
Allegany	2012	0.5	1 m / 3.2 ft	13.0
Anne Arundel	2011	1.4	0.9 m / 3 ft	15.0
Baltimore	2015	0.7	0.7 m / 2.3 ft	6.79



Source: MD's iMAP

Figure 19. Illustration. LiDAR data availability for Maryland.

Depending on the bathymetry data source and locations, different formats and resolutions may be available. Taking an initiative to collect high resolution data for all regions of the country and making it available to State DOTs, consultants and researchers will lead to the development of new tools to analyze these data both pre and post-hazard.

There is also a need to develop freely available software modules and guidelines to combine all available and collected bathymetric data into one resolution digital bathymetric map for the bridge and its surrounding. Such map is necessary for performing advanced 2D hydraulic and scour analysis around bridge foundations through software such as SRH-2D (Lai 2010).

(ii) Sensor Technologies

Although there has been rapid progress in various nondestructive and sensor technologies, there is little information on standard configuration of UAS with these sensors to collect assessment data during different hazard. There is a need to carry out more detailed field study on identification of resolution of different sensors for their use during post-hazard assessment.

(iii) Data Management and Analysis

Assessment of bridges using UAS depend on photogrammetry to collect large amount of data. Use, storage and management of these data for State DOTs is still a major challenge. State DOTs collect large amount of data through regular bridge inspections and store those data in bridge management databases. Similar database, although with much larger capacity, need to be developed for storing data collected by UAS.

(iv) Data Collection Preparedness

Immediate response during a post-hazard event is required in order to be able to collect data that most closely reflects current conditions. In the hours following such an event, attempts to collect such data can be hindered by inaccessibility to a site and/or dangerous conditions. Therefore, during- and post-hazard event, the collection team must have a plan in place to safely and effectively collect the required data, including having equipment ready to use on short notice. This includes both manual methods and use of remote platforms and sensors to take measurements. No matter the size of the agency or team, detailed preparedness and safety plans must be created before data collection should take place during or immediately following a hazardous event.

Additionally, if the data collection includes electronic equipment, all batteries should be charged prior to the hazardous event, including any backup batteries. As is the case in many instances, electricity is lost during the hazardous event and may not be restored for many days (or weeks/months as the case is for Puerto Rico following Hurricane Maria). Therefore, data collection by platforms such as UAS or remote controlled bathymetric survey boats will be limited based on how many batteries are charged, and how long the batteries last. Hence, contingency power supply plans, such as the use of generators to charge equipment and batteries and storage of sufficient amount of fuel for generators, should be in place. Solar charging can help but may not be readily available for post-disaster responses. Likewise, plans on how to store or backup data must also be taken into account to ensure that the data is not lost.

(v) Perishability of the Collected Data

Collecting perishable data is one of the most important gaps in the current post-hazard engineering data collection assessment. Collecting data during and post-event can prove to be difficult and dangerous, if not impossible. However, collecting perishable data provides the most accurate and timely information that can be used for further assessment, modeling, and to aid in future design and rehabilitation (Okeil and Cai 2008). Following Hurricane Katrina, data concerning the pre- and post-hazard condition of the bridge and its elements was collected at multiple sites. Through the analysis of the data and portions of bridge structure that failed (or did not fail), a number of recommendations on preventing such damage during future hazard have indicated that vulnerable bridges need to be identified prior to a hazardous event, storm surge forces on transportation infrastructure need to be further investigated, and that design procedures must be formulated to minimize the impact from storm surge (Okeil and Cai 2008). One rapidly evolving method being deployed to collect this valuable data includes the use of UWS as discussed by Murphy et al. (2011b). They could detect and visualize piers that were and were not experiencing any scour as well as a submerged pallet in post-hurricanes Ike and Wilma environments. Although this nearly-autonomous technology was able to collect vital data, human interaction was still required to operate the platform, analyze the data, and provide safety oversight.

CHAPTER 2. FIELD DEMONSTRATION OF SELECTED REMOTE SENSING TECHNOLOGIES

INTRODUCTION

From the literature review and discussion in the previous chapter, it is observed that the UAS have the most potential for post-hazard damage assessment of bridges impacted by seismic and Geo-hazards. Additionally, Unmanned Water Systems (UWS) technologies, such as those in figures 20 and 21, have the potential of inspecting underwater elements of bridges, such as foundation, scour hole or countermeasures, after an extreme hydraulic hazard, such as flooding or hurricane. UAS and UWS technologies have capabilities to help meet special needs in immediate post-event time periods. For example, UAS can be flown near impacted bridges to assess issues such as movement, cracking, conditions of components, presence of materials blocking traffic, etc. UWS can potentially help with obtaining data in the worst scour conditions, depending on the hardware used (newer systems can handle faster water, for example). Since major events are normally unpredictable, this evaluation focused on locations where useful measurements could be collected. These measurements represented the type of data needed in post-event investigations and inspections.

Hence, field evaluation of UAS and UWS was carried out on two bridges in Maryland during September 5-8, 2017. The research team consisted of research scientists and engineers from Michigan Tech, the City College of New York and FHWA.

Two Maryland bridges—MD-328 over Tuckahoe Creek (Bridge # 050012001 located at 38.831041, -75.913941) and MD-450 over Bacon Ridge Branch (Bridge # 020072010 located at 38.986135, -76.608927)—were selected for a detailed investigation. The technologies for field evaluation included a remote controlled bathymetric sonar boat (see figure 20 and figure 21) and UAS (see figure 22). Sensor technologies included a single-beam sonar mounted on UWS and high-resolution optical imagery from UAS. The researchers from Michigan Tech had previously worked with the Maryland State Highway Administration (MDSHA) on inspection of these bridges. An overview of the data collection and analysis at both sites are presented in the following.



Figure 20. Photo. UWS platform collecting data at the Tuckahoe Creek bridge site. (UWS is highlighted in the grey circle).

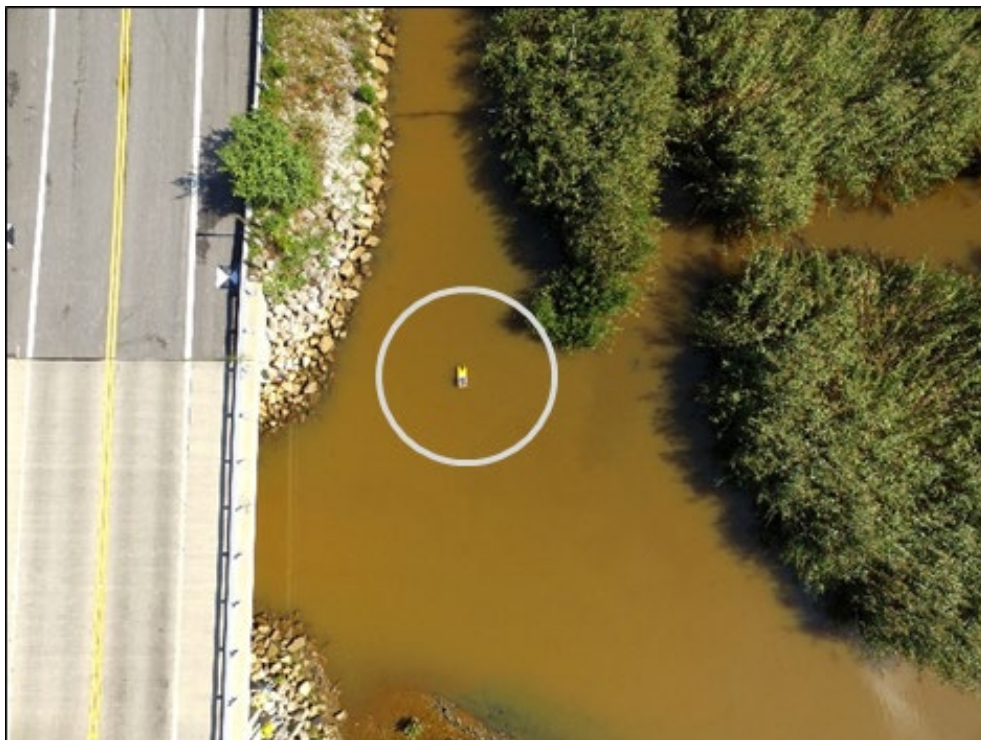


Figure 21. Photo. UWS platform collecting data at the Bacon Ridge Branch site (UWS is highlighted in the grey circle).



Figure 22. Photo. The hexacopter platform collecting bridge image data at the Tuckahoe Creek site.

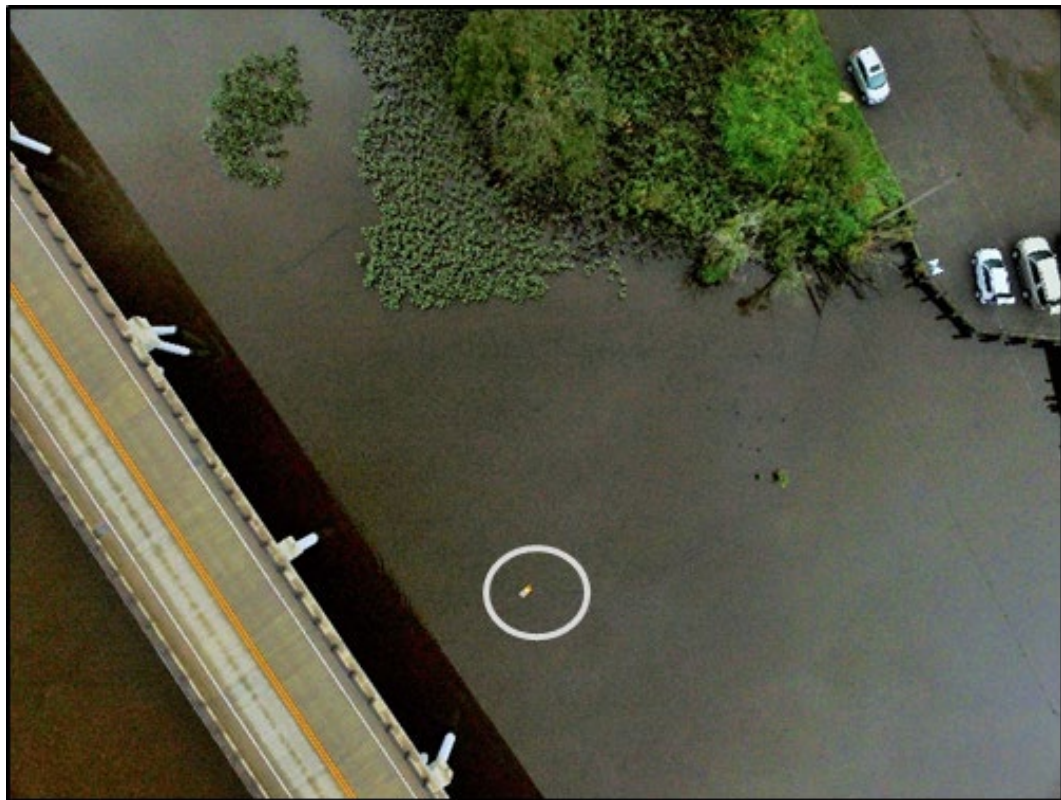


Figure 23. Photo. UWS (highlighted by grey circle) can be seen returning to Tuckahoe Landing in a UAS-collected image after obtaining sonar data near the bridge.

ASSESSMENT OF TUCKAHOE CREEK BRIDGE

Data were collected at Tuckahoe Creek on September 6, 2017 and during the afternoon hours of September 7th, 2017. After arriving on site and making observations for safe flying, five GPS targets were set up on the ground to provide ground truth location data, and to transform the optical imagery collected by UAS platform into 3D models of the site. GPS location data were collected using a cell phone app. The team preferred higher-accuracy sub-meter quality data that could be collected with units such as the Trimble GeoXH series, but the Trimble unit was not operational due to an unanticipated software problem that required further technical support. Additionally, upon returning to the site on September 7, one of the GPS targets had been removed for unknown reasons. The remaining four GPS targets and datasets were still useful for modeling purposes during post-collection processing. The UWS was deployed from the boat launch located onsite just north of the bridge. Figure 23 shows UWS returning to this area after collecting sonar data near the bridge piers. Conveniently, the boat launch also included a water depth reader on the side of one of the deck piers. Since Tuckahoe Creek is influenced by the tides, interval measurements of water depths were taken to assist in the normalization of data recorded by the UWS.

The UWS system consisted of a vessel equipped with a high-resolution GPS unit, a precision depth sounder (including both side scan sonar and single-beam sonar), water temperature sensor, a data recording and storage device, and a radio communication package for remote control. Multiple deployments of UWS were conducted with navigation covering an area approximately 230 ft (70 m) upstream and 328 ft (100 m) downstream of the bridge, with the complete track being seen in figure 24 (for a total area of approximately 4.7 acres (1.9 ha).) Post-processing of the UWS data indicated that depths in the area extended to 30 ft (9.1 m) (see figure 25), with the deepest area being in the vicinity of piers 8 and 9. More specifically, the area that reached this depth was located near a bridge pier and could indicate the presence of local scour. As such, follow on investigation may be warranted to monitor changes in the potential scour hole area.

The UWS sonar dataset and the NOAA bathymetry data were also combined with terrestrial LiDAR elevation data collected by the State of Maryland so that the detailed elevation map output could be used for SRH-2D hydraulic modelling (see figure 26 A and B, and figure 27). The bathymetric contours in Figure 26A were part of a dataset published in March 2017, consisting of 2006 NOAA contour data from Caroline County, Maryland, which are different but similar to the field data collected by Michigan Tech using a UWS. As Figure 27 shows, combining data can create edge issues, but these can be addressed through further data processing. The NOAA bathymetry and Maryland LiDAR data were combined into a single data set using ESRI ArcGIS raster merge tools, with a common sea level value selected to transition from terrestrial elevation to bathymetric values. The UWS sonar data were inserted into the NOAA bathymetry values, but were not otherwise smoothed to refine the combination of these two bathymetric data sets. Edge adjustments, such as smoothing of elevation values, could be made to improve the transition from different data sets, such as the NOAA bathymetry to sonar data collected by the UWS.

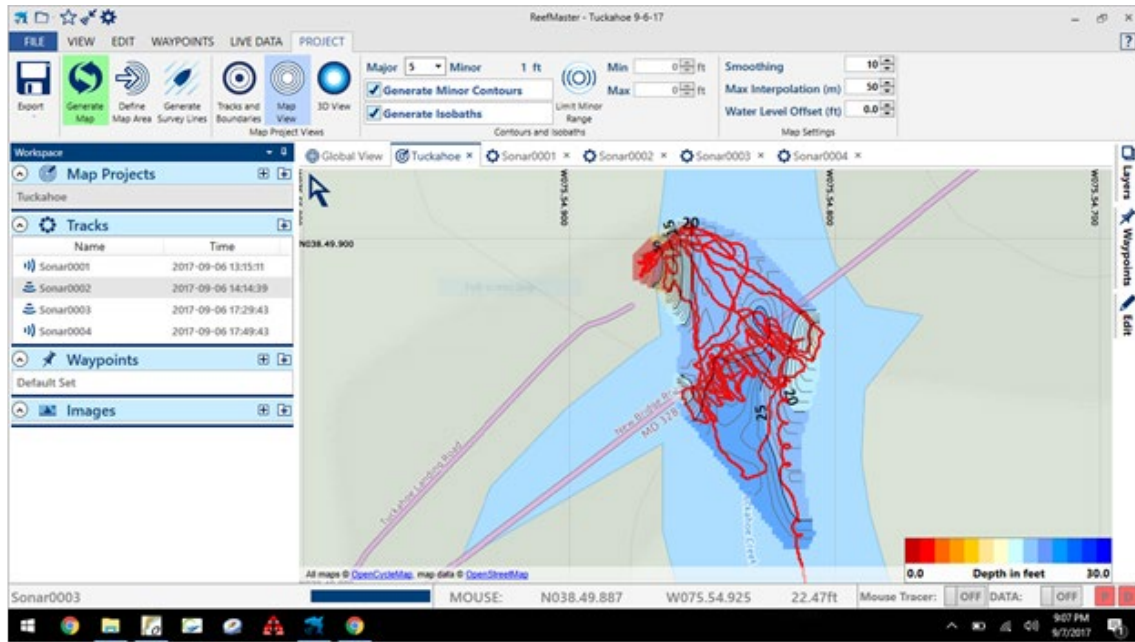


Figure 24. Illustration. Data collection paths (shown in red) of the UWS at Tuckahoe Creek.

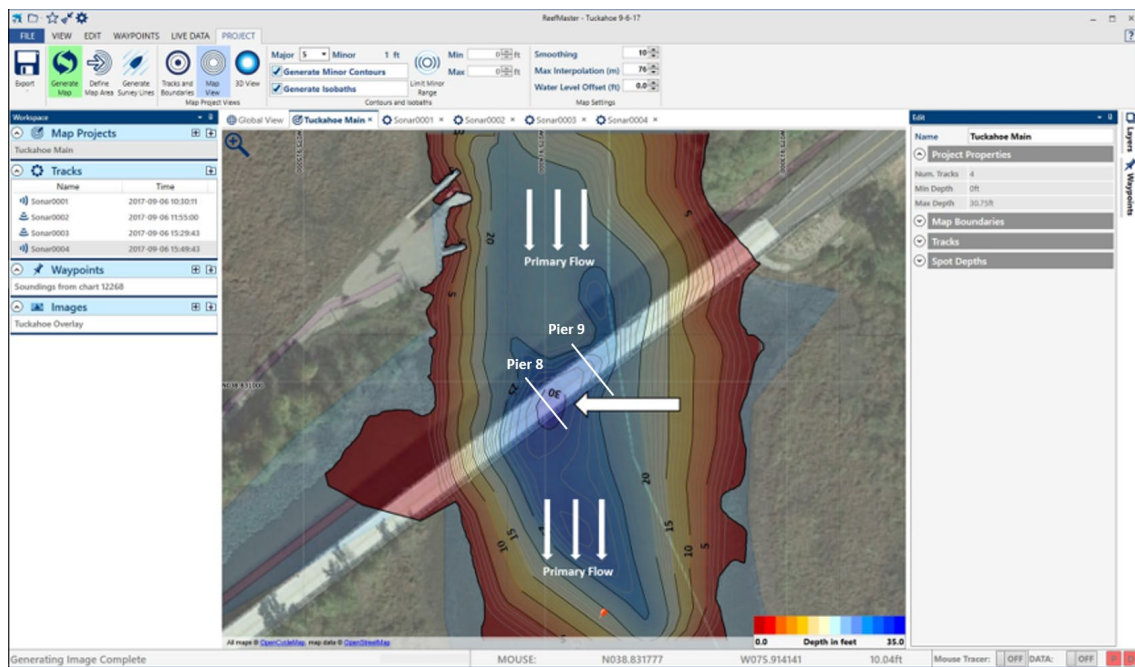
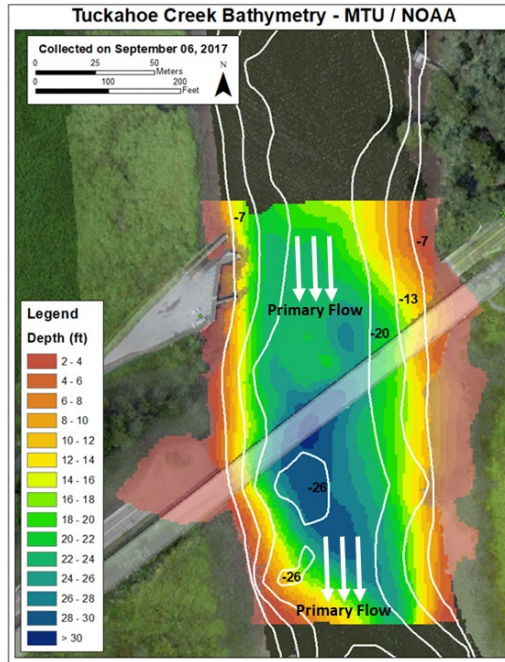
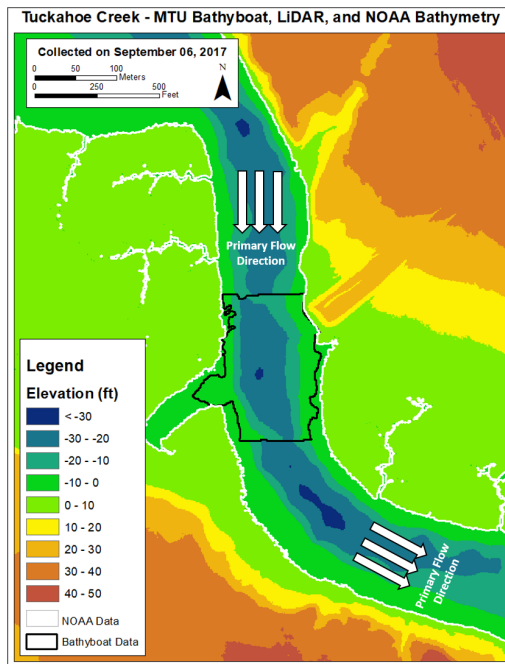


Figure 25. Illustration. Contour bathymetry measurements at Tuckahoe Creek reached 30 ft (9.1m) near bridge piers 8 and 9 (white arrow).



A. NOAA bathymetry contours.



B. Bathymetry data combination

Figure 26. Illustration. A combination of collected bathymetry data (black outline), NOAA bathymetry data (white outline), and LiDAR elevation data (outside white outline) that can be used as an input for hydraulic modeling (Tuckahoe Creek).

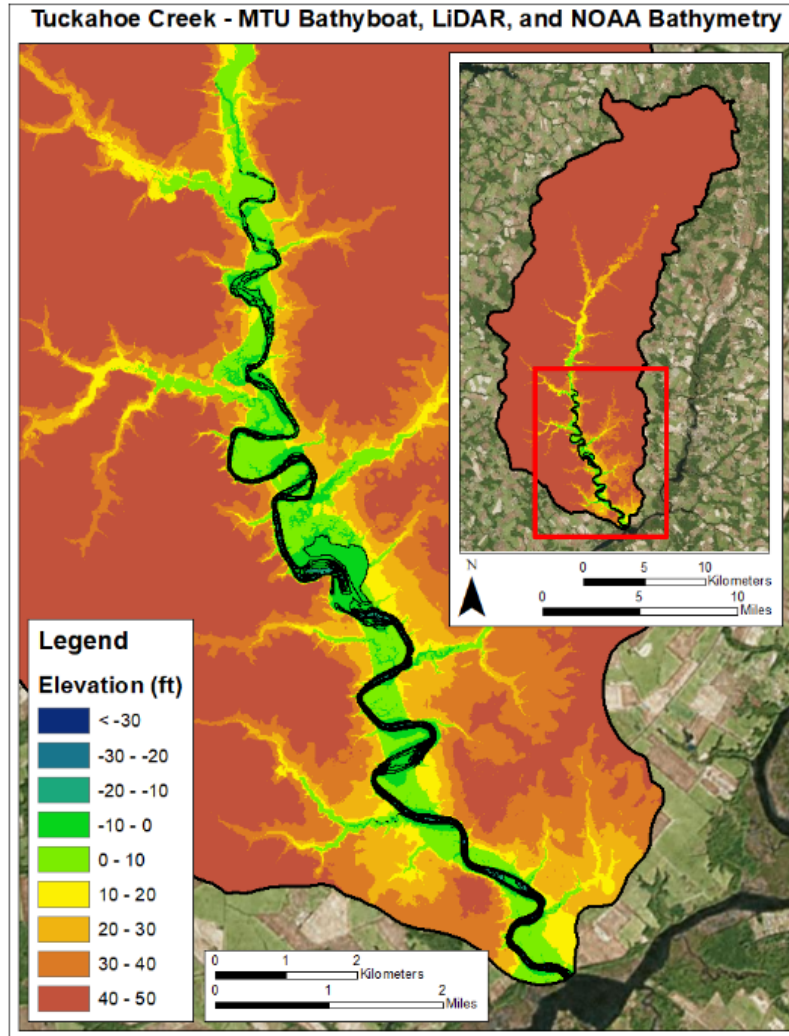


Figure 27. Illustration. Wider scale of watershed data in Tuckahoe Creek.

UAS data was collected at Tuckahoe Creek Bridge to provide overviews of the stream environment and models of the bridge and surrounding area. First, the DJI Phantom 3 Advanced (3A) was flown over the area to collect aerial imagery that could be used to create 3D models of the surrounding landscape. The DJI Phantom 3A included an onboard optical sensor with 12Mp resolution that produced imagery similar to a GoPro. Since the platform's batteries typically last approximately 20 minutes, multiple flights were conducted to cover an area approximately 1150 ft (350 m) upstream and 500 ft (150 m) downstream of the bridge, totaling approximately 40 acres. Airspace was checked ahead of time using the current FAA charts at both sites and was determined to be acceptable for UAS flights. Imagery collected was reconstructed into a model using a software for creating professional 3D content from still images. This produced a 0.8 in (2 cm) georeferenced model of the surrounding landscape (see figure 28). Figure 29 includes a representative picture of the Tuckahoe Creek site collected.



Figure 28. Illustration. DJI Phantom 3A aerial imagery (outlined in black) reconstructed into an orthophoto image with 3D elevation data shown on top of an GIS Basemap displaying WorldView satellite imagery (Tuckahoe Creek).



Figure 29. Photo. Photo of the Tuckahoe Creek bridge site taken with the Phantom 3A UAS.

A smaller but newer UAS, the DJI Mavic Pro, was also used to collect up-close optical imagery of the side of the bridge as both photos and 4K (3840x2160 resolution at 30 frames per second) video. This platform was selected due to its stability and ability to sense and avoid front-end collisions using on-board stereo vision cameras from up to 50 ft (15 m) distance, enabling it to be safely operated close to bridge elements, such as fascia and piers. The onboard 12 mp / 4K optical sensor is similar to a GoPro, which provided sufficient resolution for visual condition assessment of bridge elements (see figure 30 and figure 31).



Figure 30. Photo. Close-up photo of the Tuckahoe Creek Bridge taken with the Phantom 3A UAS.



Figure 31. Photo. DJI Mavic imagery of a pier cap and the side of the bridge.

Additional UAS data was collected at the site using high-resolution optical imagery collected by a camera of 36 megapixel resolution onboard of one of the team's larger Bergen hexacopter UAS. The heavy-lift capabilities of the hexacopter allowed it to lift heavier sensors. Imagery of the side of the bridge and piers was collected and processed into 3D models. These models were used to demonstrate how detailed measurements can be made of the piers to determine if scour

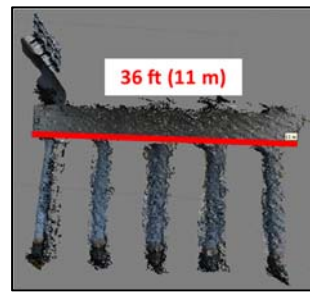
has caused any movement of the piers or bridge deck (see figure 32). For example, according to the reconstructed model, the length of the pier cap in figure 26 is 4.3 ft (1.3 m), whereas it is x4 ft (1.2 m) as per bridge plans, resulting in =a 9 percent difference. Likewise, the length of the modeled pier cap was measured to be 36 ft (11 m), which according to bridge plans is 36 ft (11 m) in length (see figure 33). These type of measurements can be made in a post-hazard scenario to understand if they have experienced lateral or rotational movements or settlement.



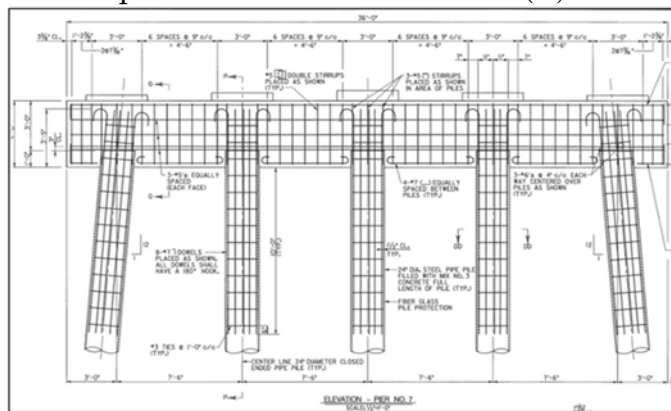
Figure 32. Illustration. Model of bridge cap-beam (Tuckahoe Creek Bridge) with its measured height.



(A) Model of the pier



(B) Measured length



Source: MDOT

(C) Drawing details

Figure 33. Illustration. (A) Model of a bridge pier (Tuckahoe Creek Bridge) and (B) its measured length compared to that shown in (C) its drawing details.

Data was collected at Bacon Ridge Branch / MD-450 bridge site during the morning hours of September 7, 2017. Michigan Tech had previously collected data at the site during a USDOT funded project in 2013 and 2014 focused on bridge scour monitoring with scour posts (Swartz et al. 2014). The site is smaller than Tuckahoe Creek and therefore was more challenging to collect data due to the restricted proximity to active traffic. Extra precautions were taken to ensure safety for all personnel involved. GPS targets were placed along the side of the road and data were recorded using the cell phone app. Figure 34 shows photograph of the Bacon Ridge Branch bridge site taken by the UAS.



Figure 34. Photo. The Bacon Ridge Branch site as collected from the DJI Phantom 3A UAS.

A UWS was deployed from the abutment side riprap located on the north side of the bridge. Unlike Tuckahoe Creek, there was an absence of a water depth reader onsite. Multiple deployments of UWS were conducted and covered an area approximately 66 ft (20 m) upstream and 148 ft (45 m) downstream of the bridge (for a total area of approximately 0.52 acres (0.21 ha) (see figure 35). Operation of the UWS was more complicated at this site due to shallower waters, with maximum depths of 3 ft (0.9 m). During a previous 2014 data collection, a potential scour hole was detected on the southwest corner of the bridge that had not been present during a 2013 survey, with depths greater than 5 ft (1.5 m). However, during the present data collection, the potential scour hole was not detected. This could indicate that it had been in-filled during the three-year period (see figure 36). While local tide levels were not available for the location, the change in depth of at least 3 ft (0.9 m) and the circular shape at the potential scour hole most likely indicate real change, rather than just changes in water levels.

UAS data were collected at Bacon Ridge Branch to provide site overviews and measurements of the bridge and scour countermeasures (riprap) located at the abutments (see figure 37). DJI Phantom 3A imagery was collected to build an overview model (2.75 in (7 cm) resolution) of the surrounding landscape. The Bergen Hexacopter was used to collect high-resolution optical imagery of riprap along both sides of the bridge. This imagery was imported into the software to build a three-dimensional model of the riprap with a ground pixel resolution of 0.08 in (2 mm). Measurements can be made from the imagery (see figure 38). Riprap gradation can be

determined for the above the water portion and extrapolated to underwater using sonar for the rock mass and its footprint.

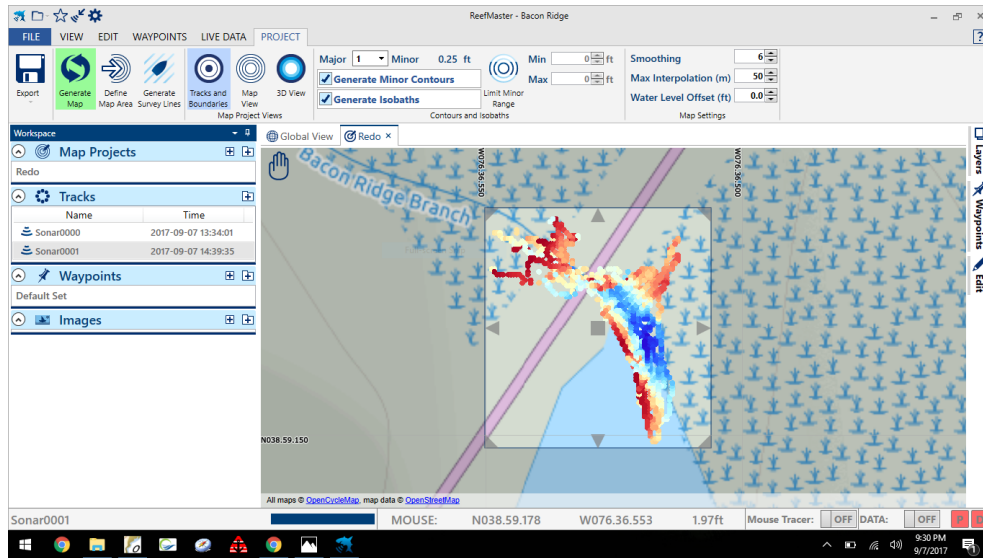
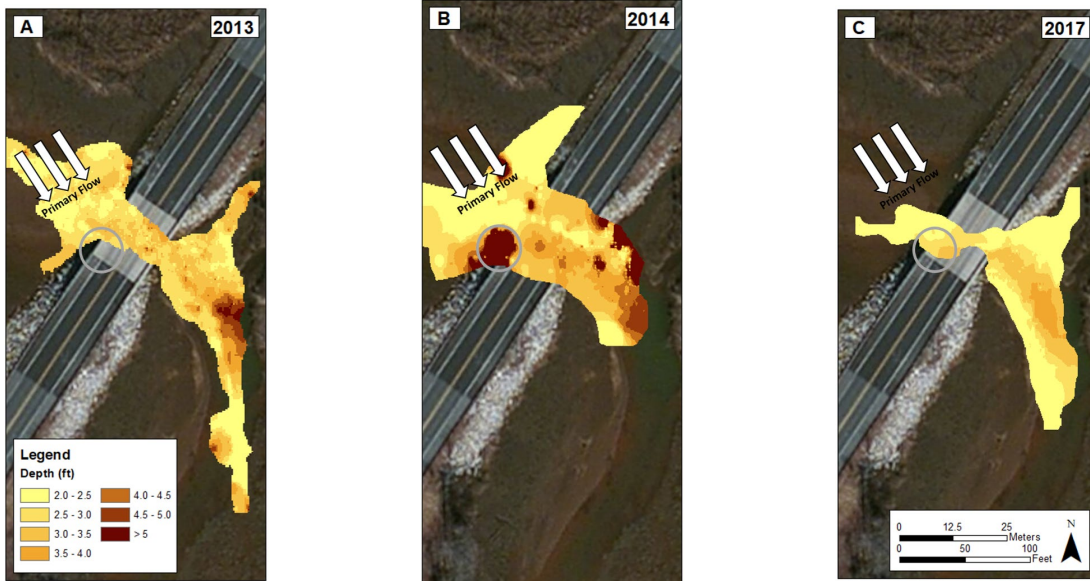


Figure 35. Illustration. Data collection paths of UWS with depths at Bacon Ridge Branch (Note: Red color indicates deeper values).

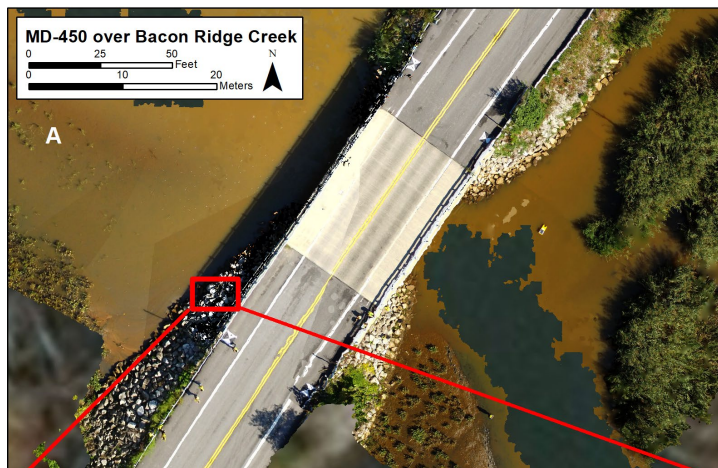


© MTRI
 A. No scour hole is visible in from March, 2013 sonar data at the location of the grey circle.
 B. A likely scour hole can be seen in the June, 2014 sonar data at the location of the grey circle.
 C. In September, 2017, the same grey circle location does not show evidence of a scour hole.

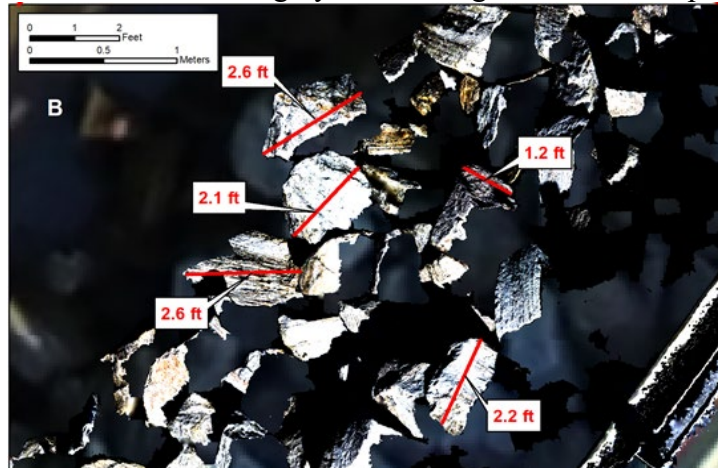
Figure 36. Illustration. Comparison of bathymetric sonar data from Bacon Ridge Branch collected using UWS in 2013, 2014, and 2017.



Figure 37. Photo. High-resolution UAS-collected imagery of riprap at Bacon Ridge Bridge.



A. Overview UAS imagery of the bridge with visible riprap.



B. Measurements of riprap size made from the UAS imagery (see the red rectangle highlighted in figure 38-A).

Figure 38. Photo. Data collection by UWS at Bacon Ridge Branch (1 ft = 0.3048 m).

CONCLUDING REMARKS

Through the remote sensing platforms (UAS, UWS) and sensors at two bridges sites in Maryland, the following conclusions relevant to post-storm assessments can be made:

Debris Field and Structural Stability Assessment: UAS can collect high-resolution imagery (and video) that can be used to evaluate the debris field and create models in which the overall position and condition of bridge elements can be assessed. The latter measurements can be compared to the bridge plans to determine the amount of change that the elements have experienced. With the simplicity of using a UAS to conduct this type of assessment, multiple flights can be conducted throughout a defined time period to determine the change between data collections.

Scour Hole Detection: Unmanned water systems can be used to collect bathymetry data around bridge piers in a relatively short amount of time. Processed data can be used to identify potential (clear-water) scour holes near bridge piers and abutments (more challenging for detecting live-load scour). This type of data collection and processing can be used for periodic assessment of scour holes to help inspectors determine how scour is progressing.

Assessing Stability of Scour Countermeasures: For the exposed portion of the scour countermeasure such as riprap, UAS can be used to collect high-resolution images above the water and sonar for the underwater portion. By processing the imagery into a 3D model, quantitative measurements and positional information can be obtained. This data could be extended to show that the movement of the countermeasures could be identified and quantified with multiple rounds conducted during different time periods.

Bathymetry and DEM for 2D and 3D Modeling: Processed bathymetry data collected by an unmanned surface vehicle, when combined with bathymetry data and terrestrial elevation data from other sources, can potentially be used as input for 2D and 3D hydraulic modeling. The work presented in this research demonstrates an example of a multi-source dataset. A combined bathymetry/terrestrial elevation dataset for all coastal regions usable in hydraulic models does not yet exist and would potentially benefit the hydraulic modelers. Best practices should be established on how to most effectively combine different data sets for rapid post-event evaluations, including hydraulic analysis.

CHAPTER 3. LABORATORY EVALUATION OF SELECTED REMOTE SENSING TECHNOLOGIES OF A MOCK BRIDGE FOR MOVEMENT DETECTION

INTRODUCTION

A detailed field evaluation of both UAS and UWS has been discussed in Chapter 2. Determination of bridge movement during an extreme-hazard event, such as earthquake, flooding or hurricane, is critical and time-sensitive information for emergency response and engineering analysis.

Mock-up experiment is a cost-effective approach to evaluate the capability of UAS in post-hazard damage assessment of bridges. For example, Otero et al. (2016) conducted indoor and outdoor UAS tests to collect LiDAR data of bridge structures for developing 3D models. Figure 39 shows the UAS equipped by a camera flying indoor over a mockup bridge. The authors concluded that the LiDAR data collection using an UAS is an effective approach for developing 3D models of high practical value during bridge inspections. This technology has the potential to improve performance, effectiveness, and safety associated with bridge inspections significantly (Otero et al. 2016). During post-hazard assessment of bridges, this technology can be used to assess movement of bridge components and construct 3D models of the bridge along with water levels and water marks after a flood or hurricane.

A model mock-up scaled bridge experiment (scale $\cong 1/10$) was carried out at the Michigan Tech University to evaluate the accuracy of UAS in measuring movements of bridge components. The main objective of this experiment was to simulate post-hazard assessments using an UAS with high-resolution optical imagery capabilities, and to characterize and document the uncertainty in photogrammetric methods for quantifying bridge movements caused by scour, such as translation, rotation, and settlement.

To this end, a representative model bridge, shown in figure 40, was constructed and was manipulated to simulate movements, and was photographed from multiple angles to create the imagery that could be used to create 3D measurable outputs. Imagery efforts included ground-based photo imagery representative of data collected using an UAS from bridge fascia and substructures, along with overhead photos from a UAS to measure example bridge settlement. Photography of the model bridge was used as input information in a Structure-from-Motion (SfM) software package, where photogrammetric equations were applied for 3D model reconstruction. The 3D model output was used for measuring the amount of movement in elements of the model bridge. Verification of estimated accuracy was recorded through comparison of photogrammetric results with manually measured movements.



Source: TRB

A. UAS



Source: TRB

B. Gimbal mount



Source: TRB

C. Indoor test of a mockup scaled bridge using an UAS with LiDAR sensor

Figure 39. Photo. Mounting LiDAR sensor on a UAS.

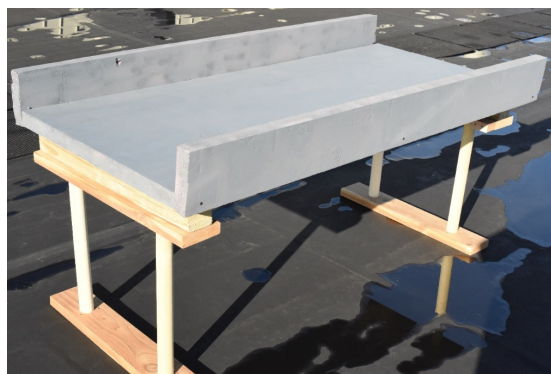


Figure 40. Photo. Photo of the scaled model bridge. The bridge dimensions are 3 ft High \times 6 ft Wide \times 2.7 ft Deep (91 cm H / 183 cm W / 83 cm D).

This chapter presents the experiment methodology, results, and a brief discussion for future applications. The methodology has been presented in the following five sections:

1. Model bridge and equipment;
2. Translation movement experiment;
3. Rotation movement experiment;
4. Settlement movement experiment; and,
5. Post-processing.

The results are presented for three possible types of structural movements: (i) translation, (ii) rotation, and (iii) settlement.

MODEL BRIDGE AND EQUIPMENT

Model Bridge

The model bridge was constructed in-house at Michigan Tech Research Institute (MTRI) using wood for the support feet, piers, and pier caps and two-inch-thick foam insulation board for the bridge surface and fascia (see figure 40). The piers, pier caps, and foam bridge face were not attached to one another to allow easy transportation and for easy representation of bridge translation, rotation, and settlement.

Camera System

A digital single lens reflex (DSLR) camera with 36 megapixel full-frame sensor was used for bridge photography. The camera was equipped with a 2 in (50 mm) f/1.4G lens. Aperture and shutter rate were adjusted throughout the experiment to correct for outdoor lighting, distance to target, and UAS movement. This is the same high-resolution camera system that MTRI has been using since 2012 for its high-resolution UAS photogrammetry work (Dobson et al. 2014; Brooks et al. 2015, 2016, and 2017; Wolf et al. 2017; Wolf, et al. 2015; Bouali et al. 2017). An upgrade to the new high megapixel cameras would enable even higher-resolution data collection in the future. The camera in this study was thus used for both the ground and aerial imagery data collection.

Unmanned Aircraft System (UAS)

Hexacopters (“Hex”) have been found to be a low-cost, reliable, and US-manufactured system that can deploy a variety of flexible payloads, including DSLR cameras, thermal imaging systems, and multi-spectral cameras. The Hex used in this study can fly for up to 20 minutes with a 11 lb (5 kg) payload. It has a global positioning system (GPS) and an inertial measurement unit (IMU), which allows for flying programmed way points that are assigned through Ground Station software that uses a Google Earth interface. With a stabilized gimbal that keeps the camera pointed from forwards to down regardless of the motion of the hexacopter, this provides a stable data platform for bridge imaging and other applications. The added FPV

allows the pilot to see the field of view of the camera as well as provides a read out of the altitude, speed and battery voltage.

TRANSLATION MOVEMENT EXPERIMENT

Data collection for capturing translation movement was carried out outdoors on December 21-22, 2017. The sky conditions were overcast on both days with a light to moderate wind. The experiment for capturing bridge translation was conducted at two distances from the bridge target: 50 ft (15 m) and 25 ft (7.6 m), which represented two distances that an UAS might collect data from a bridge. An 8 ft (2.44 m) transect was established parallel to the bridge opposite side of the distance-to-target transect (see figure 41). The 8 ft (2.4 m) transect was positioned 1 ft (0.3 m) past either side of the bridge target. Photo were taken in 6 in (15 cm) steps along the 8 ft (2.4 m) transect at a height of 36 in (0.9 m) above the ground, with the 6 in (15 cm) steps representing how often an UAS would collect data as it flew alongside the bridge fascia.

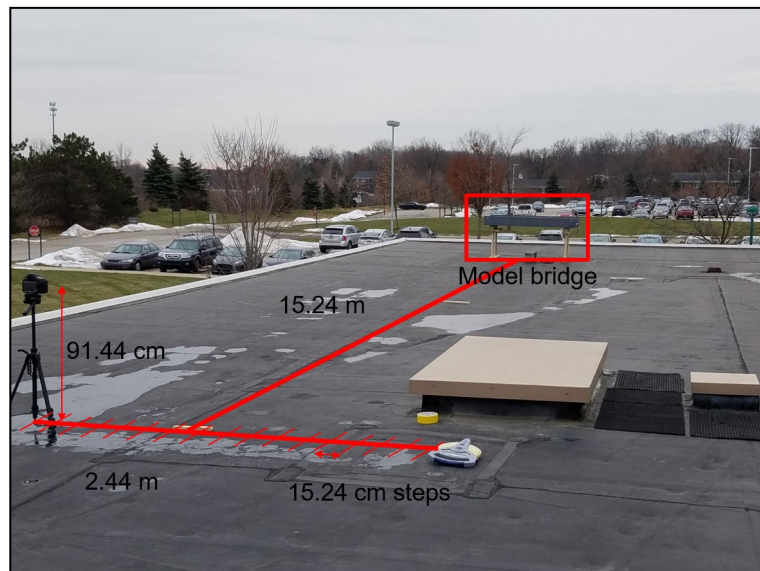


Figure 41. Illustration. Data collection set-up. Red lines indicate position of transects which were used to create distance from target and path for camera system positions. The figure also illustrates the height of the camera system.

Two translational movement experiments were carried out. The first translation movement design, termed as “design 1”, simulated the movement of an entire pier (the left pier in this experiment) from left to right. The second translation movement design, termed as “design 2”, simulated the movement of a separated pier cap (left pier cap in this experiment) from left to right. In total, 10 positions were photographed for each movement experiment at each distance-to-target (DTT) configuration photographed in 0.4 in (1 cm) steps between 0.4 in (1 cm) and 3.9 in (10 cm). A total of 17 photos were captured along the 8 ft (2.44 m) transect for each position, totaling in 680 photos. Of these photos, photos for eight positions were processed at 50 ft (15.2 m) from target for “design 2” movement case.

A total of seven markers were used to set up a local coordinate system, which was used for computing location, volume, and distance as well as optimizing photo alignment in the image processing steps (see figure 42).

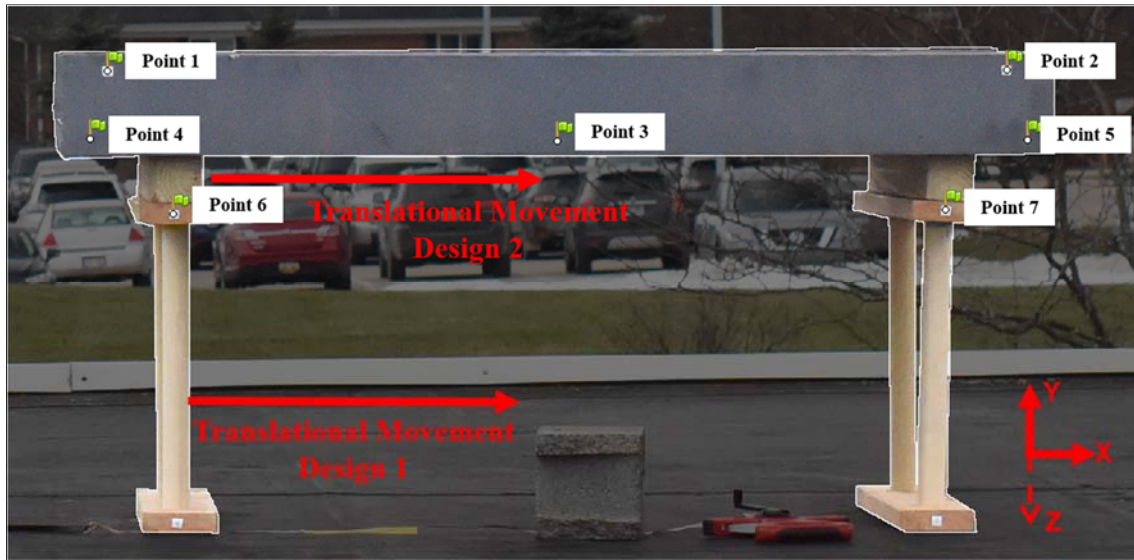


Figure 42. Illustration. Picture of model bridge with position of markers 1 to 7.

Three of the seven markers were established using natural properties of the bridge model (i.e., exposed screws in the foam board) while the remaining four were made using printed targets which were placed on the model bridge before image acquisition so that precise measurements could be made. All marker and camera position coordinates were calculated using the relative position of marker point 1 (which was set to zero in all axes). Coordinates increase from left to right on the x-axis, from down to up on the y-axis, and from away to towards the camera on the z-axis. The local coordinates of control points as measured on the data collection day are presented in table 2. Differences of up to 2 cm in position reflect the overall accuracy of the 3D data sets.

Table 2. Coordinates of markers for the translation experiment (Unit: cm)

Marker	X	Y	Z
1	0.0	0.0	0.0
2	165.4	0.2	0.0
3	83.0	-12.5	0.0
4	-2.9	-12.2	0.0
5	169.5	-12.4	0.0
6	10.8	-26.0	-7.0
7	154.8	-25.8	-6.3

Bridge translation movement for the “design 1” was quantified as the distance between markers 1 and 6. As the pier with marker 6 was moved from left to right in 0.4 in (1 cm) steps, the distance between 1 and 6 increased in 0.4 in (1 cm) steps. Bridge translation movement for

“design 2” was quantified as the distance between marker 1 and an additional marker placed on the upper right hand corner of the pier cap, marker 8 (see figure 43). Note that marker 8 was not used as input in software for computing location, volume, distance, or for optimizing photo alignment in model reconstruction, but rather was used as a measurement point for estimating total movement.

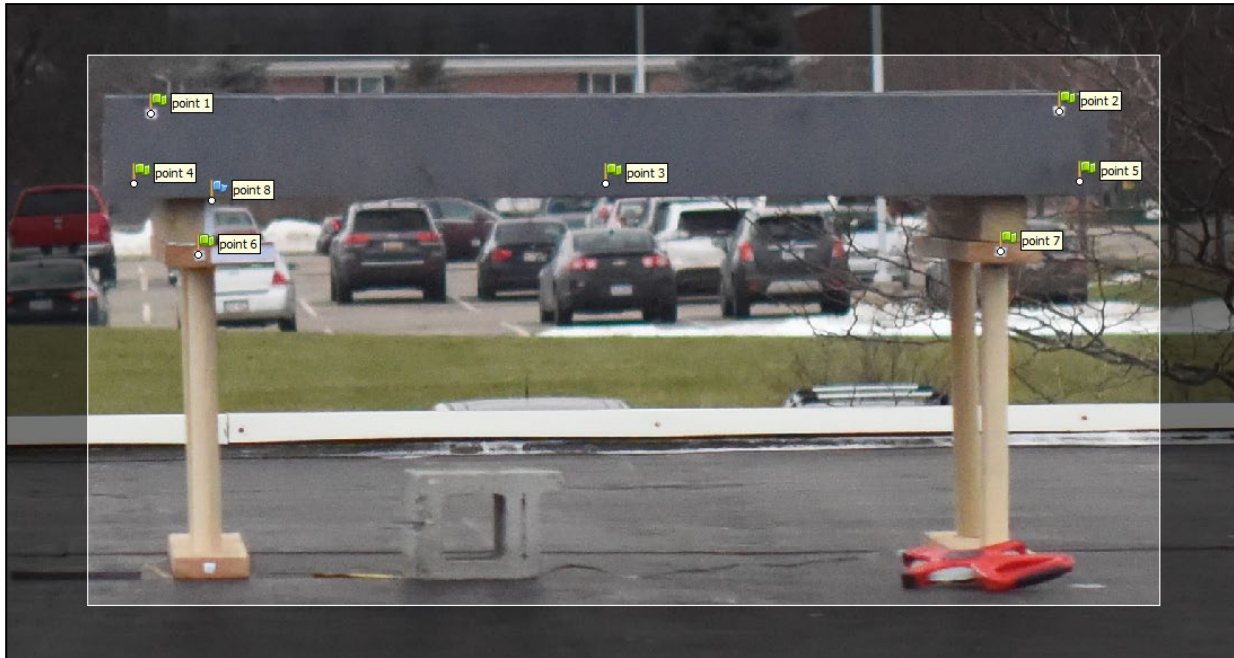


Figure 43. Illustration. Picture of model bridge with position of markers 1 to 8.

ROTATION MOVEMENT EXPERIMENT

Data collection for capturing rotation movement was carried out outdoors on February 15, 2018. Weather conditions were overcast with light wind and intermittent precipitation. The experiment for capturing pier rotation was conducted at 25 ft (7.6 m) from the target, but followed the same configuration for photo acquisition as the translation experiment (see figure 44). The entire wooden pier, including pier feet, pier, and pier cap, was rotated counter clockwise by 20, 30, and 40 degrees, positions 2, 3, and 4 respectively, from parallel orientation, position 1, with the 25 ft (7.6 m) distance-to-target transect. A total of 17 photos were collected for each position, totaling in 68 photos. A total of four markers were used to set up a local coordinate system which was used for computing location, volume, and distance as well as optimizing photo alignment in the image processing steps (see figure 44).

The four markers used in this experiment were printed and placed on the piers before the experiment. All marker and camera position coordinates were calculated using the relative position of marker point 3 (which was set to zero along all three coordinates). Coordinates increase from left to right on the x-axis, from down to up on the y-axis, and from away to towards the camera on the z-axis. The local coordinates of control points are presented in table 3.

With each rotation movement, the position of marker 2 was marked on the pavement using duct-tape and marker (see figure 45). Marked locations were used to trace to a common origin of

rotation. The degrees were measured with a compass positioned at the origin of rotation as the angle between the traced line to marker position and the starting position line parallel to the distance-to-target transect (see figure 45).

Table 3. Coordinates of markers for the rotation experiment (Unit: cm)

Marker	X	Y	Z
1	-70.5	0.0	0.0
2	-70.6	-57.4	0.0
3	0.0	0.0	0.0
4	-1.4	-57.5	-6.3

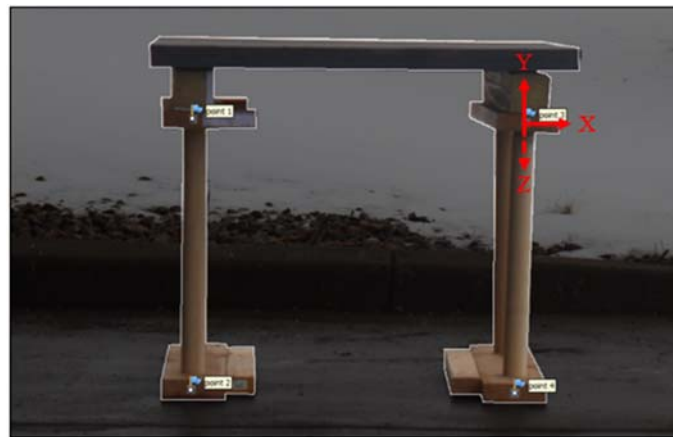


Figure 44. Illustration. Picture of model bridge with position of markers 1 to 4.



A. Measurement with a compass



B. Top view

Figure 45. Photo. Amount of rotation in the model bridge element was verified with ground measurements.

To estimate the degree of rotation using the software, marker 2 movement from position 1 was estimated on the X and Z axis to establish two points (x_1, z_1) and (x_2, z_2) , where the distance between points could be calculated. Half the calculated distance and radius of the circle around the origin of rotation were used to solve for the new angle:

$$\theta = 2 \sin^{-1} \left(\frac{d}{2r} \right)$$

Figure 46. Equation. Estimated angle of rotation.

where d is the estimated distance between (x_1, z_1) and (x_2, z_2) , r is the radius of the circle around the origin of rotation, and θ is the estimated angle of rotation.

SETTLEMENT MOVEMENT EXPERIMENT

Data collection for capturing settlement was carried outdoors on February 15, 2018. Weather conditions were overcast with light wind and intermittent precipitation. Photos were captured using the hexacopter UAS equipped with a camera system at 50 ft (15 m) altitude above the target. Photos were collected at one frame per second (fps) with the UAS passing overhead at approximately 2.5 m/s (5.6 mph), a speed used for sufficient overlap to create 3D data using SfM photogrammetry.

A total of six markers were used to set up a local coordinate system, which was used for computing location, volume, and distance as well as optimizing photo alignment in the image processing steps (See figure 47). Table 4 shows coordinates of markers 1 to 6 for the settlement experiment.



Figure 47. Illustration. Picture of model bridge with position of coordinate markers 1-6. Additional markers 7 and 8 used for reporting Z-axis position.

Table 4. Coordinates of markers for the settlement experiment (Unit: cm)

Marker	X	Y	Z
1	0.0	0.0	0.0
2	0.3	-31.8	0.0
3	-0.6	-59.0	0.0
4	162.0	29.0	0.0
5	162.0	-30.3	0.0
6	161.0	-64.1	0.0

The foam bridge face was cut in half before photo acquisition to simulate bridge settlement. The half with markers 4-6 was elevated between positions using wooden boards under the pier base to represent settlement (see figure 48). Bridge settlement was quantified as the distance between bridge half surfaces on the z-axis. The settlement was recorded with a ruler before photo acquisition. Figure 49 shows the UAS flying over the model bridge, while figure 50 is an example image of how the model bridge appeared from the air with the settlement in place.



Figure 48. Photo. The model bridge with a raised section used to represent bridge settlement for the UAS data collection.



Figure 49. Photo. Certified remote pilot collecting imagery from the UAS of the model bridge in the settlement scenario.



Figure 50. Photo. The model bridge with settlement in place as collected from the UAS with 36 megapixel camera at 50 ft (15m) height.

Similar to “design 2” case of the translation movement experiment, additional markers 7 and 8 were used to report position coordinates for estimated difference in bridge surface elevation, but were not used for computing photo alignment or for any other 3D model optimizing function.

POST-PROCESSING OF DATA

Post-processing of photos was carried out using a photogrammetric 3D image processing software. The photos taken for each position were brought into the software as a photo chunk. Markers were manually set for each photo using the marker tool and the coordinates were set for each marker using their measured distances from the origin marker. Finally, each photo was masked using the masking tool to exclude non-pertinent information in the foreground.

Photo alignment was calculated using marker coordinates reported in tables 2 to 4. Camera positions were not considered for photo alignment calculation, and instead was estimated during alignment with the marker coordinate information. The marker coordinates were not adjusted from the initial position coordinates throughout each of the movement experiments. Instead, it was assumed that no movement had occurred from one experiment to the next. Estimated marker positions were exported after photo alignment.

RESULTS AND DISCUSSION

Translation

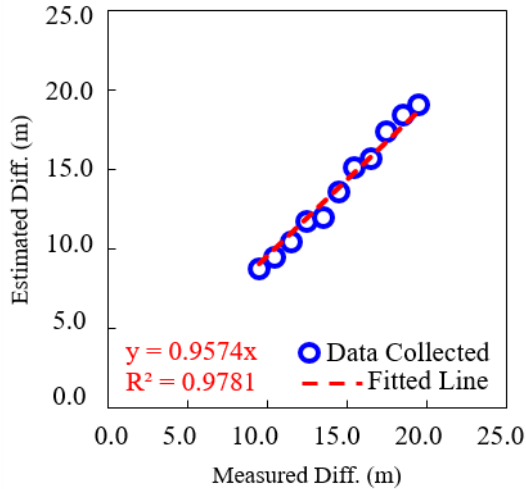
The results from design 1 at 25 ft (7.6 m) and 50 ft (15.2 m) are presented in table 5. The results from design 2 at 50 ft (15.2 m) are presented in table 6. Two scatter plots comparing the estimated translational movement with the measured translational movement for design 1 are presented in figure 51.

Table 5. Measured vs. estimated distance between markers 1 and 6 for the translation design 1 movement experiment (Unit: cm)

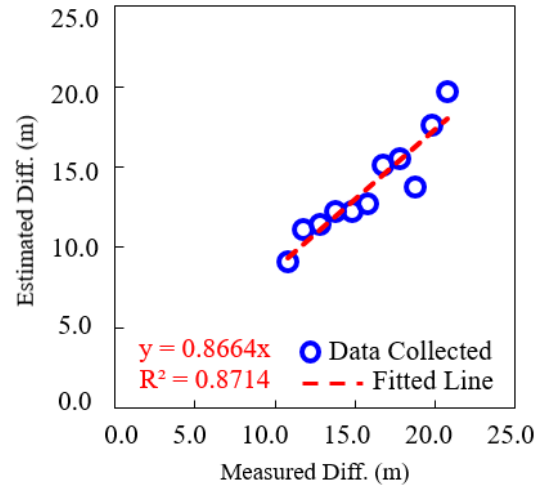
Position	Meas. (DDT ₁) ^a	Est. (DDT ₁)	Avg. X,Y,Z		Meas. (DDT ₂) ^a	Est. (DDT ₂)	Avg. X,Y,Z	
			RMS Error (DDT ₁)	Abs. Diff. (DDT ₁) ^b			RMS Error (DDT ₂)	Abs. Diff. (DDT ₂) ^b
0	9.5	8.8	0.5	0.7	10.8	9.1	0.8	1.7
1	10.5	9.5	0.7	1	11.8	11.1	1.1	0.7
2	111.5	10.5	20	1	12.8	11.4	0.9	1.4
3	12.5	11.7	1.2	0.8	13.8	12.2	1.2	1.6
4	13.5	12	1.1	1.5	14.8	12.2	0.8	2.6
5	14.5	13.6	1.9	0.9	15.8	12.7	1.1	3.1
6	15.5	15.1	2.6	0.4	16.8	15.1	1.9	1.7
7	16.5	15.7	2.5	0.8	17.8	15.6	2	2.2
8	17.5	17.4	3.1	0.1	18.8	13.7	38.3	5.1
9	18.5	18.4	3.5	0.1	19.8	17.6	2.8	2.2
10	19.5	19.1	3.8	0.4	20.8	19.7	4.4	1.1

a. DDT₁=7.62 m (25 ft) and DDT₂=15.24 m (50 ft)

b. The value of the average absolute difference for DDT₁ and DDT₂ are equal to 0.7 cm and 2.1 cm, respectively.



A. Estimation at 25 ft (7.6 m)



B. Estimation at 50 ft (15.2 m)

Figure 51. Graph. Scatter plots comparing the measured differences of markers 1 and 6 against estimated differences for each position.

Table 6. Measured vs. estimated distance between markers 1 and 8 for the translation design 2 movement experiment (Unit: cm)

Position	Meas.	Est.	Avg. X,Y,Z RMS Error	Abs. Diff. ^a
0	12	11.3	5	0.7
1	14.3	13.8	14.9	0.5
2	15.3	14	1.3	1.3
3	16.3	14.4	1.8	1.9
4	17.3	15.1	1.7	2.2
5	18.3	16	1.5	2.3
6	19.3	16.9	1	2.4
7	20.3	18.9	1.3	1.4

a. The value of the average absolute difference is equal to 1.6 cm.

The “design 1” results indicate that more accurate movement characterization was possible at 25 ft. An average absolute difference of approximately 0.8 in (2.1 cm) was observed between measured and estimated distance between markers 1 and 6 on the x-axis at 50 ft (15.2 m) from the target, whereas an average absolute difference of under 0.3 in (7 mm) was observed at 25 ft (7.6 m) from the target. Similar error at 50 ft (15.2 m) was observed for the “design 2” translation experiment where an average absolute difference of approximately 0.6 in (1.6 cm) was observed. For UAS observation of movement of bridge fascia and other elements that would be evaluated from a side-on view, collecting data at the 25 ft (7.6 m) distance should be preferred over the 50 ft (15 m) distance to achieve the 0.4 in (1 cm) or better accuracy.

Rotation

The results from the rotation experiment are presented in table 7.

Table 7. Measured vs. estimated degrees and distance between marker 2 at position 0 and reported row position (Unit: cm)

Position	Meas. Degrees	Est. Degrees	Meas. Distance	Est. Distance	Avg. X,Y,Z RMS Error	Abs. Diff. ^a
0	0	0.68	0.0	0.9	0.9	0.9
1	20	19.60	13.1	12.9	9.1	0.2
2	30	30.86	20.4	20.3	14.0	0.1
3	40	42.82	31.0	28.2	19.6	2.8

a. The value of the average absolute difference is equal to 1.0 cm.

An average absolute difference between measured and estimated distance travelled for marker 2 of approximately 0.4 in (1 cm) was observed using the 25 ft (7.6 m) data collection distance, similar to the translation movement results. The increase of average X, Y, Z RMSE error is expected as marker 1 and 2 positions begin to deviate from the coordinate inputs of table 3.

Settlement

The results from the settlement experiment are presented in table 8.

Table 8. Measured vs. estimated distance between bridge surfaces at markers 7 and 8 (Unit: cm)

Position	Meas.	Est.	Avg. X,Y,Z RMS Error	Abs. Diff. ^a
0	0.0	0.1	0.3	0.1
1	3.2	1.0	0.4	2.2
2	4.5	2.5	0.4	2.0

a. The value of the average absolute difference is equal to 1.4 cm.

An average absolute difference of approximately 0.55 in (1.4 cm) was observed between measured and estimated bridge surface elevation difference using the UAS imagery collected at 25 ft (7.6 m) height with the 36 Mp digital images.

Results Summary

Table 9 presents the accuracy of the UAS in measuring three different movements of the model bridge, including the translation, rotation, and settlement. For the sake of simplicity, the movement experiments were conducted separately and no combination of them was considered. As the matter of fact, the authors don't expect a significant change in measurement accuracy when a combination of three movements may occur.

The distance to target (DTT) and sensor resolution were expected to have a more significant impact on accuracy. The highest accuracy of 0.7 cm was obtained when the UAS was used to measure the translation movement of the pier with DTT=7.62 m (25 ft). This number is within range of deflection of components of a bridge under service loads, is but quite smaller than the maximum deflection that these components may experience during a strong earthquake (Buckle

et al., 2006). This clearly indicates that the UAS has a significant potential for collecting valuable and high-accuracy data on assessing post-hazard bridges movements.

Table 9. Accuracy of the UAS in measuring three different movements of the model bridge.

Movement	DDT ₁ =7.62 m (25 ft)	DDT ₂ =15.24 m (50 ft)
Translation (Design 1)	0.7 cm (0.3 in)	2.1 cm (0.8 in)
Translation (Design 2)	... ^a	1.6 cm (0.6 in)
Rotation	1 cm (0.4 in)	... ^a
Settlement	... ^a	1.4 cm (0.5 in)

a. Only one DTT was considered because of time limitation and weather condition.

CONCLUDING REMARKS

This chapter presented the results obtained from Structure-from-Motion photogrammetry to evaluate and document the accuracies that can be obtained for measuring different types of bridge movement using remote sensing. Ground-based measurements were taken for side-on measurements of translation and rotation movements, representative of a UAS data collection. A hexacopter UAS was used for demonstrating measurement of bridge settlement. The following conclusions can be made:

- 1. Minimizing error:** A potential source of error for estimated translational movement may be due the narrow angle of photo acquisition relative to the facade of the bridge. The same photo collection transect length of 2.44 m was used during collection at both distances to the target due to space constraints for the experiment. To achieve better object reconstruction and depth, the photo collection transect should be extended at larger distances to the target.
- 2. Detection of movement:** The results suggest that movement detection is possible at resolutions of 2 cm or better (with sub-centimeter possible) using high-resolution optical imagery installed in a flexible multi-rotor UAS platform.
- 3. Points of reference:** Future real-world scenario bridge photo collection experiments should test the ability of accurate coordinate, length, and volume characterization using markers based on parts of a bridge artifacts from prior information. Access to the post-hazard site for marker set up could be avoidable using known distances between bridge properties (i.e. pier caps, bolts, etc.) based on as-built plans. Future real-world scenario bridge photo collection experiments should test the ability of accurate coordinate, length, and volume characterization using markers based on bridge artifacts gathered from a priori information (i.e. as-built plans).
- 4. Recommendation:** The focal length and sensor size (together gives the range of view) are important in photogrammetric processing. Therefore, it is recommended that full scale bridge testing be followed up with a field scenario measuring likely movement of bridge elements, including use of existing bridge features as markers and availability / unavailability of baseline data / as-built plans to evaluate how the sub-centimeter capabilities represented here can be used for post-hazard scenarios.

For these experiments, the authors used the equivalent of pre-event bridge baseline data by having markers on the model bridge, and were able to have verified information about the

distances between these markers before and after a movement. This is the easiest scenario for creating 3D models and measuring change, but may not always be practical in a post-event scenario. Engineers should be able to obtain equivalent known distances between at least some bridge features based on existing bridge plans for use as references for comparing to parts of the bridge that may have moved or settled. Placing one or more objects of known size somewhere in the data collection area would also provide equivalent information, if this could be done safely in a post-event scenario. Without any baseline data that can be used to verify the size of at least some components of the affected bridge, measuring at least relative difference is possible. For example, it would be possible to evaluate if a bridge is level or if bridge components appear to have moved, if there appeared to be at least some components that likely didn't move. Ideally, however, placing a known reference, measuring some components, or having bridge plans may be the most practical way of measuring movements. As noted in the "Points of Reference" concluding remark above, a future real-world experiment should test these capabilities, especially for a situation where pre-event information is limited.

Additionally, there is room for further optimization during the photo processing stages as well. This feature was not considered for this experiment, and as a result, none of the photos were rejected before 3D model reconstruction.

CHAPTER 4. CONCLUSIONS AND RECOMMENDATIONS FOR FUTURE STUDY

CONCLUSIONS

The main objective of the research presented in this report has been to evaluate current state-of-the-art post-hazard engineering assessment of bridges using remote sensing technologies, identify potential technologies for post-hazard assessment of bridges, develop a list of data needs and gaps, perform a scaled laboratory experiment for detecting bridge movements using photogrammetry, and field demonstration of unmanned aerial and unmanned boat technologies for post-hazard applications. Currently, visual inspection and limited deployment of nondestructive technologies are the primary tools for post-hazard inspection of bridges. Several research and field studies have shown that remote sensing technologies can provide high-quality wide area data rapidly after a hazard. However, satellite-based remote sensing technologies and manned aerial surveys can be expensive, require specialized system / software and expert technical qualification (Vaghefi et al. 2012). For example, in a detailed 2015 blog post about the costs of inspection by satellite, manned aircrafts and UAS, UAS costs has been found to be 40 percent lower than satellite costs for smaller areas (<12 acres (5 ha)). On the other hand, costs for equivalent UAS coverage is 60 percent more than that for high-resolution satellite for larger areas (120 acres (50 ha)) (see <https://droneapps.co/price-wars-the-cost-of-drones-planes-and-satellites/>). Remote sensing using UAS are cost effective, can be deployed rapidly, can be equipped with high resolution digital cameras and sensors, and can be used for collecting a variety of data after an extreme natural hazard strikes a bridge site. Similarly, unmanned water systems (UWS) that are similar to UAS but can navigate on water can be used to collect sonar data for bathymetry, scour and hydraulic measurement around bridges.

In order to demonstrate the application of UAS and UWS for post-hazard assessment, field evaluation of these two tools were carried out on two bridges in Maryland, and are detailed in Chapter 2. Using the bathymetric and aerial LiDAR data collected at these two bridge sites, creation of high resolution bathymetric and DEMs that can cover an entire watershed for detailed hydraulic analysis has been demonstrated. These DEMs can be used as input for 2D and 3D hydraulic modeling to identify scour risk around the bridge pier. The field study has demonstrated that the bathymetric and LiDAR data can be used to identify potential scour holes near bridge piers and abutments. This type of data collection and processing can be used for periodic assessment of scour holes to help inspectors determine how scour is progressing. More importantly, by using UAS and UWS, data collection covering a larger area and in hard to reach areas (i.e., assessing bridge piers closer than manned boats) can be achieved in a relatively short time. For bridges with exposed scour countermeasures, such as riprap, 3D reconstruction using bathymetric and LiDAR data can give quantitative measurements and positional information of the countermeasure. The movement of the countermeasure can be measured by identifying changes in countermeasure footprint due to, for example, edge failures during different time periods. These type of high-resolution 3D UAS-based sensing can also be used for structural stability assessment and measuring debris fields in post-hazard scenarios. Finally, processed bathymetry data collected by an unmanned surface vehicle, when combined with bathymetry

data and terrestrial elevation data from other sources, can lead to high precision DEM of the watershed surrounding the bridge.

As described in Chapter 3, a field evaluation on mock scaled model of bridge was carried out to identify maximum resolutions to which bridge movements could be measured using UAS with high-resolution cameras and photogrammetric processing of images to create 3D bridge models. Results show that UAS can measure bridge displacements with a resolution of 0.5 in (1.4 cm) or better when measured from a distance of 25 ft (7.6 m), and a resolution of 0.8 in (2.1 cm) from a distance of 50 ft (15.2 m). Both rotation and settlement movement could be measured using a multi-rotor UAS that could carry a DSLR camera. For absolute measurement of movement, current methods require knowing at least some size of a bridge element or distance between them. These could be provided by using bridge plans, by placing markers on elements that could be safely reached, or by placing an object of known size somewhere in the UAS collection area. A future study should evaluate these requirements and investigate the measurement of movements when pre-event information is not available.

RECOMMENDATIONS FOR FUTURE STUDY

A detailed discussion on needs and gaps in remote sensing technology for post-hazard assessment of bridges was presented in Chapter 1. Resolution of these gaps is important for successful incorporation of remote sensing technology, particularly UAS, in future post-hazard assessment of bridges. In addition to this, following recommendations on field evaluation and testing of bridge movement using UAS should be considered.

Field Evaluation of the Technology

A combined bathymetry/terrestrial elevation dataset for all coastal regions usable in hydraulic models does not yet exist and would potentially benefit the hydraulic modelers. This shows the need for future work in cross-agency collaboration for data sharing and generation of missing data. The cross-agency collaborators should include bridge inspectors, hydraulic modelers and experts on sensors and UWS.

Evaluation of Bridge Movements

The work on measurement of bridge movements has been carried out on a mock model of a bridge by using camera mounted on fixed support for translation and rotation and by using a UAS for settlement. The future study should be done on an actual bridge using a flexible multi-rotor UAS platform. In this case, bridge photo collection experiments should test the ability of accurate coordinate, length, and volume characterization using markers based on parts of a bridge artifacts from prior information. Full scale bridge testing should be followed up with a field scenario measuring likely movement of bridge elements, including use of existing bridge features as markers, to evaluate how the sub-centimeter capabilities could be achieved for post-hazard scenarios. Because of rapid change in technology, state-of-the art UAS with higher resolution cameras should be used to determine appropriate hardware that can give sub-centimeter resolution that may be necessary for the assessment of integrity of bridges. This could also lead to a standard equipment configuration that agencies across all States in the country could adopt for post-hazard preparedness. Real world crack detection algorithms from

3D photogrammetry images should also be carried out. An ideal site for such study could be a bridge that is damaged because of hydraulic or other hazards (such as vehicular impacts). Liquefaction is another important geo-hazard that has to be taken into account for seismic post-hazard assessment of bridges on soils with loose sand. Future study should consider using UAS to assess cracking of deck/column/girders; movement of bearing pads; anchor bolts damage/fracture; column failure modes; girder bending/shear damage; rotation of deck; and ground spreading measure due to liquefaction, etc.

ACKNOWLEDGMENTS

This work was done under FHWA contract number DTFH61-14-D-00010 0209 entitled “Post-Hazard Engineering Assessment of Highway Structures: *Scanning and Convening Meeting and Demonstration of Reconnaissance Technologies*”. The authors sincerely acknowledge support of Michigan Technological University team members in carrying out the field evaluation and mock testing presented in this report.

Any opinions, findings and conclusions or recommendations expressed in this publication are those of the authors and do not necessarily reflect the views of the Federal Highway Administration.

REFERENCES

- Acton, S. (2013). *Sinkhole detection, landslide and bridge monitoring for transportation infrastructure by automated analysis of interferometric synthetic aperture radar (InSAR) imagery*, Report No. RITARS-11-H-UVA, University of Virginia, Charlottesville, VG.
- Adkins, J. (2016). "Bridge of America" (website) Available online: <http://jonahadkins.com/bridges.html>, last accessed March 22, 2017.
- Ahlborn, T.M., Shuchman, R.A., Sutter, L.L., Harris, D.K., Brooks, C.N., Burns, J.W. (2013). *Bridge condition assessment using remote sensors*, Report No. DT0S59-10-H-00001, Michigan Technological University, Houghton, MI.
- Akiyama, M., Frangopol, D.M., Arai, M., and Koshimura, S. (2013). "Reliability of bridges under tsunami hazards: Emphasis on the 2011 Tohoku-oki earthquake." *Earthquake Spectra*, 29(s1), pp. S295-S314.
- Alipour, A. (2016). *Post-extreme event damage assessment and response for highway bridges*, Report No. 20-05/Topic 46-11, Transportation Research Board, Washington, DC. doi: 10.17226/24647.
- American Red Cross (2015). *Drones for disaster response and relief operations*, Report, [<http://www.issueab.org/resources/21683/21683.pdf>].
- Anderson, N.L., Ismael, A.M., and Thitimakorn, T. (2007). "Ground-penetrating radar: a tool for monitoring bridge scour." *Environmental and Engineering Geoscience*, 13(1), pp.1-10.
- Aronoff, S. (2005). *Remote sensing for GIS managers*, ESRI Press, Redlands, CA.
- Azhari, F., Tom, C., Benassini, J., Loh, K. J., and Bombardelli, F. A. (2014). "Design and characterization of a piezoelectric sensor for monitoring scour hole evolution." Presented at Sensors and Smart Structures Technologies for Civil, Mechanical, and Aerospace Systems, International Society for Optics and Photonics.
- Baiocchi, V., Dominici, D., Mormile, M. (2013). "UAV application in post-seismic environment." *Int. Arch. Photogram. Remote Sens. Spatial Inf. Sci. XL-1 W*, 2, pp. 21–25.
- Baiocchi, V., Dominici, D., Vittoria Milone, M., Mormile, M. (2014). "Development of a software to optimize and plan the acquisitions from UAV and a first application in a post-seismic environment." *Eur. J. Remote Sens*, 47, pp.477–496. doi:10.5721/EuJRS20144727.
- Baso"z, N.I., Kiremidjian, A.S., King, S.A. and Law, K.H. (1999). "Statistical analysis of bridge damage data from the 1994 Northridge, CA, earthquake." *Earthquake Spectra*, 15(1), pp.25-54.
- Bian, H., Chen, S. E., Watson, C., and Hauser, E. (2011). "Bridge deck joints evaluation using lidar and aerial photography." Presented at Nondestructive Characterization for Composite

Materials, Aerospace Engineering, Civil Infrastructure, and Homeland Security, International Society for Optics and Photonics.

Bouali, E.H., Oommen, T. and Escobar-Wolf, R. (2016). “Interferometric stacking toward geohazard identification and geotechnical asset monitoring.” *Journal of Infrastructure Systems*, 22(2), p.05016001.

Bouali, E.H., Oommen, T., Vitton, S., Escobar-Wolf, R. and Brooks, C. (2017). “Rockfall hazard rating system: benefits of utilizing remote sensing.” *Environmental and Engineering Geoscience*, 23(3), pp.165-177.

Brooks, C.N., Dean, D.B., Dobson, R.J., Roussi, C., Carter, J.F., VanderWoude, A.J., Colling, T. and Banach, D.M. (2017). “Identification Of Unpaved Roads in a Regional Road Network Using Remote Sensing.” *Photogrammetric Engineering & Remote Sensing*, 83(5), pp.377-383.

Brooks, C.N., Dobson, R.J., Banach, D.M., Dean, D.B., Oommen, T., Escobar-Wolf, R., Havens, T.C., Ahlborn, T.M., Hart, B.E., Cook, S.J., and Clover, A. (2015). *Evaluating the Use of Unmanned Aerial Vehicles for Transportation Purposes: Final Report*, Report No. RC-1616, Michigan Technological University, Houghton, MI. (http://www.michigan.gov/mdot/0,4616,7-151-9622_11045_24249-353767--,00.html)

Brooks, C.N., Dobson, R.J., Banach, D.M., Roussi, C., Colling, T., Lefler, V., Hart, B., Garbarino, J., Lawrence, J., White, B., Aden, S., Singh, C. (2016). *Characterization of Unpaved Road Condition through the Use of Remote Sensing Project – Phase II Deliverable 8-D: Final Report*, Report No. RITARS-11-H-MTU1, Michigan Tech Research Institute, Ann Arbor, MI (http://www.mtri.org/unpaved/media/doc/deliverable_Final_Report_Del8D_Unpaved_Roads_Phase_II_RevisedB.pdf)

Brown, H.C., Jenkins, L.K., Meadows, G.A., and Shuchman, R.A. (2010). “BathyBoat: An autonomous surface vessel for stand-alone survey and underwater vehicle network supervision.” *Marine Technology Society Journal*, 44(4), pp.20-29.

Brown, J.L. (2009). “Robot inspects damaged bridge.” *Civ. Eng. Mag. Arch.*, 79, 40–40. doi:10.1061/ciegag.0000793.

Buckle, I. G., Friedland, I. M., Mander, J. B., Martin, G. R., Nutt, R., & Power, M. (2006). *Seismic retrofitting manual for highway structures: Part 1-bridges*, Report No. FHWA-HRT-06-032, Federal Highway Administration.

Burgess, D., Ortega, K., Stumpf, G., Garfield, G., Karstens, C., Meyer, T., Smith, B., Speheger, D., Ladue, J., Smith, R., and Marshall, T. (2014). “20 May 2013 Moore, Oklahoma, tornado: Damage survey and analysis.” *Weather and Forecasting*, 29(5), pp. 1229-1237.

Campbell, J.B., Wynne, R.H. (2011). *Introduction to remote sensing*, 5th ed. The Guilford Press, New York City, NY.

- Chen, G., Schafer, B. P., Lin, Z., Huang, Y., Suaznabar, O., Shen, J., and Kerenyi, K. (2015). "Maximum scour depth based on magnetic field change in smart rocks for foundation stability evaluation of bridges." *Structural Health Monitoring*, 14(1), pp. 86-99.
- Chen, H.P. (2018). *Structural Health Monitoring of Large Civil Engineering Structures*, John Wiley and Sons.
- Chen, S. E., Rice, C., Boyle, C., and Hauser, E. (2011). "Small-format aerial photography for highway-bridge monitoring." *Journal of Performance of Constructed Facilities*, 25(2), pp. 105-112.
- Chen, S.E. (2010). "*Forensic applications of commercial remote sensing and spatial information technologies*." Presented at Indo-US Forensic Practices: Investigation Techniques and Technology.
- Chen, S.E., Sumitro, P., and Boyle, C. (2016). "Remote sensing techniques for geo-problem applications." *Japanese Geotechnical Society Special Publication*, 2(3), pp.207-211.
- Craft, Andrew. (2017). "How Drones Are Playing a Larger Role in Hurricane Relief Efforts." (website) *Fox News*, September 8, 2017. Available online: <http://www.foxnews.com/tech/2017/09/08/how-drones-are-playing-larger-role-in-hurricane-relief-efforts.html>.
- Cusson, D., Ghuman, P., Gara, M. and McCardle, A. (2012). "*Remote monitoring of bridges from space*." Presented at the Proceedings of the 54th Brazilian Congress of concrete, Maceio-Alagoas, Brazil.
- Darrow, M., Meyer, F., Cunningham, K. Gong, W., Gyswyt, N.L., McCoy, R.P., Daanen, R.P., and McAlpin, D. (2016). *Monitoring and Analysis of Frozen Debris Lobes Using Remote Sensing*, Report No. OASRTRS-14-H-UAF-B, Office of the Assistant Secretary for Research and Technology, U.S. Department of Transportation.
- Deng, L. and Cai, C.S. (2009). "Bridge scour: Prediction, modeling, monitoring, and countermeasures." *Practice periodical on structural design and construction*, 15(2), pp.125-134.
- Dobson, R., Colling, T., Brooks, C., Roussi, C., Watkins, M., and Dean, D. (2014). "Collecting decision support system data through remote sensing of unpaved roads." *Transportation Research Record: Journal of the Transportation Research Board*, (2433), pp.108-115.
- Duwadi, P. (2010). *Hazard Mitigation R&D Series: Article 1: Taking a Key Role in Reducing Disaster Risks*, Public Roads, Vol. 73, No. 6, Federal Highway Administration.
- Ettema, R., Nakato, T., and Muste, M.V.I. (2006). *An illustrated guide for monitoring and protecting bridge waterways against scour*, Report No. Project TR-515, IIHR-Hydroscience & Engineering, University of Iowa, Iowa City, IA.
- Falkner, E. (1995). *Aerial mapping: Methods and applications*, CRC Press, Boca Raton, FL.

FAA (2016). Advisory Circular 107, Part 2, dated June 21, 2016 issued by the Federal Aviation Administration. https://www.faa.gov/documentLibrary/media/Advisory_Circular/AC_107-2.pdf. Last Accessed February 28, 2019.

Federal Highway Administration. (2018). "National Bridge Inventory, Deficient Bridges by Highway System in 2017." (website) McLean, VA. Available online: <https://www.fhwa.dot.gov/bridge/nbi/no10/defbr17.cfm>, Last accessed March 15, 2018.

Gao, Q., & Yu, X. B. (2015). Design and evaluation of a high sensitivity spiral TDR scour sensor. *Smart Materials and Structures*, 24(8), 085005.

Gong, J. (2016). *Mobile Hybrid LiDAR & Infrared Sensing for Natural Gas Pipeline Monitoring*, Report No. RITARS-14-H-RUT, U.S. Department of Transportation.

Gostnell, C., and Yoos, J. (2005). "Efficacy of an Interferometric Sonar for Hydrographic Surveying: Do interferometers warrant an in-depth examination?" *Hydrographic Journal*, 118, p.17-24.

Graettinger, A.J., Ramseyer, C.C., Freyne, S., Prevatt, D.O., Myers, L., Dao, T., Floyd, R.W., Holliday, L., Agdas, D., Haan, F.L., and Richardson, J. (2014). *Tornado damage assessment in the aftermath of the May 20th 2013 Moore Oklahoma tornado*. National Science Foundation.

Guo, J., Kerényi, K., and Pagan-Ortiz, J.E. (2009). *Bridge pressure flow scour for clear water conditions*, Report No. FHWA-HRT-09-041, Turner-Fairbank Highway Research Center.

Han, Q., Du, X., Liu, J., Li, Z., Li, L., and Zhao, J. (2009). "Seismic damage of highway bridges during the 2008 Wenchuan earthquake." *Earthquake Engineering and Engineering Vibration*, 8(2), pp.263-273.

Hatta, H., Aly-Hassan, M. S., Hatsukade, Y., Wakayama, S., Suemasu, H., and Kasai, N. (2005). "Damage detection of C/C composites using ESPI and SQUID techniques." *Composites Science and Technology*, 65(7-8), pp. 1098-1106.

Hauser, E.W., Chen, S.-E. (2009). *Integrated remote sensing and visualization (IRSV) system for transportation infrastructure operations and management*, Report No. DTOS59-07-H-0005, University of North Carolina, Charlotte, NC.

Helmerich, R., Niederleithinger, E., Trela, C., Bień, J., Kamiński, T., and Bernardini, G. (2012). "Multi-tool inspection and numerical analysis of an old masonry arch bridge." *Structure and Infrastructure Engineering*, 8(1), pp. 27-39.

Holzer, T.L., Borchardt, R. D., Comartin, C.D., Hanson, R.D., Scawthorn, C. R. Tierney, K. and Youd, T.L. (2002). *The Plan to Coordinate NEHRP Post-Earthquake Investigations*. Circular 1242, United States Geological Survey.

Hoppe, E., Bruckno, B., Campbell, E., Acton, S., Vaccari, A., Stuecheli, M., Bohane, A., Falorni, G., and Morgan, J. (2016). "Transportation Infrastructure Monitoring Using Satellite Remote Sensing." *Materials and Infrastructures 1*, pp.185-198.

- Huizinga, R. (2017), *Bathymetric and Velocimetric Surveys at Highway Bridges Crossing the Missouri and Mississippi Rivers on the Periphery of Missouri*, Report No. 2017–5076, U.S. Geological Survey, Reston, Virginia.
- Hutt, T., and Cawley, P. (2008). “Feasibility of digital image correlation for detection of cracks at fastener holes.” *NDT Int.*, 42(2), pp. 141-149.
- Irish, J.L., McClung, J.K., and Lillycrop, W.J. (2016). “Airborne lidar bathymetry: the SHOALS system.” *Bulletin-International Navigation Association*, p.43–54.
- Jáuregui, D.V., White, K.R., Woodward, C.B., and Leitch, K.R. (2003). “Noncontact photogrammetric measurement of vertical bridge deflection.” *Journal of Bridge Engineering*, 8(4), pp. 212-222.
- Jiang, R., Jáuregui, D.V., and White, K. R. (2008). “Close-range photogrammetry applications in bridge measurement: Literature review.” *Measurement*, 41(8), pp. 823-834.
- Jordan, S., Moore, J., Hovet, S., Box, J., Perry, J., Kirsche, K., Lewis, D., and Tse, Z.T.H. (2018). “State-of-the-art technologies for UAV inspections.” *IET Radar, Sonar & Navigation*, 12(2), p.151-164.
- Kalooop, M. R., and Li, H. (2009). “Monitoring of bridge deformation using GPS technique.” *KSCE Journal of Civil Engineering*, 13(6), pp. 423-431.
- Karpowicz, R., Tymli F., and Jessica L. (2014). “*The Use of Unmanned Aerial Systems for Steep Terrain Investigations.*” Caltrans Division of Research, Innovation and System Information (DRISI), Sacramento, CA.
- Kerenyi K., and Guo J. (2010). *Hazard Mitigation R&D Series: Article 2: Scour, Flooding, and Inundation*, Public Roads, Vol. 74, No. 1, Federal Highway Administration.
- Kornus, W., Magariños, A., Pla, M., Soler, E., and Perez, F. (2015). “Photogrammetric processing using ZY-3 satellite imagery.” *The International Archives of Photogrammetry, Remote Sensing and Spatial Information Sciences*, 40(3), p.109-113.
- Kosa, K. (2014). “Damage analysis of bridges affected by the tsunami in the Great East Japan Earthquake.” *Journal of JSCE*, 2(1), pp. 77-93.
- Lai, Y.G. (2010), “Two-Dimensional Depth-Averaged Flow Modeling with an Unstructured Hybrid Mesh”, *Journal of Hydraulic Engineering*, Vol. 136(1).
- Lee, W. F., Cheng, T. T., Huang, C. K., Yen, C. I., and Mei, H. T. (2012). “Performance of a Highway Bridge under Extreme Natural Hazards: Case Study on Bridge Performance during the 2009 Typhoon Morakot.” *Journal of Performance of Constructed Facilities*, 28(1), pp. 49-60.
- Liang, X. (2017). *Improving Hydrologic Disaster Forecasting and Response for Transportation by Assimilating and Fusing NASA and other Data Sets*, Report No. OASRTRS-14-H-PIT, U.S. Department of Transportation.

- Liao, C. L., Wang, C. Y., Wang, H., and Chen, M. H. (2010). “*Damage Investigation of Bridges Affected by Mudslides and Flood during 2009 Morakot Typhoon in Taiwan.*” Presented at the 5th Civil Engineering Conference in the Asian Region (CECAR5) and Australasian Structural Engineering Conference.
- Liu, J., Mason, P.J., and Bryant, E.C. (2018). “Regional assessment of geohazard recovery eight years after the Mw7. 9 Wenchuan earthquake: a remote-sensing investigation of the Beichuan region.” *International Journal of Remote Sensing*, 39(6), pp.1671-1695.
- Mallet, L., Lee, B. C., Staszewski, W. J., and Scarpa, F. (2004). “Structural health monitoring using scanning laser vibrometry: II. Lamb waves for damage detection.” *Smart materials and structures*, 13(2), pp. 261-269.
- Mansour, M. F., Morgenstern, N. R., and Martin, C. D. (2011). “Expected damage from displacement of slow-moving slides.” *Landslides*, 8(1), pp. 117-131.
- McGlone, C., Mikhail, E., and Bethel, J. (1980). *Manual of photogrammetry*, American Society for Photogrammetry and Remote Sensing.
- Melville, B. W. (1992). “Local scour at bridge abutments.” *Hydraulic Engineering*, 118(4), pp. 615-631.
- Meng, X., Gogoi, N., Dodson, A.H., Roberts, G.W., and Brown, C.J. (2011). “*Using multi-constellation GNSS and EGNOS for bridge deformation monitoring.*” Presented at the joint international symposium on deformation monitoring, Hong Kong, China.
- Milillo, P., Giardina, G., DeJong, M. J., Perissin, D., and Milillo, G. (2018). “Multi-Temporal InSAR Structural Damage Assessment: The London Crossrail Case Study.” *Remote Sensing*, 10(2), 287.
- Morey, R. M. (1998). *Ground penetrating radar for evaluating subsurface conditions for transportation facilities*, Transportation Research Board.
- Murphy, R.R., Dreger, K.L., Newsome, S., Rodocker, J., Steimle, E., Kimura, T., Makabe, K., Matsuno, F., Tadokoro, S., and Kon, K. (2011a). “*Use of remotely operated marine vehicles at Minamisanriku and Rikuzentakata Japan for disaster recovery.*” Presented at the 2011 IEEE International Symposium on Safety, Security, and Rescue Robotics. IEEE, Kyoto, Japan.
- Murphy, R.R., Steimle, E., Hall, M., Lindemuth, M., Trejo, D., Hurlebaus, S., Medina-Cetina, Z., and Slocum, D. (2011b). “Robot-assisted bridge inspection”, *J. Intell. Robot. Syst.*, 64, p.77–95. doi:10.1007/s10846-010-9514-8
- Nakamura, S. (2000). “GPS measurement of wind-induced suspension bridge girder displacements.” *J. Struct. Eng.*, 126, pp.1413–1419. doi:10.1061/(ASCE)0733-9445(2000)126:12(1413)

Nassif, H., Ertekin, A.O., and Davis, J. (2002). *Evaluation of bridge scour monitoring method*, Report No. FHWA-NJ-2003-009, U.S. Department of Transportation, Federal Highway Administration.

Nassif, H.H., Gindy, M., and Davis, J. (2005). “Comparison of laser Doppler vibrometer with contact sensors for monitoring bridge deflection and vibration.” *NDT & E International*, 38(3), pp. 213-218.

Nedjati, A., Vizvari, B., and Izbirak, G. (2016). “Post-earthquake response by small UAV helicopters.” *Nat. Hazards*, 80, pp.1669–1688. doi:10.1007/s11069-015-2046-6.

Niu, X., Tang, H., and Wu, L. (2018). “Satellite scheduling of large areal tasks for rapid response to natural disaster using a multi-objective genetic algorithm.” *International Journal of Disaster Risk Reduction*, 28, pp.813-825.

O’Connor, J. (2010). *Post-earthquake bridge inspection guidelines*. Report No. C-06-14. New York Department of Transportation, Albany, NY.

O’Neil-Dunne, J. (2015). *Rapid exploitation of commercial remotely sensed imagery for disaster response & recovery*, Report No. RITARS-12-H-UVM, University of Vermont, Burlington, VT.

O’Brien, E. J., and Malekjafarian, A. (2016). “A mode shape-based damage detection approach using laser measurement from a vehicle crossing a simply supported bridge.” *Structural Control and Health Monitoring*, 23(10), pp. 1273-1286.

Okeil, A.M., and Cai, C.S. (2008). “Survey of short-and medium-span bridge damage induced by Hurricane Katrina.” *Journal of Bridge Engineering*, 13(4), pp.377-387.

Olson, M.J., Barbosa, A., Burns, P., Kashani, A., Wang, H., Veletzos, M., Chen, Z., Roe, G., and Tabrizi, K., (2016a). *Assessing, Coding, and Marking of Highway Structures in Emergency Situations, Volume 1: Research Overview*. National Academies of Sciences, Engineering, and Medicine, Washington, DC. <https://doi.org/10.17226/24608>.

Olson, M.J., Barbosa, A., Burns, P., Kashani, A., Wang, H., Veletzos, M., Chen, Z., Roe, G., and Tabrizi, K., (2016b). *Assessing, Coding, and Marking of Highway Structures in Emergency Situations, Volume 2: Assessment Process Manual*. National Academies of Sciences, Engineering, and Medicine, Washington, DC. <https://doi.org/10.17226/24610>

Olson, M.J., Barbosa, A., Burns, P., Kashani, A., Wang, H., Veletzos, M., Chen, Z., Roe, G., and Tabrizi, K., (2016c). *Assessing, Coding, and Marking of Highway Structures in Emergency Situations, Volume 3: Coding and Marking Guidelines*. National Academies of Sciences, Engineering, and Medicine, Washington, DC. <https://doi.org/10.17226/24609>

Oštir, K., Veljanovski, T., Podobnikar, T., and Stančič, Z., (2003). “Application of satellite remote sensing in natural hazard management: the Mount Mangart landslide case study.” *International Journal of Remote Sensing*, 24(20), pp.3983-4002.

- Otero, L.D., Adrian, P., Moyou, M. (2016). *Remote sensing with mobile LiDAR and imaging sensors for railroad bridge inspections*, Florida Institute of Technology, Melbourne, FL.
- Padgett, J., DesRoches, R., Nielson, B., Yashinsky, M., Kwon, O.S., Burdette, N., and Tavera, E., (2008). “Bridge damage and repair costs from Hurricane Katrina.” *Journal of Bridge Engineering*, 13(1), pp.6-14.
- Palermo, A., Wotherspoon, L., Wood, J., Chapman, H., Scott, A., Hogan, L., Kivell, A., Camnasio, E., Yashinsky, M., Bruneau, M., and Chouw, N. (2011). “Lessons learnt from 2011 Christchurch earthquakes: analysis and assessment of bridges.” *Bulletin of the New Zealand Society for Earthquake Engineering*, 44(4), pp.319-333.
- Pamuk, A., E. Kalkan, and H. I. Ling. (2005). “Structural and Geotechnical Impacts of Surface Rupture on Highway Structures during Recent Earthquakes in Turkey.” *Soil Dynamics and Earthquake Engineering*, 25(7–10), p. 581–89.
- PCI Journal (2005). “Special Report: Damage in the gulf, impact of hurricane Katrina on precasting plants and precast/prestressed concrete structures.” *PCI J.*, 50, pp. 117–120.
- Pittore, M., and Wieland, M. (2013). “Toward a rapid probabilistic seismic vulnerability assessment using satellite and ground-based remote sensing.” *Natural Hazards*, 68(1), pp.115-145.
- Placzek, Gary, and Haeni, F.P. (1995), *Surface-geophysical techniques used to detect existing and infilled scour holes near bridge piers*, Report No. 95-4009, U.S. Geological Survey Water-Resources Investigations.
- Radchenko, A., Pommerenke, D., Chen, G., Maheshwari, P., Shinde, S., Pilla, V., and Zheng, Y. R. (2013). “Real time bridge scour monitoring with magneto-inductive field coupling.” Presented at Sensors and Smart Structures Technologies for Civil, Mechanical, and Aerospace Systems, International Society for Optics and Photonics.
- Ramirez, J.A., Frosch, R.J., Sozen, M.A. and Turk, A.M. (2000). Handbook for the post-earthquake safety evaluation of bridges and roads. JTRP Contract No. 2377. Indiana Department of Transportation.
- Ranf, R.T., Eberhard, M.O. and Malone, S. (2007), “Post-earthquake Prioritization of Bridge Inspections”, *Earthquake Spectra*, Volume 23, No. 1, pages 131–146, February 2007; © 2007, Earthquake Engineering Research Institute.
- Renslow, M. (2012). *Manual of Airborne Topographic Lidar*. American Society for Photogrammetry and Remote Sensing.
- Richardson, E.V., Harrison, L.J., Richardson, J.R., and Davis, S.R. (1993). *Evaluating scour at bridges*, Report No. FHWA-HIF-12-003, U.S. Department of Transportation, Federal Highway Administration.

Robertson, I.N., Riggs, H.R., Yim, S.C., and Young, Y.L., (2007). “Lessons from Hurricane Katrina storm surge on bridges and buildings.” *Journal of Waterway, Port, Coastal, and Ocean Engineering*, 133(6), pp.463-483.

Rockwell, M. (2017). “FAA Speeds Drone Approvals for Irma Recovery.” (website), Available online: <https://gcn.com/articles/2017/09/19/faa-drone-authorizations.aspx>, last accessed September 19, 2017.

Ruggles, S., Clark, J., Franke, K.W., Wolfe, D., Reimschiessel, B., Martin, R.A., Okeson, T.J., and Hedengren, J.D. (2016). “Comparison of SfM computer vision point clouds of a landslide derived from multiple small UAV platforms and sensors to a TLS-based model.” *J. Unmanned Veh. Syst.*, 4, pp. 246–265. doi:10.1139/juvs-2015-0043.

Schierenbeck, Tim (2018). “Surveying Beyond the Water’s Edge” (website) XYHT, February 27, 2018. Available online: <https://www.xyht.com/hydromarine/surveying-beyond-the-waters-edge/>.

Sofi, M., Lumantarna, E., Mendis, P. A., Duffield, C., and Rajabifard, A. (2017). “Assessment of a pedestrian bridge dynamics using interferometric radar system IBIS-FS.” *Procedia Engineering*, 188, pp. 33-40.

Sotiropoulos, F., and Khosronejad, A. (2016). *Three-Dimensional Simulation of Bridge Foundation Scour on Mississippi River Bridges 9321 & 27801*, Report No. CTS 16-03, Center for Transportation Studies, University of Minnesota.

Sousa, J.J., Hlaváčová, I., Bakoň, M., Lazecký, M., Patrício, G., Guimarães, P., Ruiz, A.M., Bastos, L., Sousa, A., and Bento, R. (2014). “Potential of multi-temporal InSAR techniques for bridges and dams monitoring.” *Procedia Technology*, 16, pp.834-841.

Stearns, M., and Padgett, J.E. (2011). “Impact of 2008 Hurricane Ike on bridge infrastructure in the Houston/Galveston region.” *Journal of Performance of Constructed Facilities*, 26(4), pp.441-452.

Steimle, E. T., and Hall, M. L. (2006). “*Unmanned surface vehicles as environmental monitoring and assessment tools.*” Presented at OCEANS 2006, IEEE, Boston, MA.

Steimle, E.T., Murphy, R.R., Lindemuth, M., and Hall, M.L. (2009). “*Unmanned marine vehicle use at Hurricanes Wilma and Ike.*” Presented at the OCEANS 2009, MTS/IEEE Biloxi-Marine Technology for Our Future: Global and Local Challenges, Biloxi, MS.

Stow, D.A., Lippitt, C.D., Coulter, L.L. and Loerch, A.C. (2018). “Towards an end-to-end airborne remote-sensing system for post-hazard assessment of damage to hyper-critical infrastructure: research progress and needs.” *International Journal of Remote Sensing*, 39(5), pp.1441-1458.

Stow, D.A., Lippitt, C.D., Coulter, L.L., and Davis, B.A. (2015). “Time-Sensitive Remote Sensing Systems for Post-Hazard Damage Assessment.” *Time-Sensitive Remote Sensing*, pp.13-28.

Stramondo, S., Bignami, C., Chini, M., Pierdicca, N. and Tertulliani, A. (2006). “Satellite radar and optical remote sensing for earthquake damage detection: results from different case studies.” *International Journal of Remote Sensing*, 27(20), pp.4433-4447.

Stumpf, A., Michéa, D., and Malet, J.P. (2017), “*Generation of Digital Surface Models from satellite photogrammetry: the DSM-OPT service of the ESA Geohazards Exploitation Platform (GEP)*.” Presented at 19th EGU General Assembly, EGU2017, Vienna, Austria.

Sumitro, S., and Hodge, M.H. (2006). “Global smart bridge monitoring system.” *Bridge Maintenance, Safety, Management, Life-Cycle Performance and Cost*, pp. 673–674.

Swartz, R.A., Brian, B., Colin, B., and Alison F. (2016). *Automated Scour Detection Arrays Using Bio-Inspired Magnetostrictive Flow Sensors*. Report No. RITARS-12-H-MTU, U.S. Department of Transportation.

Sydell, L. (2017). “Telecom Companies Turn To Drones for Help After Hurricanes.” (webpage) *NPR*, Available online: <https://www.npr.org/2017/09/10/549922317/telecom-companies-turn-to-drones-for-help-after-hurricanes>, last accessed September 10, 2017.

Tabatabai, H., Mehrabi, A.B., and Yen, W.-H. P. (1998). “*Bridge stay cable condition assessment using vibration measurement techniques*”, Presented at Proc. SPIE 3400, Structural Materials Technology III: An NDT Conference.

Toth, C., and Józków, G. (2016). “Remote sensing platforms and sensors: A survey.” *ISPRS Journal of Photogrammetry and Remote Sensing*, 115, pp. 22-36.

Tralli, D.M., Blom, R.G., Zlotnicki, V., Donnellan, A., Evans, D.L. (2005). “Satellite remote sensing of earthquake, volcano, flood, landslide and coastal inundation hazards.” *ISPRS J. Photogram. Remote Sens.*, 59, pp. 185–198. doi:10.1016/j.isprsjprs.2005.02.002

Vaghefi, K., Oats, R.C., Harris, D.K., Ahlborn, T., M., Brooks, C.N., Endsley, K.A., Roussi, C., Shuchman, R., Burns, J.W., Dobson, R. (2012). “Evaluation of commercially available remote sensors for highway bridge condition assessment.” *J. Bridg. Eng.*, 17, pp. 886–895. doi:10.1061/(ASCE)BE.1943-5592.0000303.

Wang, Z., and Lee, G.C. (2009). “A comparative study of bridge damage due to the Wenchuan, Northridge, Loma Prieta and San Fernando earthquakes.” *Earthquake Engineering and Engineering Vibration*, 8(2), pp.251-261.

Washer, G.A. (2010). *Long-term remote sensing system for bridge piers and abutments*, Report No. NCHRP-123, University of Missouri, Columbia, MO.

Watanabe, E., Sugiura, K., Nagata, K., and Kitane, Y. (1998). “Performances and damages to steel structures during the 1995 Hyogoken-Nanbu earthquake.” *Engineering Structures*, 20(4-6), pp.282-290.

Waters, N., and Cervone, G. (2014). *Using social networks and commercial remote sensing to assess impacts of natural events on transportation infrastructure*, Report No. RITARS-12-H-GMU Geographic Information Science, Center of Excellence, Fairfax, VA.

Wipf, T.J., Phares, B.M., and Greimann L. (2011). *Evaluation of Bridge Movement Measurement Using GPS*. Institute of transportation, Iowa State University.

Wolf, R.E, Oommen, T., Brooks, C.N., Dobson, R.J. and Ahlborn, T.M., and (2017). “Unmanned Aerial Vehicle (UAV)-Based Assessment of Concrete Bridge Deck Delamination Using Thermal and Visible Camera Sensors: A Preliminary Analysis.” *Research in Nondestructive Evaluation*, pp.1-16.

Wolf, R.E., Bouali, E.H., Oommen, T., Dobson, R., Vitton, S., Brooks, C., and Lautala, P. (2015). *Sustainable Geotechnical Asset Management Along the Transportation Infrastructure Environment Using Remote Sensing*, Report No. RITARS-14-H-MTU, Michigan Technological University, Houghton Geological and Mining Engineering and Sciences, Houghton, MI.

Wolf, R.E., Oommen, T., Brooks, C., and Dobson, R. (2016). “*Monitoring Geotechnical Assets along Pipeline Corridors Using Manned and Unmanned Aerial Platform-Based Photogrammetry*.” Presented at the Pipelines 2016, Reston, VA.

Xing, C., Yu, Z. Q., Zhou, X., and Wang, P. (2014). “*Research on the Testing Methods for IBIS-S System*.” Presented at IOP Conference Series: Earth and Environmental Science, IOP Publishing.

Yen, W. H. (2010). *Hazard Mitigation R&D Series: Article 3: Earthquake*, Public Roads, Vol. 74, No. 2, Federal Highway Administration.

Zebker, H., McParland, M.A., Kubanski, M., Greene, F., and Eppler, J. (2017). *Advanced Space-Based InSAR Risk Analysis of Planned and Existing Transportation Infrastructure*, Report No. OASRTRS-14-H-SUI, U.S. Department of Transportation.

Zhang, L., Maizuar, M., Mendis, P., Duffield, C., and Thompson, R. (2016). “Monitoring the dynamic behaviour of concrete bridges using non-contact sensors (IBIS-S).” *Applied Mechanics & Materials*, 846, pp. 225-230.

Zink, J., and Lovelace, B. (2015). *Unmanned aerial vehicle bridge inspection demonstration project*, Report No. MN/RC 2015-40, Minnesota Department of Transportation, Saint Paul, MN.